DOCTORAL SCHOOL

UNIVERSITY OF MILANO-BICOCCA

School of Medicine and Surgery

PhD Program in Translational and Molecular Medicine (DIMET)

Cycle XXX

Molecular mechanisms of cholangiocarcinoma progression: emphasizing the role of tumor-stroma interactions

Dr. Simone Brivio
Registration number: 708864

Tutor: Prof. Mario Strazzabosco
Co-tutor: Prof. Luca Fabris

Coordinator: Prof. Andrea Biondi

ACADEMIC YEAR 2016/2017

Table of contents

CHAPTER 1

General introduction

1. Cholangiocarcinoma

Cholangiocarcinoma (CCA) is a highly aggressive epithelial malignancy stemming from varying locations within the biliary tree. Nowadays, CCA carries a very poor prognosis, mainly due to an early metastatic propensity, and an impressive resistance to conventional chemotherapy [1-3]. The median survival is below 2 years, and the survival rate is less than 10% [4]. Liver failure, biliary tract sepsis, and cachexia are the most common causes of CCA-related mortality [4,5]. According to its anatomical location, CCA is classified as either intrahepatic (iCCA) (also called peripheral) or extrahepatic (eCCA), with the latter being further divided into perihilar (pCCA) (also called Klatskin tumor) and distal (dCCA). iCCA occurs within the liver parenchyma, involving the intrahepatic biliary system in its entirety, from segmental bile ducts to small bile ductules. pCCA arises from the right and left hepatic ducts at or near their confluence, whereas dCCA grows along the common bile duct (Figure 1) [6]. pCCA represents about 50% of CCA cases, whereas dCCA and iCCA roughly accounts for 40% and 10% of tumors, respectively [3]. Classically, CCA is thought to originate from the neoplastic transformation of the epithelial cells lining the bile ducts, named cholangiocytes. However, recent evidence suggests that iCCA pathogenesis may also involve mature hepatocytes or hepatic progenitor cells (HPCs) [7,8]. The latter are immature, bipotential epithelial cells residing in the canals of Hering (i.e., the physiologic link between the hepatocyte canalicular system and the

biliary tree), capable of differentiating towards the cholangiocytic or hepatocytic lineage [9]. Similar to iCCA, eCCA has been proposed to arise not only from the lining epithelium of the extrahepatic biliary tree, but also from peribiliary glands, i.e., mucin-producing glandular elements scattered throughout the wall of perihilar and extrahepatic bile ducts, representing a reservoir of multipotent stem cells of endodermal origin [7,10].

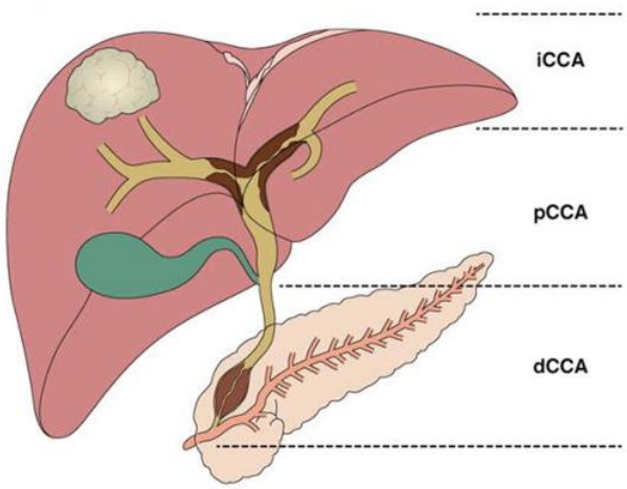

Figure 1 Anatomical classification of cholangiocarcinoma. According to its location within the biliary tree, cholangiocarcinoma (CCA) can be classified as either intrahepatic (iCCA) or extrahepatic (eCCA), with the merging point of the second order bile ducts representing the separation point. eCCA can be further divided into perihilar (pCCA) or distal (dCCA), with the insertion of the cystic duct acting as the anatomic boundary. Adapted from [7].

1.1 Classification and pathological features

Going beyond the anatomical location, CCA can be also classified on the basis of its macroscopic growth pattern, which can be

identified as mass-forming, periductal-infiltrating, or intraductal-growing [11,12]. The mass-forming type produces a well-delimited, polylobulated mass that early occludes the bile duct lumen, and then expands beyond the bile duct wall, within the periductal tissue. Periductal-infiltrating tumors extend lengthwise along the bile duct, thereby causing wall thickening and eventually, luminal obstruction. Intraductal-growing tumors preferentially grow towards the lumen of the bile duct, which undergoes a marked dilatation, and infiltrate the bile duct wall only at very late stages (Figure 2). Of note, intraductal-growing CCAs typically spread superficially along the mucosal layer, thereby generating multiple masses on the inner surface of the bile ducts [6,11,13]. The most frequent growth pattern of iCCA is the mass-forming type, with the periductal-infiltrating and intraductal-growing types exclusively arising at the level of large intrahepatic bile ducts. pCCA typically originates as a periductal-infiltrating tumor, but it tends to acquire additional mass-forming features in the course of its progression. Finally, dCCA are almost exclusively periductal-infiltrating or intraductal-growing [2,6]. Importantly, mass-forming and periductal-infiltrating CCAs are generally associated with a poorer prognosis compared to intraductal-growing tumors [11,14].

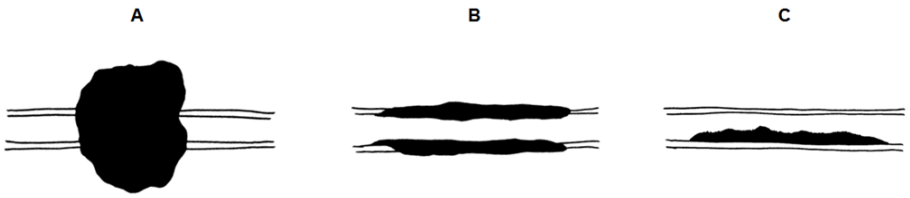

Figure 2 Morphologic classification of cholangiocarcinoma. Based on its macroscopic growth characteristics, cholangiocarcinoma can be classified as mass-forming (A), periductal-infiltrating (B), and intraductal-growing (C). See text for further details. Adapted from [11].

At the microscopic, histopathological level, 90-95% of CCAs are well to moderately differentiated adenocarcinomas, with an abundant fibrous stroma surrounding the neoplastic glands [11,15]. However, iCCAs are histologically heterogeneous tumors, which likely reflects the different anatomical sites of origin and therefore, the topographical heterogeneity of cholangiocytes all along the biliary tree [14,16]. Indeed, large intrahepatic ducts (i.e., segmental, area and septal ducts), similarly to extrahepatic bile ducts, are lined by mucin-producing, columnar cholangiocytes, whereas small bile ductules (or terminal cholangioles) and interlobular ducts are delimited by mucin-negative, cuboidal cholangiocytes [16,17]. Although different classification systems have been proposed over time, iCCA can be substantially subcategorized in two main histological phenotypes, which we refer to as bile duct (mucinous) type and bile ductular (mixed) type. The bile duct type is composed of cylindrical tumor cells organized in large glandular patterns, with extensive mucin

production. The bile ductular type shows similar mucin-producing, adenocarcinomatous components, but also focally consists of small, anastomosing glands lined by mucin-negative, cuboidal tumor cells, which are reminiscent of a ductular reaction (Figure 3) [2,14,16]. The latter is a dynamic reparative response to severe liver damage, based on the expansion of the epithelial cells lining the smallest ramifications of the biliary tree, giving rise to irregular, highly branched ductules devoid of lumen at the portal interface [17,18]. Indeed, bile ductular iCCAs are thought to originate from HPC-containing small intrahepatic bile ducts, whereas bile duct iCCAs are supposed to arise from large intrahepatic bile ducts. This hypothesis is further supported by the fact that bile ductular iCCAs are generally located in the peripheral area, whereas bile duct iCCAs mostly display a perihilar location [16]. Importantly, this histological heterogeneity also results in divergent clinicopathological features. In fact, bile ductular iCCAs predominantly adopt a mass-forming growth pattern, and typically arise as large masses with low invasive potential. Conversely, bile duct iCCAs do not display a preferential growth pattern, and tends to be more aggressive compared with bile ductular tumors, thus carrying a poorer prognosis [2,16,19]. Interestingly, bile duct iCCAs share clinical, morphological and immunohistochemical features with both eCCA and pancreatic ductal adenocarcinoma, suggesting that all these tumors may be derived from similar cells of origin. On the other hand, bile ductular iCCAs clinicopathologically and genotypically overlap with

cholangiolocellular carcinoma (CLC), an HPC-derived tumor that is almost exclusively arranged in small, monotonous glands, with no mucin production, showing both hepatocellular and cholangiocellular differentiation characteristics [2,16]. In this regard, it was suggested that bile ductular iCCAs, CLC, and combined hepatocellular-cholangiocarcinoma actually all originate from HPCs, though the neoplastic transformation apparently occurs at distinct stages of HPC differentiation towards biliary or hepatocyte lineage [2]. In conclusion, as the anatomical-based classification of CCA is challenged by the highly branched, three-dimensional structure of the biliary system, the histological subtyping has drawn increasing attention over time, also because it carries more detailed information about tumor biology and clinical course [2,16].

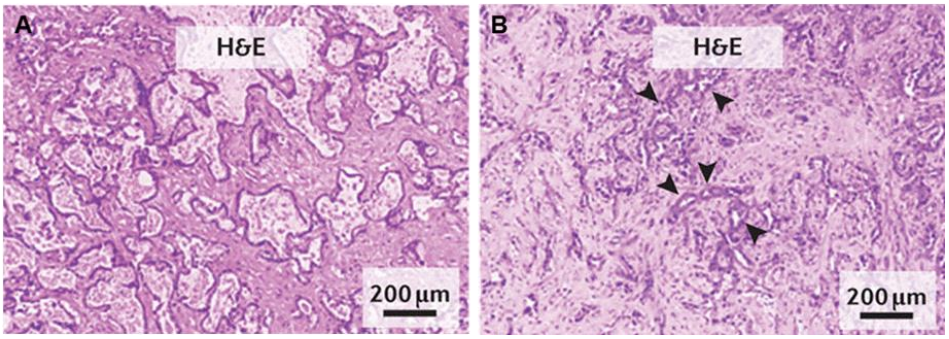

Figure 3 Hematoxylin and eosin staining of distinct histopathological subtypes of intrahepatic cholangiocarcinoma. The bile duct type intrahepatic cholangiocarcinoma (iCCA) is solely composed of large tubular, acinar, or papillary structures arising from the abnormal proliferation of columnar cholangiocytes lining the large intrahepatic ducts (A). The bile ductular type iCCA also focally consists of small glandular patterns with irregular lumen (arrowheads) arising from the

abnormal proliferation of cuboidal cholangiocytes lining the small bile ductules and the interlobular ducts (B). Modified from [2].

1.2 Epidemiology

CCA is the second most common primary neoplasm of the liver after hepatocellular carcinoma (HCC), and overall accounts for 10-20% of the deaths for hepatobiliary malignancies. Whereas liver tumors are the second cause of cancer-related mortality worldwide, it is clear that CCA represents a global health problem [5,20]. Of note, CCA incidence rates are geographically heterogeneous, likely due to a differential exposure to environmental risk factors, as well as to genetic diversity among various populations [21]. The highest incidence rates are found in China, South Korea and North Thailand, which indeed are all areas where infestation with liver flukes is endemic (see below). Conversely, CCA is a rare cancer (i.e., less than 6 cases per 100,000 people) in Europe, United States and Australia. For instance, the incidence rate of CCA in Italy is 3.36/100,000 [2]. However, the occurrence of CCA, more specifically of iCCA, markedly increased in Western Countries during the last three decades of the twentieth century, thus strongly renewing the interest of the scientific community towards this malignancy, though the underlying reasons have not yet been fully understood [2]. It is also worth noting that, owing to the poor outcome, mortality and incidence rates are nearly comparable [5].

1.3 Etiology

Unlike HCC, CCA typically occurs in the absence of an evident pre-existing chronic liver disease. Nevertheless, several risk factors have been identified over time, and recent observations also point out that iCCA is increasingly detected in the context of cirrhotic liver [1]. Hepatobiliary fluke infestation (e.g., *Opisthorchis viverrini*, *Clonorchis sinensis*), hepatitis B viral infection, and hepatolithiasis are common risk factors for CCA in Southeast Asia, where the prevalence of these conditions is high. Conversely, the association between CCA and primary sclerosing cholangitis (PSC) or chronic hepatitis C infection is statistically relevant in Western Countries [2-4]. More specifically, 8-40% of PSC patients eventually develop CCA in their lifetime, and this usually occurs at a younger age (30-50 years) compared to the general population (60-70 years) [15]. Interestingly, the burden of viral hepatitis C has been even claimed to partly account for the increasing incidence of iCCA in Europe and United States [2]. Other major risk factors for CCA are metabolic syndrome and congenital malformations of the bile ducts (e.g., Caroli's disease, choledochal cysts) [2-4].

1.4 Molecular pathogenesis

The molecular pathogenesis of CCA is a complex, multistep process relying on genomic (point mutations, copy number variations, chromosome fusions) and epigenetic (promoter hypermethylation, histone deacetylation) alterations, as well as on non-genetically

determined signaling pathway deregulations [3,8]. In this regard, chronic inflammation of the biliary tract is unanimously recognized as a paramount force behind the neoplastic transformation, regardless of etiology. Indeed, a persistent inflammatory state is capable of generating a pro-carcinogenic microenvironment abnormally enriched with cytokines and growth factors, which are broadly released by both inflammatory and epithelial cells. On the one hand, pro-inflammatory cytokines elicit DNA damage by fueling the generation of nitric oxide, ultimately leading to an increased mutation rate. On the other hand, the wide web of local inflammatory cues directly prompts cholangiocytes to undertake a sustained proliferative program, generally coupled with apoptosis evasion. Of note, the acceleration of the cell cycle, along with the impossibility of eliminating dysfunctional cells by programmed cell death, further supports the accumulation of somatic mutations potentially conducive to neoplastic growth [5,22]. In addition, chronic inflammation is typically comorbid with cholestasis, which for its part, dangerously promotes cholangiocyte turnover in this hectic microenvironment, again increasing the risk of malignant transformation (Figure 4) [3,22].

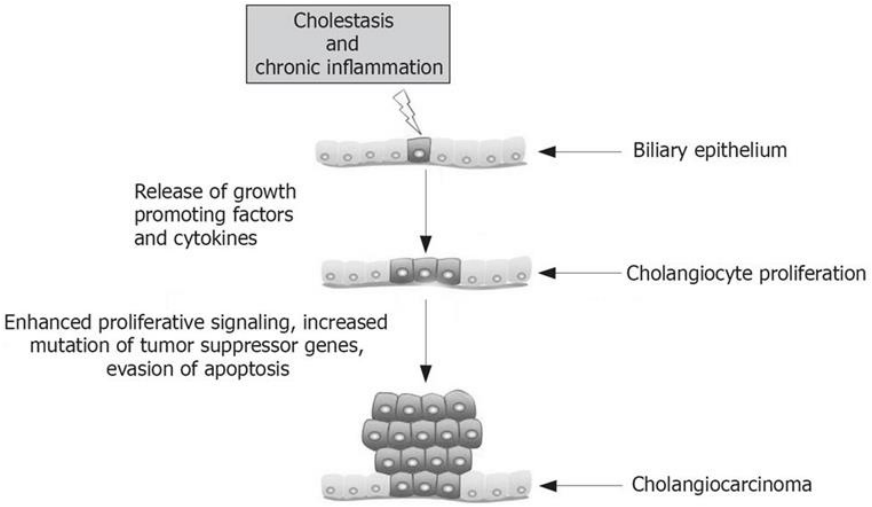

Figure 4 Cellular mechanisms driving cholangiocarcinogenesis. Chronic inflammation of the biliary tract, coupled with sever obstruction of bile flow, may trigger the pathogenesis of cholangiocarcinoma, both by directly fostering the unrestrained growth of the biliary epithelium, and by leading to nitric oxide-mediated DNA damage. Modified from [22].

1.4.1 Deregulated signaling pathways

Among cytokines promoting cholangiocarcinogenesis, interleukin (IL)-6, a well-known biliary mitogen, is recognized to play a key role. IL-6 is constitutively expressed by both normal and neoplastic cholangiocytes, and its secretion can be further enhanced by inflammatory mediators such as IL-1β and tumor necrosis factor (TNF)-α [23]. At the mechanistic level, IL-6 markedly promotes CCA cell survival by up-regulating the anti-apoptotic protein myeloid cell leukemia (Mcl)-1, via activation of signal transducer and activator of transcription (STAT)3, phosphatidylinositol-3 kinase (PI3K), and p38 mitogen-activated protein kinase (MAPK) pathways [24-26].

Mitogenic effects of IL-6 on CCA cells are also reported, and mainly rely on p44/p42 (also known as extracellular signal-regulated kinase (ERK)1/2) and p38 MAPK activation [23]. Importantly, in mice with genetically primed biliary tract, the pro-inflammatory cytokine IL-33 was shown to greatly facilitate CCA development by promoting IL-6 expression, further validating the intimate relationship between chronic inflammation and biliary carcinogenesis [27].

Deregulation of growth factor signaling also represents a major pro-tumorigenic mechanism in CCA. In particular, epidermal growth factor receptor (EGFR) (also called ErbB1 or HER1), ErbB2/HER2, and MET pathways, which generally involve the activation of MAPKs, are deeply connected to the acquisition of malignant traits by biliary epithelial cells, as a result of sustained ligand stimulation, receptor overexpression or inactivation of negative feedback mechanisms. Classically, constitutive activation of these signaling cascades exerts potent mitogenic effects on the biliary epithelium, ultimately encouraging tumor outgrowth in an autocrine fashion [7,12]. For instance, EGFR and ErbB2 are potent inducers of cyclooxygenase (COX)-2 expression, which fosters CCA growth by favoring uncontrolled proliferation and evasion of apoptosis [4]. Of note, COX-2 up-regulation may also be induced by inflammatory cytokine (e.g., TNF-α), bile acids, nitrosative stress, and oxysterols (i.e., cholesterol oxidation products) [5].

Notch and Hedgehog (Hh) signaling are evolutionarily conserved morphogen pathways fulfilling essential roles in both liver morphogenesis and liver regeneration following chronic injury. Therefore, it is not surprising that the aberrant activation of both pathways has been widely related to cholangiocarcinogenesis [2]. In particular, studies in mice have shown that a persistent hepatic Notch1 activation contributed to the development of CCA, based on an abnormal transdifferentiation of normal adult hepatocytes into neoplastic cholangiocytes [28,29]. Of note, inducible NO synthase (iNOS) was reported to substantially promote Notch1 expression in murine cholangiocytes via production of NO [30]. Similarly, the pharmacological inhibition of autocrine Hh signaling dramatically impaired CCA cell viability, both *in vitro* and in xenograft mouse models, arguing for a leading role of this pathway in the emergence of malignant growth features [31]. The molecular mechanisms underlying Hh overactivation have yet to be elucidated, though the accumulation of oxysterols in bile has been suggested to play a role [32].

Cholangiocytes, especially those lining the intrahepatic portion of the biliary tree, are potentially able to secrete and respond to a wide range of neuropeptides and hormones, since they classically adopt a neuroendocrine-like phenotype in the course of chronic liver injury [5,33]. In this regard, several endocrine factors have been claimed to boost the neoplastic transformation of biliary epithelial cells, either by

chronically fueling proliferation or by preventing apoptosis. For instance, malignant cholangiocytes up-regulate estrogen receptor (ER)α, whose stimulation actually results in enhanced cell growth, as well as in increased expression of IL-6 and vascular endothelial growth factor (VEGF), both critical mediators of CCA biology. Moreover, a relevant role in promoting CCA cell proliferation has also been attributed to dopamine, serotonin, histamine, and leptin [2].

1.4.2 Genetic and epigenetic abnormalities

Somatic mutations in well-known proto-oncogenes (e.g., *KRAS*, *FGFR2*, *EGFR*, *ERBB2*, *MET*, *IDH1/2*) or tumor suppressor genes (e.g., *TP53*, *SMAD4*, *ARID1A*, *PBRM1*, *BAP1*) have been widely documented in CCA [34,35]. Importantly, the pattern of oncogenic mutations in CCA is heavily influenced by both etiology and tumor anatomical location [2,4,35]. For instance, *TP53* mutations are more frequent in liver fluke-related CCAs compared with non-infection-related tumors, whereas *IDH1/2* and *BAP1* mutations generally show an opposite trend [36]. Regarding the anatomic subtype, *FGFR2*, *MET*, *IDH1/2*, *ARID1A*, *PBRM1*, and *BAP1* mutations are characteristic of iCCA, whereas *KRAS* and *ERBB2* mutations are more common in eCCA [34,35].

Activating mutations in *KRAS*, as well as loss-of-function mutations in *TP53* are frequent events in cancer, and CCA is no exception, with mutation frequencies of 9-40% and 3-45%, respectively [34]. Specifically, KRAS belongs to the small GTPase

superfamily, and actively regulates several cellular processes such as proliferation, survival, and motility, through the activation of its downstream effectors, including p44/42 MAPK and PI3K/Akt/mammalian target of rapamycin (mTOR) pathways [35]. p53 is deeply involved in cellular stress responses, by acting as a transcription factor to regulate cell cycle arrest, DNA repair and apoptosis. Loss of p53 activity paves the way for an uncontrolled proliferation of damaged cells, ultimately favoring tumorigenesis. In addition, alterations in p53 expression may lead to an aberrant accumulation of β-catenin, a signaling molecule that modulates the expression of several oncogenic genes [3,37,38]. Unlike *KRAS* and *TP53* point mutations, which are widespread genetic abnormalities, chromosomal translocations involving the *FGFR2* gene are almost exclusively found in CCA, thus representing a potential diagnostic marker [2]. Fibroblast growth factor receptor (FGFR)2 is tyrosine kinase protein acting as a receptor for various FGFs, which are well-known regulators of mitogenesis and differentiation [39]. Typically, FGFR2 fusion proteins undergo an enforced, ligand-independent dimerization, which is eventually responsible for an unrestrained activation of the FGFR2 kinase domain [8]. Still on the subject of receptor kinase signaling, a decreased expression of SMAD4, a common signal transducer of transforming growth factor (TGF)-β pathway, is frequently found in CCA, and undermines the tumor

suppressor functions typically exerted by TGF-β during early stages of carcinogenesis [4,40].

Interestingly, several recurrently mutated genes in CCA (e.g., *IDH1/2*, *ARID1A*, *PBRM1*, *BAP1*) directly or indirectly impinge on epigenetic dynamics and chromatin architecture, thereby deeply influencing the transcriptomic profile of cancer cells [3]. For instance, mutant forms of isocitrate dehydrogenases (IDH)1 and 2 drive the production of 2-hydroxyglutarate, an oncometabolite that elicits aberrant epigenetic changes by impairing the function of multiple enzymes involved in histone and DNA methylation [3,8,35]. Specifically, it was shown that mutant IDH1/2 could contribute to the pathogenesis of HPC-derived iCCA by epigenetically blunting the expression of hepatocyte nuclear factor 4α, a master regulator of hepatocytic differentiation [41]. Regardless of the underlying cause, epigenetic silencing via promoter hypermethylation has been frequently described in CCA, involving well-known tumor suppressor genes such as *SOCS3*, *CDKN2A*, *APC*, and *RASSF1* [7,8]. In particular, reduced expression of suppressor of cytokine signaling (SOCS)3 partially accounts for the aberrant activation of IL-6 signaling typically observed in CCA, as it acts as a negative-feedback regulator of the Janus kinases/STAT3 axis [42]. In contrast to *IDH1/2* gene, *ARID1A*, *PBRM1*, and *BAP1* genes are classically endowed with tumor suppressive functions, and frequently harbor inactivating mutations in CCA patients [43]. In particular, AT-rich interaction domain (ARID)1A and

polybromo (PBRM)1 are subunits of the switch/sucrose non-fermentable chromatin-remodeling complex, which finely regulates gene transcription by mobilizing nucleosomes [44], while BRCA1 associated protein (BAP)1 is a nuclear deubiquitylating enzyme, capable of altering chromatin architecture by modulating the ubiquitylated status of histone 2A [45].

1.5 Management

As previously mentioned, the prognosis of CCA is still very grim, basically due to the late diagnosis and the lack of effective therapeutic strategies [22]. Indeed, CCA is difficult to detect and diagnose early, since it remains clinically silent until advanced stages, when it finally presents with non-specific symptoms such as painless jaundice (eCCA), weight loss or abdominal pain (iCCA) [3,4]. Therefore, most of patients are diagnosed when metastatic dissemination has already occurred [2]. In fact, CCA is an highly invasive cancer, which tends to spread along the duct walls, and pervasively infiltrate the adjacent structures (branches of the portal vein, lymphatic vessels, nerve fibers), thereby spawning metastases within the liver, at regional lymph nodes, or at distant sites (notably, lungs or peritoneum) (Figure 5) [5,46]. Diagnosis of CCA frequently occurs as an incidental finding, and is classically based on a combination of clinical data, non-specific (biochemical and/or histological) biomarkers, and imaging modalities [2]. Surgical resection by partial hepatectomy and orthotopic liver

transplantation are the only treatments with curative intent, but their applicability is limited to early-stage disease [2]. Accordingly, only 30% of CCA patients are actually eligible for radical surgery [3]. Moreover, chances of recurrence after resection are still very high (49-64%), ultimately resulting in discouraging outcomes, with a 5-year survival after resection lower than 45% [2,12]. Although liver transplantation was initially hailed as a promising therapy for unresectable tumors without evidence of metastasis, its actual reliability remains controversial. Indeed, encouraging results were obtained only in highly specialized centers implementing stringent patient selection criteria, whereas historically, liver transplant is in turn associated with high recurrence rates and poor long-term survival [2,12]. CCA patients who are not candidate for surgical therapy have no other chance but palliative procedures, which, by definition, are merely aimed at turning the tumor into a clinically manageable chronic disease and improving the quality of life [4]. The median survival of patients diagnosed at inoperative stage is 6-12 months, with a 5-year overall survival of 5% [4,5,8]. Systemic chemotherapy with gemcitabine plus cisplatin currently represents the standard of practice in the palliative setting, though pledging a median overall survival of only 11.7 months [2,47]. In fact, CCA is characterized by a remarkable resistance to conventional chemotherapeutic agents, directly resulting from the intrinsic ability of CCA cells to efficiently escape from drug-induced cytotoxicity [5,48].

Unfortunately, there are still no targeted molecular therapies approved for the treatment of CCA, likely owing to the poor knowledge on the molecular mechanisms driving its development and progression [35].

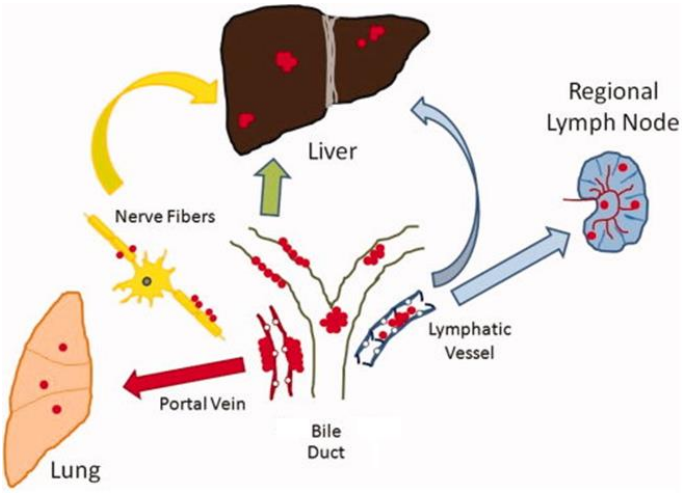

Figure 5 Metastatic patterns of cholangiocarcinoma. Cholangiocarcinoma is characterized by a highly invasive behavior. Lymphatic vessels, nerve fibers, and branches of the portal vein offer CCA cells multiple routes to escape from the primary site of growth. Moreover, the periductal wall may be directly invaded by tumoral infiltrates. Early metastases are more common within the liver and at regional lymph nodes rather than at distant sites (notably, lung or peritoneum). Adapted from [46].

2. The tumor reactive stroma

Normal tissues encompass two distinct but interdependent compartments, namely the parenchyma, which accounts for the specific tissue function, and the stroma, which provides a multifaceted support for the parenchyma, and predominantly consists of

extracellular matrix (ECM) proteins (notably, type I collagen and fibronectin), resting fibroblasts, a few resident leukocytes, and vascular elements. The structure of solid tumors is roughly similar, with the parenchymal component being represented by the malignant cells themselves [49,50]. However, in sharp contrast to a normal stroma, which typically contains a small amount of quiescent fibroblasts embedded within a physiological ECM, the tumor stroma is characterized by a large number of activated fibroblasts, an abnormally rich inflammatory infiltrate, and an enhanced capillary density. By undergoing activation, fibroblasts not only increase their proliferative activity, but also secrete starkly higher amounts of ECM components (e.g., fibrillar collagens, fibronectin, tenascin C, and proteoglycans), thereby generating a highly desmoplastic microenvironment that is reminiscent of organ fibrosis [51]. Of note, in human cancers, the stromal compartment can represent up to 90% of the total mass [52]. However, its relative amount is highly variable among tumors, and does not necessarily correlate with the degree of malignancy [49].

In 1986, Harold F. Dvorak first called attention to the similarities existing between the generation of tumor stroma and wound healing [52]. Indeed, both processes are initially triggered by an increased microvascular permeability, which enables a massive extravasation of plasma proteins such as fibrinogen, plasminogen, and fibronectin, ultimately resulting in the deposition of an extravascular

clot of cross-linked fibrin enriched with fibronectin. This bulk of fibrin acts as a promiscuous substrate supporting the migration of inflammatory cells (mainly macrophages), endothelial cells, and fibroblasts, which in the tumoral context, are powerfully recruited and activated by a plethora of cancer cell-derived soluble factors. A broad synthesis of matrix components, coupled with extensive angiogenesis, then leads to a gradual transformation of the original fibrin-fibronectin gel matrix into a collagenous and vascularized stroma, which in wound healing, is usually referred to as granulation tissue. Upon further deposition of interstitial collagens, the fibrin clot is little by little degraded, new vessels are partially resorbed, and the number of activated fibroblasts markedly decreases, thus giving rise to a poorly vascularized, densely collagenous, and nearly acellular connective tissue. However, unlike physiological wound healing, which is a self-limiting process, the remodeling of tumor stroma is continuously evolving, since in tumors, the molecular cues that classically evoke the wound healing cascade are released in an unrestrained manner, which led Dvorak to describe neoplastic lesions as “wounds that do not heal”. As a result, the tumor core is typically associated with a scar tissue-like stroma, whereas cancer cells located at the invasive front are generally encased within a highly cellular stroma mimicking the active stages of wound healing. Among the mediators of tumor stroma generation, VEGF is suggested to play a paramount role, since it is constitutively expressed at high levels by the vast majority of human neoplasms, and

may potentially account for both chronic vascular hyperpermeability and tumor angiogenesis. Of note, besides being secreted by cancer cells, VEGF can also be plentifully produced by macrophages and fibroblast populating the tumor microenvironment [50-52].

In summary, by behaving like self-perpetuating wounds, tumors can effectively hijack a physiological host process, in an effort to build up a personalized microenvironment that may adequately satisfy their high metabolic needs, and actively support their malignant growth [50,53,54]. Indeed, a dense, mutual paracrine communication typically takes place between cancer and stromal cells, giving rise to a hectic microenvironment that is increasingly recognized as a key determinant of tumor progression. As mentioned above, neoplastic cells act as leading actors in the remodeling of the neighboring stroma, by chronically recruiting, activating, and co-opting several inflammatory and mesenchymal cell types. Stromal cells, for their side, secrete a plethora of cyto/chemokines, growth factors, and proteinases that directly foster the emergence of malignant phenotypes, and/or contribute to the recruitment and aberrant activation of additional stromal components [55,56]. Furthermore, intratumoral hypoxia and aberrant changes in the ECM may further impinge on cancer cell behavior [57]. Interestingly, a growing body of evidence suggests that oncogenic signals emanating from the TRS may even modify the epigenome of cancer cells [58-60]. In the light of the above, it is clear that the naïve stroma represents a

highly plastic and dynamic compartment that is prone to pandering to the neoplastic evolution of the adjacent parenchyma, thereby undergoing a change from gatekeeper of tissue homeostasis to pathological niche fueling cancer aggressiveness [61,62]. Therefore, the complex milieu harboring tumor growth is currently termed as "tumor reactive stroma" (TRS). It is worth noting that normal epithelia, as well as early-stage carcinomas, are surrounded by a well-delineated basement membrane that effectively separates epithelial cells from the adjoining connective tissue. Although there is evidence that a primal tumor-stroma crosstalk still occurs despite the presence of an intact (but altered) basal lamina, reactive stromal cells are empowered to fully exert their pro-neoplastic effects only upon basement membrane degradation, which represents one of the first steps of the invasion-metastasis cascade (Figure 6) [51,63].

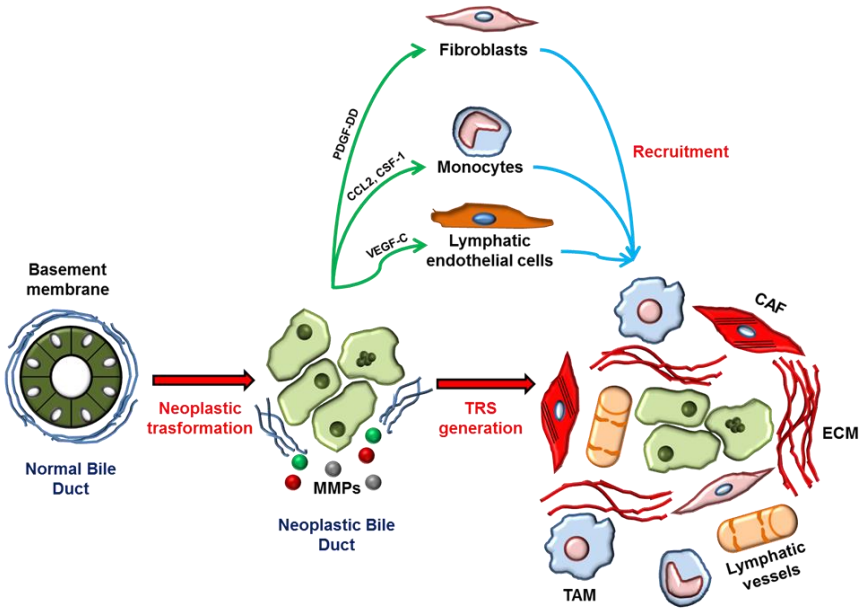

Figure 6 Cellular and molecular mechanisms underlying the generation of the tumor reactive stroma in cholangiocarcinoma. Upon neoplastic transformation, cholangiocytes acquire the ability to broadly secrete a rich repertoire of cyto/chemokines and growth factors that enable them to establish an intense crosstalk with various cell types (e.g., portal fibroblasts, hepatic stellate cells, inflammatory cells, endothelial cells). Moreover, the basement membrane is progressively dismantled through the massive release of matrix metalloproteinases (MMPs), further supporting the interplay between the neoplastic epithelium and its stromal microenvironment. It is against this background that multiple mesenchymal and inflammatory cells are plentifully recruited to the tumor mass through paracrine signals chronically released by malignant cholangiocytes. For instance, platelet-derived growth factor (PDGF)-DD triggers the chemotaxis of resident fibroblasts, C-C motif chemokine ligand (CCL)2 and colony stimulating factor (CSF)-1 dictate the monocyte homing from blood circulation, and vascular endothelial growth factor (VEGF)-C orchestrates lymphangiogenesis by stimulating the proliferation and migration of lymphatic endothelial cells. Under the influence of the tumor microenvironment, fibroblasts and monocytes transdifferentiate into cancer-associated fibroblasts (CAFs) and tumor-associated macrophages (TAMs), respectively, and then foster tumor aggressiveness in a paracrine fashion (see text for further details). Importantly, cholangiocarcinoma cells, CAFs, and TAMs all

contribute to the aberrant remodeling of the extracellular matrix (ECM), an additional mechanism supporting cancer progression. Modified from [53].

2.1 The pathological relevance of the tumor reactive stroma in cholangiocarcinoma

In CCA, as well as in other epithelial tumors with strong invasiveness, such as breast and pancreatic carcinomas, the stromal compartment is particularly prominent, thus representing a histological hallmark (Figure 7). More importantly, it is now a fact that the TRS hugely promotes CCA growth and dissemination, which is why it is drawing a growing interest as a potential therapeutic target [55,56]. Interestingly, it was shown that the genomic profile of CCA-associated stroma markedly differed from that of fibrous tissue from peritumoral areas. Furthermore, specific genetic changes in the tumor stroma were found to correlate with clinicopathological variables predictive of bad prognosis. Of note, most of the differentially expressed genes were involved in cell metabolism, cell cycle progression, ECM composition, and intracellular signaling [64]. In line with these findings, a genome-wide transcriptome profiling of tumor epithelium and stroma from resected CCAs revealed a stromal gene signature significantly associated with poor prognosis. In particular, the stromal compartment was markedly enriched with inflammatory cyto/chemokines, including IL-6, IL-33, TGF-β3, and C-C motif chemokine ligand (CCL)2 (also called monocyte chemoattractant protein (MCP)-1) [65]. Overall, these studies highlight not only the

uniqueness of the TRS as a biological entity, but also the prognostic relevance of the molecular aberrations underlying its pathological remodeling. In the next paragraphs, we will discuss in detail the characteristics of the main (cellular and non-cellular) components of the TRS, particularly focusing on how they are supposed to elicit the emergence of malignant phenotypes in CCA cells.

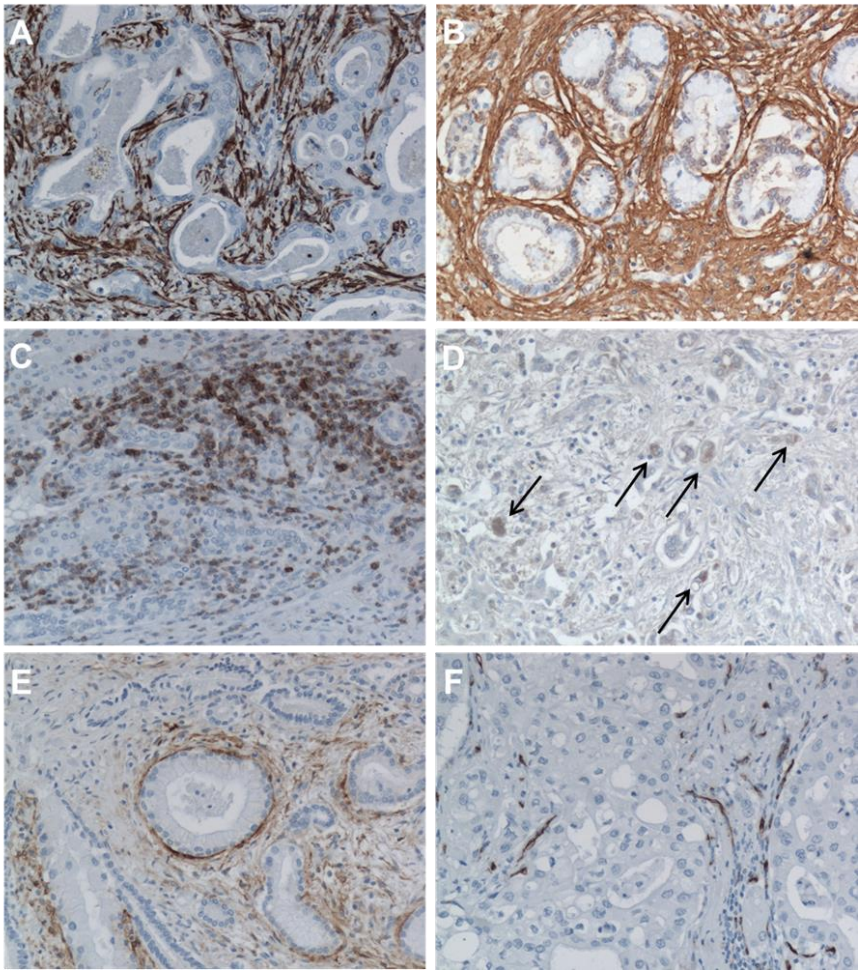

Figure 7 Phenotyping the tumor reactive stroma in cholangiocarcinoma. Immunohistochemistry of multiple markers to characterize the main cellular and structural components of the tumor reactive stroma in intrahepatic cholangiocarcinoma. Cancer-associated fibroblasts (α-SMA) (A); extracellular matrix (fibronectin) (B); inflammatory cells (CD45) (C); tumor-associated macrophages (arrows) (CD206) (D); lymphatic endothelial cells (podoplanin) (E); vascular endothelial cells (CD34) (F). Original magnification: 200x. Modified from [53].

2.2 Cancer-associated fibroblasts

Cancer-associated fibroblasts (CAFs) are perpetually activated fibroblasts, phenotypically characterized by the expression of vimentin, S100A4 (otherwise called fibroblast-specific protein 1), fibroblast activation protein (FAP), and especially, α-smooth muscle actin (α-SMA), a widely recognized hallmark of fibroblast activation [66,67]. Gene expression profiling of CAFs from CCA specimens unveiled thousands of differentially expressed genes compared to fibroblasts from matched peritumoral tissue, with the majority of them being involved in cellular metabolism [68]. Indeed, CAFs feature a high proliferation rate, and are deeply engaged in the remodeling of tumor-associated ECM, due to the enhanced production of both matrix components (e.g., collagen type I, fibronectin, tenascin C) and matrix-degrading enzymes. Furthermore, CAFs are capable of secreting a rich repertoire of cyto/chemokines and growth factors, which mediate the crosstalk with cancer, endothelial and inflammatory cells [49,51]. For instance, CAF-derived CCL2 effectively triggers macrophage recruitment to the tumor neighborhood [53,69], whereas the broad

secretion of VEGF accounts for the ability of CAFs to sustain tumor-associated angiogenesis and lymphangiogenesis [70]. Hepatic stellate cells (HSCs) and portal fibroblasts are the main precursors of CAFs, with a minor contribution by bone marrow-derived mesenchymal stem cells (MSCs) [71]. Interestingly, conditioned medium from CCA cells was found to foster the activation of HSCs [72] and primary liver myofibroblasts [73], as well as to induce the differentiation of MSCs into myofibroblast-like cells [74], further confirming that cancer cells are largely responsible for the generation of CAFs. In particular, among the pro-fibrotic factors driving the recruitment and/or activation of fibroblasts within the tumor microenvironment, TGF-β, FGF, and platelet-derived growth factor (PDGF), which may be released by both cancer and inflammatory cells, have been widely reported to play a prominent role [51,57,75]. In this regard, our group has recently unveiled that PDGF-DD, which is aplenty released by CCA cells under severe hypoxia, can massively promote the migration of fibroblasts towards the tumor mass, by activating the small Rho GTPases Rac1 and Cdc42, as well as the c-Jun N-terminal kinases (JNK) pathway, through PDGFRβ binding [75].

Co-culture and conditioned medium experiments clearly demonstrated that both CAFs and their precursors (i.e., HSCs) are able to provide CCA cells with enhanced proliferative, survival, and migratory capabilities, *in vitro* [67,72,76-82]. Furthermore, co-transplantation of CCA cells with hepatic myofibroblasts [73] or HSCs

[72] into the flank of nude mice markedly boosted the growth of CCA xenografts. Similarly, the selective depletion of CAFs by navitoclax in a syngeneic, orthotopic rat model of CCA dramatically impaired tumor burden and metastasis, while improving host survival [83]. Overall, these studies argue for a tumor-promoting role of CAFs in CCA, which is further validated by the finding that α-SMA expression proved to be an independent negative prognostic factor for survival in iCCA patients [77]. In particular, various soluble factors have been shown to mediate the pro-neoplastic effects of CAFs, including C-X-C motif chemokine ligand (CXCL)12 (also named stromal cell-derived factor (SDF)-1), heparin-binding epidermal growth factor (HB-EGF), and PDGF-BB. For instance, both CXCL12 [78] and PDGF-BB [81,82] strongly encourage apoptosis resistance in CCA cells, by up-regulating the anti-apoptotic protein B-cell lymphoma (Bcl)-2, and activating the Hh signaling, respectively. CXCL12 also promotes CCA cell invasiveness, through activation of ERK1/2 and PI3K pathways [78,79]. The migratory and invasive properties of neoplastic cholangiocytes are also enhanced by HB-EGF, which binds to EGFR on the cancer cell surface, and thus starts a transcriptional program that involves ERK1/2, STAT3 and β-catenin [73]. It is worth noting that CCA cells and CAFs are engaged in an intricate network of reciprocal, self-perpetuating paracrine loops, which well exemplify the ability of cancer cells to tirelessly shape the behavior of their stromal neighbors. For instance, the expression of HB-EGF by CAFs can be induced by CCA cell-derived TGF-β1, whose

production is in turn sustained by HB-EGF in a paracrine fashion [73]. Similarly, studies in rats showed that CCA cells lead CAFs to massively secrete hepatocyte growth factor (HGF), which in turn can up-regulate C-X-C motif chemokine receptor (CXCR)4 (the cognate receptor for CXCL12) on the surface of CCA cells, thus making them hyper-responsive to CAF-derived CXCL12 [84].

2.3 Tumor-associated macrophages

In contrast to other immune cell types that populate the tumor microenvironment and overall preserve tumor-suppressive functions (e.g., natural killer cells), macrophages are mostly "corrupted" by the tumor compartment, which prompts their differentiation towards the so-called M2 (or alternatively activated) phenotype through a number of paracrine signals, including colony stimulating factor (CSF)-1, IL-4, IL-10, IL-13, and TGF-β [49,71,85]. In CCA, bulk tumor cells [86], CAFs [87], and regulatory T cells [86] have all been reported to contribute to the M2 polarization of recruited macrophages. Unlike M1 (or classically activated) macrophages, which massively produce pro-inflammatory cytokines (e.g., TNF-α, IL-12), prime tissue destruction, and possess strong microbicidal and tumoricidal activities, M2 macrophages preferentially express anti-inflammatory cytokines (e.g., IL-10), down-regulate major histocompatibility complex molecules, and promote tissue remodeling and tumor progression [85,88]. Whilst tumor-associated macrophages (TAMs) are classically identified as M2

macrophages, it is worth considering that the boundary between the M1 and M2 activation states is quite blurred. In fact, macrophages feature a considerable degree of plasticity, and actually go through a wide spectrum of highly changing phenotypes [88]. Therefore, it is not surprising that the tumor-promoting functions of TAMs frequently rely on ‘‘M1 cytokines”, such as IL-6 and TNF-α [85]. Furthermore, in CCA, Raggi et al. identified a peculiar subset of TAMs that is directly molded by cancer stem cells (CSCs), and is characterized by a mixed expression of M1 and M2 markers. Interestingly, CSC-associated TAMs exhibit pronounced adhesive and invasive properties, as well as a heightened expression of matrix-remodeling-related genes (e.g., *ADAM17*, *MMP2*), suggesting a critical role in ECM reorganization [89]. Importantly, TAM accumulation within the TRS mainly results from the recruitment of blood monocytes (notably, $CD14^+/CD16^+$ monocytes) by tumor- or CAF-derived chemoattractants (e.g., CCL2, CSF-1/2/3, VEGF), rather than from the *in situ* proliferation of resident ($CD68^+$) macrophages [49,90-92].

Similar to CAFs, TAMs are believed to play a critical part in CCA progression. Indeed, high tumor infiltration by M2 ($CD163^+$) macrophages was found to correlate with poor disease-free survival of CCA patients [86]. Furthermore, in CCA tissue, the density of M2 TAMs is greatest at the tumor front, and positively correlated with tumor pathological grade [89], and the development of extrahepatic metastases [93]. In line with the immunohistochemical data, the

selective depletion of macrophages by liposomal clodronate in rodent models of CCA strikingly decreased tumor burden [94]. In particular, TAMs have been suggested to foster CCA growth by sustaining the chronic activation of the Wnt/β-catenin signaling in cancer cells, through the release of Wnt ligands [94,95]. In fact, the canonical Wnt pathway is able to promote the unrestrained proliferation of neoplastic cholangiocytes by up-regulating a number of cell cycle-related genes [94,96]. In addition, macrophages may paracrinally contribute to the aberrant activation of the IL-6/STAT3 axis frequently observed in CCA cells [97,98], a fundamental mechanism underlying their heightened survival abilities [24]. TAMs are also likely to mediate cancer invasion, by both directly impinging on cancer cell behavior, and shaping the tumor microenvironment. For instance, TAMs are the primary source of TNF-α [99], which has been shown to provide CCA cells with increased migratory functions by activating transcription factors Snail and ZEB2 [97,100,101]. Consistently, conditioned medium from M2 macrophages was found to foster CCA cell motility, *in vitro* [93]. On the other hand, in several epithelial cancers, including CCA, TAMs aplenty produce various MMPs, most notably MMP-9 [102], thereby aiding tumor cells in degrading the surrounding ECM, a process of utmost importance for local invasion [103]. Finally, a variety of pro-angiogenic and/or pro-lymphangiogenic factors, such as VEGF, FGF-2, and angiopoietin 1, are typically released by TAMs, which thus promote the generation of a microenvironment conducive to

metastatic dissemination [49,88]. Indeed, in CCA samples, the number of M2 macrophages was directly associated with microvascular density [86].

2.4 Lymphatic endothelial cells

In CCA, tumor-associated angiogenesis and lymphangiogenesis are both markedly induced, and were found to confer a significant survival disadvantage on patients [104-106]. However, the formation of new blood vessels within the tumor mass is generally not as striking as the expansion of the lymphatic vasculature, which actually represents the preferential route for CCA cells to escape from the primary site of growth [53]. In this regard, immunohistochemical staining of resected iCCAs and eCCAs for the lymphatic vessel marker D2-40 (otherwise named podoplanin) revealed that a high lymphatic microvessel density correlated with lymph node involvement [104,106]. Importantly, lymph node metastasis is a well-known negative prognostic factor for the survival of patients with CCA [107-110]. The lymphatic capillaries, also called initial lymphatics, are physiologically responsible for the continuous uptake of the interstitial fluids, and their structure is particularly suitable for the intravasation of metastasizing cancer cells. Indeed, they are only composed of a monolayer of lymphatic endothelial cells (LECs), joined together by weak cell-cell junctions, and surrounded by a discontinuous basement membrane. However, the caliber of the initial

lymphatics gradually increases to form the pre-collecting lymphatics first, and then the collecting lymphatics, which are lined by an intact basal lamina, and contain both smooth muscle cells in their walls, and intraluminal valves regulating the fluid flow. During the transit from the collecting lymphatics to the thoracic duct, the fluid goes through the regional lymph nodes, where metastasizing cancer cells can reside before disseminating to distant organs [92,111].

Tumor-associated lymphangiogenesis essentially consists in the formation of new lymphatic vessels arising from pre-existing lymphatic capillaries, through the proliferation and migration of LECs. However, both the recruitment of bone marrow-derived endothelial progenitor cells, and the transdifferentiation of mature blood endothelial cells have been suggested to play a role in this context, though providing a minor contribution. Overexpression of the archetypical lymphangiogenic factor VEGF-C by cancer and reactive stromal cells is widely recognized as the main driver of neo-lymphangiogenesis. Indeed, VEGFR-3, the cognate receptor for VEGF-C, is selectively and highly expressed by LECs, and the maintenance of the VEGF-C/VEGFR-3 signaling is of crucial importance for the expansion of the lymphatic vasculature network in the embryo [92,112]. In CCA, a high expression of VEGF-C was shown to correlate with lymph node metastasis, and was also reported as an independent prognostic factor for the survival of patients [113-115]. Additional VEGF family members, namely VEGF-A and VEGF-D, are also claimed

to participate in tumor-associated lymphangiogenesis, even though they are just ancillary mediators of embryonic lymphatic vessel development [92,112]. Of note, VEGF-C and VEGF-D selectively bind to VEGFR-2 and VEGFR-3, whereas VEGF-A selectively binds to VEGFR-1 and VEGFR-2. Unlike VEGFR-3, VEGFR-2 is primarily expressed by vascular endothelial cells, where it acts as a positive modulator of angiogenesis [116]. Nevertheless, critical functions for VEGFR-2 in the lymphatic biology are emerging, and VEGFR-2 overexpression on tumor-associated LECs has been described [117]. In addition to VEGF ligands, other well-recognized tumor lymphangiogenic growth factors include angiopoietins 1 and 2 (i.e., growth factors classically involved in lymphatic remodeling and maturation), PDGF-BB, and FGF-2 [92,112].

Besides being involved in lymphangiogenesis, the initial lymphatics may also be driven by cancer cell-derived factors (notably, VEGF-C) to undergo a substantial enlargement, which is mediated by the proliferation of LECs, and ultimately increases the interface for lymphatic invasion by cancer cells. Enlargement of the collecting lymphatics has also been reported, and likely results in an increased lymph flow that further supports the metastatic dissemination. Of further interest, VEGF-C is capable of altering the structure of pre-existing and/or newly formed vessels by inducing the formation of intercellular gaps, which can be deleteriously exploited by metastasizing cancer cells. It is finally worth noting that LECs are not

only passively "educated" by cancer cells to build up a pro-metastatic lymphatic network, but also actively promote the intravasation of tumor cells by generating a chemoattracting gradient. Indeed, they broadly release endogenous chemokines, such as CCL21 and CXCL12, whose cognate receptors are generally located on the surface of cancer cells [92,112].

2.5 Non-cellular components of the tumor reactive stroma

2.5.1 The extracellular matrix

The so-called ECM encompasses the interstitial connective tissue matrix, and the basement membrane (or basal lamina). The interstitial matrix is a three-dimensional network of collagens (especially, type I collagen), proteoglycans, and glycoproteins (e.g., fibronectin, tenascin C, elastin), which fills the intercellular spaces, and constitutes a structural scaffold for the tissue. Specifically, collagen bundles confer tensile strength upon the whole tissue, while proteoglycans mostly perform hydration functions. On the other hand, the basement membrane is a specialized, sheet-like type of ECM, interposed between the epithelium and the stroma, and mainly composed of type IV collagen and laminin. Importantly, the ECM not only provides a physical support to cells, but also actively impinges on their behavior by communicating with them. Indeed, several ECM constituents, especially glycoproteins, may act as ligands for cell

surface receptors such as integrins. Furthermore, both proteoglycans and glycoproteins physically interact with a number of growth factors and cyto/chemokines, which are thus efficiently sequestered within the ECM, and may be subsequently locally unleashed through proteolytic cleavage. Therefore, it is not surprising that the extensive, dysregulated ECM remodeling that typically accompanies the emergence of neoplastic lesions has been widely reported to support cancer progression at multiple levels, including the induction of angiogenesis, the activation of stromal cells, and the direct promotion of cancer cell aggressiveness [49,51,118]. Throughout carcinogenesis, the ECM progressively becomes stiffer, due to type I collagen deposition and cross-linking, and concomitantly undergoes compositional changes, resulting from both the proteolytic activity of overexpressed MMPs, and the accumulation of newly synthesized glycoproteins [55]. Importantly, the unrestrained ECM breakdown by proteases leads to the generation of reactive ECM fragments endowed with unique signaling functions, which in turn may elicit specific biological responses [49,118]. In addition, ECM stiffening also profoundly affects cell behavior, by impinging on the activity of intracellular mechanosensors [55,118].

Similar to reactive stromal cells, the TRS-associated ECM has been shown to foster CCA aggressiveness. Indeed, CCA cells cultured on a mixture of collagen type IV and laminin demonstrated greater invasive abilities than cells grown on uncoated plates, an effect likely

mediated by the up-regulation of the actin-binding protein L-plastin [119]. Furthermore, in CCA tissue, increased stromal expression of certain non-structural ECM proteins, namely tenascin [120], periostin [68], and osteopontin [64], correlated with poor outcome and tendency to invade. In particular, the tumor-promoting functions of tenascin are suggested to rely on its binding to EGFR [120], while periostin was found to promote CCA cell invasiveness in a α5β1 integrin-dependent manner [68,121]. Of note, such ECM constituents are primarily produced by CAFs, though CCA cells themselves may represent an ancillary source [68,120,121].

2.5.2 Intratumoral hypoxia

In most of solid tumors, the unrestrained proliferation of neoplastic cells, and the concomitant formation of an inadequate and highly disorganized vascular bed, necessarily lead to the generation of a markedly hypoxic microenvironment. Nowadays, hypoxia is widely recognized as a critical tumor-promoting player, deeply involved in the emergence of the main hallmarks of tumor progression. In fact, malignant cells are able to deleteriously hijack the adaptive cellular responses to oxygen deprivation, which are physiologically aimed at enabling injured cells to survive, migrate towards less hypoxic regions, and orchestrate compensatory angiogenesis. Moreover, hypoxia represents a potent microenvironmental stressors, and thus exerts a selective pressure on cancer cells, ultimately resulting in the clonal

expansion of the most aggressive tumor phenotypes. Cellular responses to hypoxia are primarily mediated by the activation of the hypoxia-inducible factors (HIFs), i.e., helix-loop-helix transcription factors that bind to specific DNA sequences known as hypoxia-response elements. HIFs consist of an α (HIF-1α, HIF-2α, or HIF-3α) and a β (HIF-1β) subunit. Among HIF-α isoforms, HIF-1α is the best characterized, due to its ubiquitous expression. Under normoxic conditions, HIF-1α is continuously primed for proteasome-mediated degradation by prolyl hydroxylase domain-containing (PHD) enzymes, whereas in the absence of adequate oxygen levels, PHD enzymes are unable to properly hydroxylate HIF-1α, which can thus accumulate and translocate to the nucleus. Here, HIF-1α dimerizes with HIF-1β, which is constitutively expressed regardless of the oxygen concentration. The resulting heterodimer interacts with transcriptional co-activators, and regulates the expression of hundreds of genes involved in cell survival and motility, glucose metabolism, and angiogenesis [122-124].

In CCA tissue, HIF-1α is typically overexpressed compared with bile ducts of peritumoral areas [125,126], and its high expression was reported as an independent prognostic factor for overall and disease-free survival [127,128]. Consistently, *in vitro* studies clearly demonstrated that hypoxia-induced signaling leads CCA cells to gain a more malignant phenotype. For instance, low-oxygen culture conditions, as well as treatment with cobalt chloride (i.e., a chemical

inducer of HIF-1α), promoted a substantial increase in CCA cell motility and invasiveness [126,128,129]. Specifically, the pro-invasive effects of hypoxia were suggested to rely on the aberrant activation of the pro-oncogenic MET/ERK axis [126], as well as on the induction of autophagy [128], which is actually emerging as a key regulator of cell invasion in several carcinomas, including CCA [130]. Of further interest, hypoxia was found to boost the resistance of CCA cells to both radiation- and drug-induced cytotoxicity [131], an effect likely dependent on the up-regulation of the anti-apoptotic protein X-linked inhibitor of apoptosis (XIAP) at the translational level [132]. It is worth noting that, in sharp contrast to CCA cells, normal cholangiocytes proved to be highly sensitive to oxygen deprivation [131,132], further highlighting the ability of cancer cells to adapt to otherwise detrimental conditions. Despite this growing amount of evidence, the overall impact of hypoxia on CCA progression has yet to be fully understood. In this regard, it was shown that a reduced oxygen availability extensively impinged on the transcriptomic profile of neoplastic cholangiocytes, altering the expression of several genes involved in cancer cell invasion and apoptosis resistance (e.g., *TFF1*, *ADAM12*, *ITGA5*, *BIRC5*, *UMPS*, *S100P*) [131]. A hypoxic microenvironment could also endow CCA cells with heightened pro-angiogenic and/or pro-lymphangiogenic functions, since HIF-1α stabilization by cobalt chloride was shown to promote a massive up-regulation of VEGF [129]. Finally, HIF-1α accumulation could drive

genomic instability by directly triggering the expression of iNOS, which may indeed be responsible for NO-mediated DNA damage [125].

3. Molecular mechanisms underpinning cholangiocarcinoma progression: an overview

3.1 Molecular mechanisms of chemoresistance

As previously discussed, CCA cells are characterized by a substantial lack of sensitivity to drug-induced cytotoxicity, which accounts for the disappointing results of conventional chemotherapy [5]. The mechanisms of chemoresistance typically employed by CCA cells are redundant and multifaceted, and most of them are borrowed by normal cholangiocytes, which are required to chronically deal with toxic compounds from bile and blood, and are thus equipped with appropriate defense enzymatic activities [2,48]. A first strategy to circumvent drug toxicity consists in keeping at bay the intracellular drug concentration, either by restricting its uptake, through the down-regulation of solute carriers transporters (e.g., organic anion-transporting polypeptides, organic cation transporters, nucleoside transporters), or by encouraging its efflux, through the up-regulation of ATP-binding cassette (ABC) transporters (e.g., multidrug resistance protein 1 or P-glycoprotein, multidrug resistance-associated proteins (MRP)). Alternatively, CCA cells may selectively decrease the intracellular amount of the active drug metabolite, thanks to an

impaired expression (or activity) of the enzymes responsible for pro-drug activation, or to an enhanced expression (or activity) of the enzymes involved in the detoxification of the active compound [2]. For instance, glutathione S-transferase P1-1 is highly expressed in CCA cells, and promotes cellular resistance to various xenobiotics (e.g., adriamycin, cisplatin, melphalan, cyclophosphamide) by catalyzing their conjugation with reduced glutathione [133]. A large fraction of anti-cancer drugs are DNA-damaging agents; therefore, the optimization of DNA repair strategies also represents an efficient mechanisms of chemoresistance [2]. In this regard, in CCA cells, the up-regulation of uracil-DNA glycosylases, which initiates the base excision repair pathway, is likely to underlie the acquired resistance to 5-fluorouracil [134], whereas high expression of the p53-inducible ribonucleotide reductase subunit M2B, which supplies deoxyribonucleoside diphosphates throughout DNA repair, is associated with decreased sensitivity to gemcitabine [135]. Regardless of the nature of the primary cytotoxic insult, drug-induced cell death typically results from the activation of the apoptotic machinery. It is no accident that in CCA cells, the balance between anti-apoptotic and pro-apoptotic proteins is dramatically altered in favor of the former [2]. Anti-apoptotic factors that are frequently overexpressed or aberrantly activated in CCA include Mcl-1 [136], XIAP [137], and survivin [138]. Mcl-1 is a member of the Bcl-2 protein family, upon which the intrinsic apoptosis pathway is based. Specifically, Mcl-1 binds to the pro-

apoptotic member Bak, thereby preventing its oligomerization and activation. However, different intracellular stresses (e.g., trophic factor withdrawal, DNA damage) can lead to the activation of BH3-only proteins (e.g., Noxa, Bim, Puma), which effectively displace Bak by competitively interacting with Mcl-1. Once unleashed, Bak permeabilizes the outer mitochondrial membrane, thus allowing the release of cytochrome c, which eventually triggers the activation of the caspase cascade [139-141]. In this context, XIAP and survivin (also called BIRC5) counteract cell death by inhibiting caspase activity (notably, caspase-3, -7, and -9) [142]. Importantly, a defective activation of the extrinsic apoptosis pathway, which is triggered by the stimulation of cell surface death receptors (e.g., Fas receptor or CD95, death receptor (DR)4) by cognate ligands (e.g., Fas ligand, TNF-related apoptosis inducing ligand (TRAIL)), and in turn converges on caspase activation, is also believed to underpin CCA chemoresistance [48]. It is finally worth noting that, even where the drug cytotoxic mechanisms cannot be intrinsically neutralized, chemoresistance may still be acquired through an altered expression of molecular therapeutic targets. For instance, in CCA cells, a decreased expression of ERs, and an increased expression of thymidylate synthase can markedly hampered the therapeutic effectiveness of tamoxifen and 5-fluorouracil, respectively [2].

All these mechanisms of chemoresistance are fueled by microenvironmental signals originating from either cancer or reactive

stromal cells, which thus enable CCA cells to chronically avoid cell death [48]. In addition to the already mentioned anti-apoptotic effects of IL-6 and PDGF-BB, the aberrant activation of morphogenetic signaling pathways is also crucial for the emergence of chemoresistant phenotypes. For instance, the scarce sensitivity of CCA cells to different chemotherapeutics (i.e., 5-fluorouracil, cisplatin, vincristine) was found to largely rely on the overactivation of the Wnt/β-catenin pathway, which is indeed responsible for the up-regulation of the efflux pump P-glycoprotein [143]. Interestingly, both TAMs [95] and MSCs [144] were identified as important contributors to the activation of the Wnt/β-catenin axis in CCA cells and consistently, conditioned medium from MSCs was found to endow CCA cells with enhanced apoptosis resistance [144]. The overexpression of ABC transporters, namely P-glycoprotein and MRP1, is also sustained by Notch1 signaling, whose down-modulation dramatically increased the apoptotic rate of CCA cells upon 5-fluorouracil exposure [145]. Unlike Wnt and Notch signaling, the oncogenic Hh pathway decreased the sensitivity of CCA cells to TRAIL-mediated apoptosis by down-regulating the expression of DR4 at the transcriptional and post-transcriptional level [146,147]. Indeed, the Hh-related transcription factor glioma-associated oncogene (GLI)3 can negatively modulate the DR4 promoter activity [146], while DR4 mRNA is a direct target of microRNA (miR)-25, whose expression is strongly promoted by Hh signaling [147]. Of further interest, the Hh-related transcription

factors GLI1 and GLI2 directly stimulate the expression of polo-like kinase 2 (PLK2), a serine/threonine kinase classically involved in the regulation of cell division. In CCA cells, PLK2 may also inhibit the proteasomal degradation of Mcl-1, thereby further providing cells with potent pro-survival signals [148]. Interestingly, the expression of TRAIL in CCA cells can be transcriptionally down-modulated by the Hippo pathway through its downstream effector yes-associated protein (YAP), whose forced overexpression actually dampened the induction of cancer cell apoptosis by Nutlin-3, a small molecule supporting p53 activity [149].

3.2 Molecular mechanisms of cancer cell invasiveness

The acquisition of an invasive phenotype by cancer cells is a fist and crucial step towards the development of metastases, which in CCA represents a major hindrance to therapeutic success [46,150]. Cancer cells need to be equipped with pronounced invasive properties in order to degrade the surrounding basement membrane, detach from the primary tumor mass, and easily move across the stroma towards the blood and/or lymphatic vessels [150,151]. Basically, the emergence of pro-invasive changes results from an aberrant and incomplete rehash of an embryonic program known as epithelial-to-mesenchymal transition (EMT), through which epithelial cells can transdifferentiate into mesenchymal cells [63]. Regardless of the background (i.e., morphogenesis, wound healing, cancer), the EMT

program is ultimately driven by a set of master transcription factors, notably Snail (or Snail1), Slug (or Snail2), Twist1/2 and ZEB1/2, which directly repress the expression of cardinal epithelial genes, while simultaneously inducing the *de novo* expression of mesenchymal genes. For instance, a major outcome of the EMT-associated gene expression reprogramming is the so-called "cadherin switch", that is the exchange of E-cadherin, the main constituent of adherens junctions, for N-cadherin, which allows dynamic interactions among invading cells. Importantly, upon E-cadherin down-regulation, β-catenin can be no longer retained at the membrane, and either is degraded by the proteasome (in the absence of Wnt ligands) or enter the nucleus to regulate gene expression (upon Wnt pathway activation). The destabilization of adherens junctions occurs alongside the repression of tight junctions proteins (e.g., occludin, claudins), desmosomal proteins (e.g., desmoplakin), and polarity complex proteins (e.g., Crumbs complex), overall leading to a definitive loss of cell-cell adhesion and apical-basal polarity. In addition, the expression pattern of integrins is deeply modified, and the cytoskeleton is throughout remodeled, due to the down-regulation of cytokeratins (CK) and the up-regulation of vimentin. The production of MMPs is also greatly enhanced, thus enabling cells to massively degrade the ECM [152,153]. The expression of prototypical EMT features by neoplastic bile ducts is a well-established fact, generally predicting metastatic behavior and poor survival [63,154]. CCA cells, especially

those located at the invasive front, typically exhibit an elongated, spindle-shaped morphology, and express high levels of N-cadherin, vimentin, S100A4, and nuclear β-catenin, and low levels of E-cadherin and CK19. Overexpression of EMT master transcription factors is also frequently observed [75,154,155].

Although there is still a long way to go, the molecular mechanisms orchestrating this pro-invasive phenotypic switch are gradually emerging. They rely on secreted factors permeating the tumor microenvironment, as well as on aberrantly expressed intracellular players that directly or indirectly interact with the EMT machinery. For instance, TGF-β1 [156-160] and EGF-like family members (notably, EGF and HB-EGF) [73,161-163] are prototypical EMT inducers that are generally overexpressed by either CCA cells or reactive stromal cells, and are well-known to provide malignant cholangiocytes with strong migratory and invasive capabilities. Similarly, TAM-derived TNF-α up-regulates the expression of Snail and ZEB2 [100,101], and dramatically enhances the production of MMP-9 by activating focal adhesion kinase [164], and promoting the expression of COX-2 [165]. Other pro-invasive microenvironmental cues encompass IL-6 [166,167], SDF-1 [78,79,168-170], HGF [171,172] and FGF-19 [173]. On the other hand, stochastic mutations and oncogenic pathways may deleteriously impinge on the expression or activity of several intracellular proteins and miRNAs that in turn can potentially modulate the invasive potential of CCA cells. In this context,

pro-invasive transcription factors such as Notch1 [145,174-177], YAP [178], and sal-like protein (SALL)4 [179,180], which are typically up-regulated in CCA, are suggested to play a prominent role. For example, SALL4 may unleash the pro-metastatic PI3K/Akt and Wnt/β-catenin pathways by down-regulating phosphatase and tensin homolog, a negative regulator of Akt, and up-regulating BMI-1, an epigenetic repressor of Wnt inhibitors [180]. Conversely, the E3 ubiquitin ligase F-box and WD repeat domain-containing (FBXW)7 [181], and the MAPK kinase kinase (MAP3K)4 [155] counteract the invasive functions of CCA cells and consistently, are frequently down-regulated in neoplastic bile ducts. FBXW7 keeps at bay the protein levels of its direct target mTOR, which can otherwise induce EMT through ZEB1 up-regulation [181]; MAP3K4 triggers the activation of p38 MAPK, which then prevents nuclear factor κB from entering the nucleus and promoting Snail expression [155].

Scope of the thesis

During my PhD studies, I sought to dissect the nature and the biological relevance of the dense, multifaceted paracrine communications between stromal and cancer cells in CCA, in an effort to unveil the intimate molecular mechanisms driving tumor progression.

Chapter 2: Leukemia inhibitory factor protects cholangiocarcinoma cells from drug-induced apoptosis via a PI3K/AKT-dependent Mcl-1 activation.

Leukemia inhibitory factor (LIF) is a pleiotropic cytokine belonging to the IL-6 family, which can be secreted by both epithelial and stromal cell types (e.g., fibroblasts, monocytes, macrophages), and whose pro-oncogenic activity has been described in several human cancers. Our aim was to investigate the role of LIF in the progression of CCA, by evaluating the expression of LIF and its receptor in tumor tissue and cell lines, and testing the effects of LIF on the hallmarks of cancer, *in vitro*. In addition, we also intended to dissect the signaling pathways triggered by LIF in CCA cells.

Chapter 3: Low-dose paclitaxel reduces S100A4 nuclear import to inhibit invasion and hematogenous metastasis of cholangiocarcinoma.

EMT of cancer cells is a paramount process underlying carcinoma invasion and metastasis, and is widely recognized as a classic readout of tumor-stroma interactions. In a previous study, our group has revealed that in CCA, nuclear expression of the EMT-related protein S100A4 is both a powerful predictor of poor outcome, and a mechanistic determinant of cancer cell invasiveness. In this work, we aimed at clarifying the mechanisms underlying the pro-metastatic activity of nuclear S100A4 in CCA cells, as well as the mechanisms responsible for its nuclear import. Since studies from the early '90s have described the ability of paclitaxel (PTX) to downregulate the expression of S100A4 in mouse melanoma cells, we preliminary assessed whether PTX could be useful in modulating the intracellular levels of S100A4 in our cell lines.

Chapter 4: Platelet-derived growth factor D enables cancer-associated fibroblasts to promote tumor lymphangiogenesis in cholangiocarcinoma.

CAFs are recognized to play a major role in the induction of lymphangiogenesis in several human cancers, mainly due to a broad secretion of VEGFs. In a previous study, our group has identified PDGF-DD as a paramount mediator of fibroblasts recruitment by CCA cells. Interestingly, PDGF ligands, especially PDGF-BB, have been reported to stimulate the production of VEGFs in a variety of cell systems, including hepatic stellate cells and pulmonary fibroblasts. In this

study, we therefore tested the hypothesis that PDGF-DD may also endow CAFs with pro-lymphangiogenic functions. To this end, we measured the secretion of various lymphangiogenic growth factors by human fibroblasts upon PDGF-DD treatment (with a focus on the intracellular pathways activated downstream of PDGFRβ), and evaluated the effects of conditioned medium from PDGF-DD-treated fibroblasts on the behavior of LECs, in terms of motility and tubulogenesis.

References

1. Razumilava N, Gores GJ. Cholangiocarcinoma. Lancet. 2014;383:2168-79.
2. Banales JM, Cardinale V, Carpino G, Marzioni M, Andersen JB, Invernizzi P, Lind GE, Folseraas T, Forbes SJ, Fouassier L, Geier A, Calvisi DF, Mertens JC, Trauner M, Benedetti A, Maroni L, Vaquero J, Macias RI, Raggi C, Perugorria MJ, Gaudio E, Boberg KM, Marin JJ, Alvaro D. Expert consensus document: Cholangiocarcinoma: current knowledge and future perspectives consensus statement from the European Network for the Study of Cholangiocarcinoma (ENS-CCA). Nat Rev Gastroenterol Hepatol. 2016;13:261-80.
3. Høgdall D, O'Rourke CJ, Taranta A, Oliveira DV, Andersen JB. Molecular Pathogenesis and Current Therapy in Intrahepatic Cholangiocarcinoma. Dig Dis. 2016;34:440-51.
4. Brito AF, Abrantes AM, Encarnação JC, Tralhão JG, Botelho MF. Cholangiocarcinoma: from molecular biology to treatment. Med Oncol. 2015;32:245.
5. Gatto M, Bragazzi MC, Semeraro R, Napoli C, Gentile R, Torrice A, Gaudio E, Alvaro D. Cholangiocarcinoma: update and future perspectives. Dig Liver Dis. 2010;42:253-60.
6. Blechacz B, Komuta M, Roskams T, Gores GJ. Clinical diagnosis and staging of cholangiocarcinoma. Nat Rev Gastroenterol Hepatol. 2011;8:512-22.
7. Rizvi S, Gores GJ. Pathogenesis, diagnosis, and management of cholangiocarcinoma. Gastroenterology. 2013;145:1215-29.

8. Moeini A, Sia D, Bardeesy N, Mazzaferro V, Llovet JM. Molecular Pathogenesis and Targeted Therapies for Intrahepatic Cholangiocarcinoma. Clin Cancer Res. 2016;22:291-300.
9. Roskams TA, Libbrecht L, Desmet VJ. Progenitor cells in diseased human liver. Semin Liver Dis. 2003;23:385-96.
10. Cardinale V, Carpino G, Reid L, Gaudio E, Alvaro D. Multiple cells of origin in cholangiocarcinoma underlie biological, epidemiological and clinical heterogeneity. World J Gastrointest Oncol. 2012;4:94-102.
11. Lim JH. Cholangiocarcinoma: morphologic classification according to growth pattern and imaging findings. AJR Am J Roentgenol. 2003;181:819-27.
12. Blechacz B. Cholangiocarcinoma: Current Knowledge and New Developments. Gut Liver. 2017;11:13-26.
13. Vijgen S, Terris B, Rubbia-Brandt L. Pathology of intrahepatic cholangiocarcinoma. Hepatobiliary Surg Nutr. 2017;6:22-34.
14. Aishima S, Oda Y. Pathogenesis and classification of intrahepatic cholangiocarcinoma: different characters of perihilar large duct type versus peripheral small duct type. J Hepatobiliary Pancreat Sci. 2015;22:94-100.
15. Aljiffry M, Walsh MJ, Molinari M. Advances in diagnosis, treatment and palliation of cholangiocarcinoma: 1990-2009. World J Gastroenterol. 2009;15:4240-62.
16. Komuta M, Govaere O, Vandecaveye V, Akiba J, Van Steenbergen W, Verslype C, Laleman W, Pirenne J, Aerts R, Yano H, Nevens F, Topal B, Roskams T. Histological diversity in cholangiocellular carcinoma

reflects the different cholangiocyte phenotypes. Hepatology. 2012;55:1876-88.

17. Strazzabosco M, Fabris L. Functional anatomy of normal bile ducts. Anat Rec (Hoboken). 2008;291:653-60.
18. Fabris L, Brivio S, Cadamuro M, Strazzabosco M. Revisiting Epithelial-to-Mesenchymal Transition in Liver Fibrosis: Clues for a Better Understanding of the "Reactive" Biliary Epithelial Phenotype. Stem Cells Int. 2016;2016:2953727.
19. Liau JY, Tsai JH, Yuan RH, Chang CN, Lee HJ, Jeng YM. Morphological subclassification of intrahepatic cholangiocarcinoma: etiological, clinicopathological, and molecular features. Mod Pathol. 2014;27:1163-73.
20. Ferlay J, Soerjomataram I, Ervik M, Dikshit R, Eser S, Mathers C, Rebelo M, Parkin DM, Forman D, Bray F. GLOBOCAN 2012 v1.0, Cancer Incidence and Mortality Worldwide: IARC CancerBase No. 11 [Internet]. Lyon, France: International Agency for Research on Cancer; 2013. Available from: http://globocan.iarc.fr, accessed on 25/08/2017.
21. Ebata T, Ercolani G, Alvaro D, Ribero D, Di Tommaso L, Valle JW. Current Status on Cholangiocarcinoma and Gallbladder Cancer. Liver Cancer. 2016;6:59-65.
22. Wise C, Pilanthananond M, Perry BF, Alpini G, McNeal M, Glaser SS. Mechanisms of biliary carcinogenesis and growth. World J Gastroenterol. 2008;14:2986-9.
23. Park J, Tadlock L, Gores GJ, Patel T. Inhibition of interleukin 6-mediated mitogen-activated protein kinase activation attenuates

growth of a cholangiocarcinoma cell line. Hepatology. 1999;30:1128-33.

24. Isomoto H, Kobayashi S, Werneburg NW, Bronk SF, Guicciardi ME, Frank DA, Gores GJ. Interleukin 6 upregulates myeloid cell leukemia-1 expression through a STAT3 pathway in cholangiocarcinoma cells. Hepatology. 2005;42:1329-38.
25. Kobayashi S, Werneburg NW, Bronk SF, Kaufmann SH, Gores GJ. Interleukin-6 contributes to Mcl-1 up-regulation and TRAIL resistance via an Akt-signaling pathway in cholangiocarcinoma cells. Gastroenterology. 2005;128:2054-65.
26. Meng F, Yamagiwa Y, Ueno Y, Patel T. Over-expression of interleukin-6 enhances cell survival and transformed cell growth in human malignant cholangiocytes. J Hepatol. 2006;44:1055-65.
27. Yamada D, Rizvi S, Razumilava N, Bronk SF, Davila JI, Champion MD, Borad MJ, Bezerra JA, Chen X, Gores GJ. IL-33 facilitates oncogene-induced cholangiocarcinoma in mice by an interleukin-6-sensitive mechanism. Hepatology. 2015;61:1627-42.
28. Fan B, Malato Y, Calvisi DF, Naqvi S, Razumilava N, Ribback S, Gores GJ, Dombrowski F, Evert M, Chen X, Willenbring H. Cholangiocarcinomas can originate from hepatocytes in mice. J Clin Invest. 2012;122:2911–15.
29. Sekiya S, Suzuki A. Intrahepatic cholangiocarcinoma can arise from Notch-mediated conversion of hepatocytes. J Clin Invest. 2012;122:3914–18.
30. Ishimura N, Bronk SF, Gores GJ. Inducible nitric oxide synthase up-regulates Notch-1 in mouse cholangiocytes: implications for carcinogenesis. Gastroenterology 2005;128:1354-68.

31. El Khatib M, Kalnytska A, Palagani V, Kossatz U, Manns MP, Malek NP, Wilkens L, Plentz RR. Inhibition of hedgehog signaling attenuates carcinogenesis in vitro and increases necrosis of cholangiocellular carcinoma. Hepatology 2013;57:1035-45.
32. Nachtergaele S, Mydock LK, Krishnan K, Rammohan J, Schlesinger PH, Covey DF, Rohatgi R. Oxysterols are allosteric activators of the oncoprotein Smoothened. Nat Chem Biol. 2012;8:211-20.
33. Alvaro D, Mancino MG, Glaser S, et al. Proliferating cholangiocytes: a neuroendocrine compartment in the diseased liver. Gastroenterology. 2007;132:415–31.
34. Chong DQ, Zhu AX. The landscape of targeted therapies for cholangiocarcinoma: current status and emerging targets. Oncotarget. 2016;7:46750-67.
35. Rizvi S, Gores GJ. Emerging molecular therapeutic targets for cholangiocarcinoma. J Hepatol. 2017;67:632-44.
36. Chan-On W, Nairismägi ML, Ong CK, Lim WK, Dima S, Pairojkul C, Lim KH, McPherson JR, Cutcutache I, Heng HL, Ooi L, Chung A, Chow P, Cheow PC, Lee SY, Choo SP, Tan IB, Duda D, Nastase A, Myint SS, Wong BH, Gan A, Rajasegaran V, Ng CC, Nagarajan S, Jusakul A, Zhang S, Vohra P, Yu W, Huang D, Sithithaworn P, Yongvanit P, Wongkham S, Khuntikeo N, Bhudhisawasdi V, Popescu I, Rozen SG, Tan P, Teh BT. Exome sequencing identifies distinct mutational patterns in liver fluke-related and non-infection-related bile duct cancers. Nat Genet. 2013;45:1474-8.
37. Sugimachi K, Taguchi K, Aishima S, Tanaka S, Shimada M, Kajiyama K, Sugimachi K, Tsuneyoshi M. Altered expression of beta-catenin

without genetic mutation in intrahepatic cholangiocarcinoma. Mod Pathol. 2001;14:900-5.

38. Sadot E, Geiger B, Oren M, Ben-Ze'ev A. Down-regulation of beta-catenin by activated p53. Mol Cell Biol. 2001;21:6768-81.

39. Ornitz DM, Itoh N. The Fibroblast Growth Factor signaling pathway. Wiley Interdiscip Rev Dev Biol. 2015;4:215-66.

40. Principe DR, Doll JA, Bauer J, Jung B, Munshi HG, Bartholin L, Pasche B, Lee C, Grippo PJ. TGF-β: duality of function between tumor prevention and carcinogenesis. J Natl Cancer Inst. 2014;106:djt369.

41. Saha SK, Parachoniak CA, Ghanta KS, Fitamant J, Ross KN, Najem MS, Gurumurthy S, Akbay EA, Sia D, Cornella H, Miltiadous O, Walesky C, Deshpande V, Zhu AX, Hezel AF, Yen KE, Straley KS, Travins J, Popovici-Muller J, Gliser C, Ferrone CR, Apte U, Llovet JM, Wong KK, Ramaswamy S, Bardeesy N. Mutant IDH inhibits HNF-4α to block hepatocyte differentiation and promote biliary cancer. Nature. 2014;513:110-4.

42. Isomoto H. Epigenetic alterations in cholangiocarcinoma-sustained IL-6/STAT3 signaling in cholangiocarcinoma due to SOCS3 epigenetic silencing. Digestion. 2009;79:2-8.

43. Jiao Y, Pawlik TM, Anders RA, Selaru FM, Streppel MM, Lucas DJ, Niknafs N, Guthrie VB, Maitra A, Argani P, Offerhaus GJA, Roa JC, Roberts LR, Gores GJ, Popescu I, Alexandrescu ST, Dima S, Fassan M, Simbolo M, Mafficini A, Capelli P, Lawlor RT, Ruzzenente A, Guglielmi A, Tortora G, de Braud F, Scarpa A, Jarnagin W, Klimstra D, Karchin R, Velculescu VE, Hruban RH, Vogelstein B, Kinzler KW, Papadopoulos N, Wood LD. Exome sequencing identifies frequent inactivating

mutations in BAP1, ARID1A and PBRM1 in intrahepatic cholangiocarcinomas. Nat Genet. 2013;45:1470-73.

44. Kadoch C, Crabtree GR. Mammalian SWI/SNF chromatin remodeling complexes and cancer: Mechanistic insights gained from human genomics. Sci Adv. 2015;1:e1500447.
45. Carbone M, Yang H, Pass HI, Krausz T, Testa JR, Gaudino G. BAP1 and cancer. Nat Rev Cancer. 2013;13:153-9.
46. Fabris L, Alvaro D. The prognosis of perihilar cholangiocarcinoma after radical treatments. Hepatology 2012;56:800-2.
47. Valle J, Wasan H, Palmer DH, Cunningham D, Anthoney A, Maraveyas A, Madhusudan S, Iveson T, Hughes S, Pereira SP, Roughton M, Bridgewater J; ABC-02 Trial Investigators. Cisplatin plus gemcitabine versus gemcitabine for biliary tract cancer. N Engl J Med. 2010;362:1273-81.
48. Cadamuro M, Brivio S, Spirli C, Joplin RE, Strazzabosco M, Fabris L. Autocrine and Paracrine Mechanisms Promoting Chemoresistance in Cholangiocarcinoma. Int J Mol Sci. 2017;18.
49. Mueller MM, Fusenig NE. Friends or foes - bipolar effects of the tumour stroma in cancer. Nat Rev Cancer. 2004;4:839-49.
50. Dvorak HF. Tumors: wounds that do not heal-redux. Cancer Immunol Res. 2015;3:1-11.
51. Kalluri R, Zeisberg M. Fibroblasts in cancer. Nat Rev Cancer. 2006;6:392-401.
52. Dvorak HF. Tumors: wounds that do not heal. Similarities between tumor stroma generation and wound healing. N Engl J Med. 1986;315:1650-9.

53. Cadamuro M, Morton SD, Strazzabosco M, Fabris L. Unveiling the role of tumor reactive stroma in cholangiocarcinoma: An opportunity for new therapeutic strategies. Transl Gastrointest Cancer. 2013;2:130-44.
54. Bhome R, Bullock MD, Al Saihati HA, Goh RW, Primrose JN, Sayan AE, Mirnezami AH. A top-down view of the tumor microenvironment: structure, cells and signaling. Front Cell Dev Biol. 2015;3:33.
55. Brivio S, Cadamuro M, Strazzabosco M, Fabris L. Tumor reactive stroma in cholangiocarcinoma: The fuel behind cancer aggressiveness. World J Hepatol. 2017;9:455-68.
56. Cadamuro M, Stecca T, Brivio S, Mariotti V, Fiorotto R, Spirli C, Strazzabosco M, Fabris L. The deleterious interplay between tumor epithelia and stroma in cholangiocarcinoma. Biochim Biophys Acta. 2017.
57. Quail DF, Joyce JA. Microenvironmental regulation of tumor progression and metastasis. Nat Med. 2013;19:1423-37.
58. Lin HJ, Zuo T, Lin CH, Kuo CT, Liyanarachchi S, Sun S, Shen R, Deatherage DE, Potter D, Asamoto L, Lin S, Yan PS, Cheng AL, Ostrowski MC, Huang TH. Breast cancer-associated fibroblasts confer AKT1-mediated epigenetic silencing of Cystatin M in epithelial cells. Cancer Res. 2008;68:10257-66.
59. Xu L, Deng Q, Pan Y, Peng M, Wang X, Song L, Xiao M, Wang Z. Cancer-associated fibroblasts enhance the migration ability of ovarian cancer cells by increasing EZH2 expression. Int J Mol Med. 2014;33:91-6.
60. Kurashige J, Mima K, Sawada G, Takahashi Y, Eguchi H, Sugimachi K, Mori M, Yanagihara K, Yashiro M, Hirakawa K, Baba H, Mimori K. Epigenetic modulation and repression of miR-200b by cancer-

associated fibroblasts contribute to cancer invasion and peritoneal dissemination in gastric cancer. Carcinogenesis. 2015;36:133-41.

61. Coulouarn C, Clément B. Stellate cells and the development of liver cancer: therapeutic potential of targeting the stroma. J Hepatol. 2014;60:1306-09.
62. Chen F, Zhuang X, Lin L, Yu P, Wang Y, Shi Y, Hu G, Sun Y. New horizons in tumor microenvironment biology: challenges and opportunities. BMC Med. 2015;13:45.
63. Brivio S, Cadamuro M, Fabris L, Strazzabosco M. Epithelial-to-Mesenchymal Transition and Cancer Invasiveness: What Can We Learn from Cholangiocarcinoma? J Clin Med. 2015;4:2028-41.
64. Sulpice L, Rayar M, Desille M, Turlin B, Fautrel A, Boucher E, Llamas-Gutierrez F, Meunier B, Boudjema K, Clément B, Coulouarn C. Molecular profiling of stroma identifies osteopontin as an independent predictor of poor prognosis in intrahepatic cholangiocarcinoma. Hepatology. 2013;58:1992-2000.
65. Andersen JB, Spee B, Blechacz BR, Avital I, Komuta M, Barbour A, Conner EA, Gillen MC, Roskams T, Roberts LR, Factor VM, Thorgeirsson SS. Genomic and genetic characterization of cholangiocarcinoma identifies therapeutic targets for tyrosine kinase inhibitors. Gastroenterology. 2012;142:1021-31.e15.
66. Augsten M. Cancer-associated fibroblasts as another polarized cell type of the tumor microenvironment. Front Oncol. 2014;4:62.
67. Chuaysri C, Thuwajit P, Paupairoj A, Chau-In S, Suthiphongchai T, Thuwajit C. Alpha-smooth muscle actin-positive fibroblasts promote biliary cell proliferation and correlate with poor survival in cholangiocarcinoma. Oncol Rep. 2009;21:957-69.

68. Utispan K, Thuwajit P, Abiko Y, Charngkaew K, Paupairoj A, Chauin S, Thuwajit C. Gene expression profiling of cholangiocarcinoma-derived fibroblast reveals alterations related to tumor progression and indicates periostin as a poor prognostic marker. Mol Cancer. 2010;9:13.
69. Yang X, Lin Y, Shi Y, Li B, Liu W, Yin W, Dang Y, Chu Y, Fan J, He R. FAP Promotes Immunosuppression by Cancer-Associated Fibroblasts in the Tumor Microenvironment via STAT3-CCL2 Signaling. Cancer Res. 2016;76:4124-35.
70. Shiga K, Hara M, Nagasaki T, Sato T, Takahashi H, Takeyama H. Cancer-Associated Fibroblasts: Their Characteristics and Their Roles in Tumor Growth. Cancers (Basel). 2015;7:2443-58.
71. Leyva-Illades D, McMillin M, Quinn M, Demorrow S. Cholangiocarcinoma pathogenesis: Role of the tumor microenvironment. Transl Gastrointest Cancer. 2012;1:71-80.
72. Okabe H, Beppu T, Hayashi H, Ishiko T, Masuda T, Otao R, Horlad H, Jono H, Ueda M, Phd SS, Ando Y, Baba H. Hepatic stellate cells accelerate the malignant behavior of cholangiocarcinoma cells. Ann Surg Oncol. 2011;18:1175-84.
73. Clapéron A, Mergey M, Aoudjehane L, Ho-Bouldoires TH, Wendum D, Prignon A, Merabtene F, Firrincieli D, Desbois-Mouthon C, Scatton O, Conti F, Housset C, Fouassier L. Hepatic myofibroblasts promote the progression of human cholangiocarcinoma through activation of epidermal growth factor receptor. Hepatology. 2013;58:2001-11.
74. Haga H, Yan IK, Takahashi K, Wood J, Zubair A, Patel T. Tumour cell-derived extracellular vesicles interact with mesenchymal stem cells

to modulate the microenvironment and enhance cholangiocarcinoma growth. J Extracell Vesicles. 2015;4:24900.

75. Cadamuro M, Nardo G, Indraccolo S, Dall'olmo L, Sambado L, Moserle L, Franceschet I, Colledan M, Massani M, Stecca T, Bassi N, Morton S, Spirli C, Fiorotto R, Fabris L, Strazzabosco M. Platelet-derived growth factor-D and Rho GTPases regulate recruitment of cancer-associated fibroblasts in cholangiocarcinoma. Hepatology. 2013;58:1042-53.
76. Heits N, Heinze T, Bernsmeier A, Kerber J, Hauser C, Becker T, Kalthoff H, Egberts JH, Braun F. Influence of mTOR-inhibitors and mycophenolic acid on human cholangiocellular carcinoma and cancer associated fibroblasts. BMC Cancer. 2016;16:322.
77. Okabe H, Beppu T, Hayashi H, Horino K, Masuda T, Komori H, Ishikawa S, Watanabe M, Takamori H, Iyama K, Baba H. Hepatic stellate cells may relate to progression of intrahepatic cholangiocarcinoma. Ann Surg Oncol. 2009;16:2555-64.
78. Gentilini A, Rombouts K, Galastri S, Caligiuri A, Mingarelli E, Mello T, Marra F, Mantero S, Roncalli M, Invernizzi P, Pinzani M. Role of the stromal-derived factor-1 (SDF-1)-CXCR4 axis in the interaction between hepatic stellate cells and cholangiocarcinoma. J Hepatol. 2012;57:813-20.
79. Okamoto K, Tajima H, Nakanuma S, Sakai S, Makino I, Kinoshita J, Hayashi H, Nakamura K, Oyama K, Nakagawara H, Fujita H, Takamura H, Ninomiya I, Kitagawa H, Fushida S, Fujimura T, Harada S, Wakayama T, Iseki S, Ohta T. Angiotensin II enhances epithelial-to-mesenchymal transition through the interaction between activated hepatic stellate cells and the stromal cell-derived factor-1/CXCR4 axis in intrahepatic cholangiocarcinoma. Int J Oncol. 2012;41:573-82.

80. Kim Y, Kim MO, Shin JS, Park SH, Kim SB, Kim J, Park SC, Han CJ, Ryu JK, Yoon YB, Kim YT. Hedgehog signaling between cancer cells and hepatic stellate cells in promoting cholangiocarcinoma. Ann Surg Oncol. 2014;21:2684-98.
81. Fingas CD, Bronk SF, Werneburg NW, Mott JL, Guicciardi ME, Cazanave SC, Mertens JC, Sirica AE, Gores GJ. Myofibroblast-derived PDGF-BB promotes Hedgehog survival signaling in cholangiocarcinoma cells. Hepatology. 2011; 54: 2076-2088.
82. Fingas CD, Mertens JC, Razumilava N, Bronk SF, Sirica AE, Gores GJ. Targeting PDGFR-β in Cholangiocarcinoma. Liver Int. 2012;32:400-9.
83. Mertens JC, Fingas CD, Christensen JD, Smoot RL, Bronk SF, Werneburg NW, Gustafson MP, Dietz AB, Roberts LR, Sirica AE, Gores GJ. Therapeutic effects of deleting cancer-associated fibroblasts in cholangiocarcinoma. Cancer Res. 2013;73:897-907.
84. Campbell DJ, Dumur CI, Lamour NF, Dewitt JL, Sirica AE. Novel organotypic culture model of cholangiocarcinoma progression. Hepatol Res. 2012;42:1119-30.
85. Grivennikov SI, Greten FR, Karin M. Immunity, inflammation, and cancer. Cell. 2010;140:883-99.
86. Hasita H, Komohara Y, Okabe H, Masuda T, Ohnishi K, Lei XF, Beppu T, Baba H, Takeya M. Significance of alternatively activated macrophages in patients with intrahepatic cholangiocarcinoma. Cancer Sci. 2010;101:1913-19.
87. Chang J, Hisamatsu T, Shimamura K, Yoneno K, Adachi M, Naruse H, Igarashi T, Higuchi H, Matsuoka K, Kitazume MT, Ando S, Kamada N, Kanai T, Hibi T. Activated hepatic stellate cells mediate the differentiation of macrophages. Hepatol Res. 2013;43:658-69.

88. Sica A, Invernizzi P, Mantovani A. Macrophage plasticity and polarization in liver homeostasis and pathology. Hepatology. 2014; 59:2034-42.
89. Raggi C, Correnti M, Sica A, Andersen JB, Cardinale V, Alvaro D, Chiorino G, Forti E, Glaser S, Alpini G, Destro A, Sozio F, Di Tommaso L, Roncalli M, Banales JM, Coulouarn C, Bujanda L, Torzilli G, Invernizzi P. Cholangiocarcinoma stem-like subset shapes tumor-initiating niche by educating associated macrophages. J Hepatol. 2017;66:102-15.
90. Mantovani A, Allavena P, Sica A, Balkwill F. Cancer-related inflammation. Nature. 2008;454:436-44.
91. Subimerb C, Pinlaor S, Lulitanond V, Khuntikeo N, Okada S, McGrath MS, Wongkham S. Circulating CD14(+) CD16(+) monocyte levels predict tissue invasive character of cholangiocarcinoma. Clin Exp Immunol. 2010;161:471-9.
92. Duong T, Koopman P, Francois M. Tumor lymphangiogenesis as a potential therapeutic target. J Oncol. 2012;2012:204946.
93. Thanee M, Loilome W, Techasen A, Namwat N, Boonmars T, Pairojkul C, Yongvanit P. Quantitative changes in tumor-associated M2 macrophages characterize cholangiocarcinoma and their association with metastasis. Asian Pac J Cancer Prev. 2015;16:3043-50.
94. Boulter L, Guest RV, Kendall TJ, Wilson DH, Wojtacha D, Robson AJ, Ridgway RA, Samuel K, Van Rooijen N, Barry ST, Wigmore SJ, Sansom OJ, Forbes SJ. WNT signaling drives cholangiocarcinoma growth and can be pharmacologically inhibited. J Clin Invest. 2015; 125:1269-85.
95. Loilome W, Bungkanjana P, Techasen A, Namwat N, Yongvanit P, Puapairoj A, Khuntikeo N, Riggins GJ. Activated macrophages

promote Wnt/β-catenin signaling in cholangiocarcinoma cells. Tumour Biol. 2014;35:5357-67.

96. MacDonald BT, Tamai K, He X. Wnt/beta-catenin signaling: components, mechanisms, and diseases. Dev Cell. 2009;17:9-26.

97. Techasen A, Loilome W, Namwat N, Dokduang H, Jongthawin J, Yongvanit P. Cytokines released from activated human macrophages induce epithelial mesenchymal transition markers of cholangiocarcinoma cells. Asian Pac J Cancer Prev. 2012;13 Suppl:115-8.

98. Dokduang H, Techasen A, Namwat N, Khuntikeo N, Pairojkul C, Murakami Y, Loilome W, Yongvanit P. STATs profiling reveals predominantly-activated STAT3 in cholangiocarcinoma genesis and progression. J Hepatobiliary Pancreat Sci. 2014;21:767-6.

99. Ohira S, Sasaki M, Harada K, Sato Y, Zen Y, Isse K, Kozaka K, Ishikawa A, Oda K, Nimura Y, Nakanuma Y. Possible regulation of migration of intrahepatic cholangiocarcinoma cells by interaction of CXCR4 expressed in carcinoma cells with tumor necrosis factor-alpha and stromal-derived factor-1 released in stroma. Am J Pathol. 2006;168:1155-68.

100. Techasen A, Namwat N, Loilome W, Bungkanjana P, Khuntikeo N, Puapairoj A, Jearanaikoon P, Saya H, Yongvanit P. Tumor necrosis factor-α (TNF-α) stimulates the epithelial-mesenchymal transition regulator Snail in cholangiocarcinoma. Med Oncol 2012; 29:3083-91.

101. Techasen A, Namwat N, Loilome W, Duangkumpha K, Puapairoj A, Saya H, Yongvanit P. Tumor necrosis factor-α modulates epithelial mesenchymal transition mediators ZEB2 and S100A4 to promote

cholangiocarcinoma progression. J Hepatobiliary Pancreat Sci. 2014;21:703-11.

102. Subimerb C, Pinlaor S, Khuntikeo N, Leelayuwat C, Morris A, McGrath MS, Wongkham S. Tissue invasive macrophage density is correlated with prognosis in cholangiocarcinoma. Mol Med Rep. 2010;3:597-605.
103. Brown GT, Murray GI. Current mechanistic insights into the roles of matrix metalloproteinases in tumour invasion and metastasis. J Pathol. 2015;237:273-81.
104. Thelen A, Scholz A, Benckert C, Weichert W, Dietz E, Wiedenmann B, Neuhaus P, Jonas S. Tumor-associated lymphangiogenesis correlates with lymph node metastases and prognosis in hilar cholangiocarcinoma. Ann Surg Oncol. 2008;15:791-9.
105. Thelen A, Scholz A, Benckert C, Schröder M, Weichert W, Wiedenmann B, Neuhaus P, Jonas S. Microvessel density correlates with lymph node metastases and prognosis in hilar cholangiocarcinoma. J Gastroenterol. 2008;43:959-66.
106. Thelen A, Scholz A, Weichert W, Wiedenmann B, Neuhaus P, Gessner R, Benckert C, Jonas S. Tumor-associated angiogenesis and lymphangiogenesis correlate with progression of intrahepatic cholangiocarcinoma. Am J Gastroenterol. 2010;105:1123-32.
107. de Jong MC, Nathan H, Sotiropoulos GC, Paul A, Alexandrescu S, Marques H, Pulitano C, Barroso E, Clary BM, Aldrighetti L, Ferrone CR, Zhu AX, Bauer TW, Walters DM, Gamblin TC, Nguyen KT, Turley R, Popescu I, Hubert C, Meyer S, Schulick RD, Choti MA, Gigot JF, Mentha G, Pawlik TM. Intrahepatic cholangiocarcinoma: an international

multi-institutional analysis of prognostic factors and lymph node assessment. J Clin Oncol. 2011;29:3140-5.

108. Oshiro Y, Sasaki R, Kobayashi A, Murata S, Fukunaga K, Kondo T, Oda T, Ohkohchi N. Prognostic relevance of the lymph node ratio in surgical patients with extrahepatic cholangiocarcinoma. Eur J Surg Oncol. 2011;37:60-4.
109. Kiriyama M, Ebata T, Aoba T, Kaneoka Y, Arai T, Shimizu Y, Nagino M; Nagoya Surgical Oncology Group. Prognostic impact of lymph node metastasis in distal cholangiocarcinoma. Br J Surg. 2015;102:399-406.
110. Zhang JW, Chu YM, Lan ZM, Tang XL, Chen YT, Wang CF, Che X. Correlation between metastatic lymph node ratio and prognosis in patients with extrahepatic cholangiocarcinoma. World J Gastroenterol. 2015;21:4255-60.
111. Margaris KN, Black RA. Modelling the lymphatic system: challenges and opportunities. J R Soc Interface. 2012;9:601-12.
112. Stacker SA, Williams SP, Karnezis T, Shayan R, Fox SB, Achen MG. Lymphangiogenesis and lymphatic vessel remodelling in cancer. Nat Rev Cancer. 2014;14:159-72.
113. Park BK, Paik YH, Park JY, Park KH, Bang S, Park SW, Chung JB, Park YN, Song SY. The clinicopathologic significance of the expression of vascular endothelial growth factor-C in intrahepatic cholangiocarcinoma. Am J Clin Oncol. 2006;29:138-42.
114. Aishima S, Nishihara Y, Iguchi T, Taguchi K, Taketomi A, Maehara Y, Tsuneyoshi M. Lymphatic spread is related to VEGF-C expression and D2-40-positive myofibroblasts in intrahepatic cholangiocarcinoma. Mod Pathol. 2008;21:256-64.

115. Zhao R, Chang Y, Liu Z, Liu Y, Guo S, Yu J, Wang J. Effect of vascular endothelial growth factor-C expression on lymph node metastasis in human cholangiocarcinoma. Oncol Lett. 2015;10:1011-5.
116. Ellis LM, Hicklin DJ. VEGF-targeted therapy: mechanisms of anti-tumour activity. Nat Rev Cancer. 2008;8:579-91.
117. Hirakawa S, Kodama S, Kunstfeld R, Kajiya K, Brown LF, Detmar M. VEGF-A induces tumor and sentinel lymph node lymphangiogenesis and promotes lymphatic metastasis. J Exp Med. 2005;201:1089-99.
118. Bonnans C, Chou J, Werb Z. Remodelling the extracellular matrix in development and disease. Nat Rev Mol Cell Biol. 2014;15:786-801.
119. Chaijan S, Roytrakul S, Mutirangura A, Leelawat K. Matrigel induces L-plastin expression and promotes L-plastin-dependent invasion in human cholangiocarcinoma cells. Oncol Lett. 2014;8:993-1000.
120. Aishima S, Taguchi K, Terashi T, Matsuura S, Shimada M, Tsuneyoshi M. Tenascin expression at the invasive front is associated with poor prognosis in intrahepatic cholangiocarcinoma. Mod Pathol. 2003;16:1019-27.
121. Utispan K, Sonongbua J, Thuwajit P, Chau-In S, Pairojkul C, Wongkham S, Thuwajit C. Periostin activates integrin α5β1 through a PI3K/AKT-dependent pathway in invasion of cholangiocarcinoma. Int J Oncol. 2012;41:1110-8.
122. Keith B, Simon MC. Hypoxia-inducible factors, stem cells, and cancer. Cell. 2007;129:465-72.
123. Ruan K, Song G, Ouyang G. Role of hypoxia in the hallmarks of human cancer. J Cell Biochem. 2009;107:1053-62.
124. Lu X, Kang Y. Hypoxia and hypoxia-inducible factors: master regulators of metastasis. Clin Cancer Res. 2010;16:5928-35.

125. Pinlaor S, Sripa B, Ma N, Hiraku Y, Yongvanit P, Wongkham S, Pairojkul C, Bhudhisawasdi V, Oikawa S, Murata M, Semba R, Kawanishi S. Nitrative and oxidative DNA damage in intrahepatic cholangiocarcinoma patients in relation to tumor invasion. World J Gastroenterol. 2005;11:4644-9.
126. Vanichapol T, Leelawat K, Hongeng S. Hypoxia enhances cholangiocarcinoma invasion through activation of hepatocyte growth factor receptor and the extracellular signal-regulated kinase signaling pathway. Mol Med Rep. 2015;12:3265-72.
127. Morine Y, Shimada M, Utsunomiya T, Imura S, Ikemoto T, Mori H, Hanaoka J, Kanamoto M, Iwahashi S, Miyake H. Hypoxia inducible factor expression in intrahepatic cholangiocarcinoma. Hepatogastroenterology. 2011;58:1439-44.
128. Thongchot S, Yongvanit P, Loilome W, Seubwai W, Phunicom K, Tassaneeyakul W, Pairojkul C, Promkotra W, Techasen A, Namwat N. High expression of HIF-1α, BNIP3 and PI3KC3: hypoxia-induced autophagy predicts cholangiocarcinoma survival and metastasis. Asian Pac J Cancer Prev. 2014;15:5873-8.
129. Thongchot S, Loilome W, Yongvanit P, Dokduang H, Thanan R, Techasen A, Namwat N. Chloroquine exerts anti-metastatic activities under hypoxic conditions in cholangiocarcinoma cells. Asian Pac J Cancer Prev. 2015;16:2031-5.
130. Nitta T, Sato Y, Ren XS, Harada K, Sasaki M, Hirano S, Nakanuma Y. Autophagy may promote carcinoma cell invasion and correlate with poor prognosis in cholangiocarcinoma. Int J Clin Exp Pathol. 2014;7:4913–21.

131. Seubwai W, Kraiklang R, Wongkham C, Wongkham S. Hypoxia enhances aggressiveness of cholangiocarcinoma cells. Asian Pac J Cancer Prev. 2012;13 Suppl:53-8.
132. Marienfeld C, Yamagiwa Y, Ueno Y, Chiasson V, Brooks L, Meng F, Patel T. Translational regulation of XIAP expression and cell survival during hypoxia in human cholangiocarcinoma. Gastroenterology. 2004;127:1787-97.
133. Nakajima T, Takayama T, Miyanishi K, Nobuoka A, Hayashi T, Abe T, Kato J, Sakon K, Naniwa Y, Tanabe H, Niitsu Y. Reversal of multiple drug resistance in cholangiocarcinoma by the glutathione S-transferase-pi-specific inhibitor O1-hexadecyl-gamma-glutamyl-S-benzylcysteinyl-D-phenylglycine ethylester. J Pharmacol Exp Ther. 2003;306:861-9.
134. Namwat N, Amimanan P, Loilome W, Jearanaikoon P, Sripa B, Bhudhisawasdi V, Tassaneeyakul W. Characterization of 5-fluorouracil-resistant cholangiocarcinoma cell lines. Chemotherapy. 2008;54:343-51.
135. Sato J, Kimura T, Saito T, Anazawa T, Kenjo A, Sato Y, Tsuchiya T, Gotoh M. Gene expression analysis for predicting gemcitabine resistance in human cholangiocarcinoma. J Hepatobiliary Pancreat Sci. 2011;18:700-11.
136. Taniai M, Grambihler A, Higuchi H, Werneburg N, Bronk SF, Farrugia DJ, Kaufmann SH, Gores GJ. Mcl-1 mediates tumor necrosis factor-related apoptosis-inducing ligand resistance in human cholangiocarcinoma cells. Cancer Res. 2004;64:3517-24.

137. Zhou F, Xu J, Ding G, Cao L. Overexpressions of CK2β and XIAP are associated with poor prognosis of patients with cholangiocarcinoma. Pathol Oncol Res. 2014;20:73-9.
138. Obama K, Ura K, Li M, Katagiri T, Tsunoda T, Nomura A, Satoh S, Nakamura Y, Furukawa Y. Genome-wide analysis of gene expression in human intrahepatic cholangiocarcinoma. Hepatology. 2005;41:1339-48.
139. Adams JM, Cory S. The Bcl-2 apoptotic switch in cancer development and therapy. Oncogene. 2007;26:1324-37.
140. Akgul C. Mcl-1 is a potential therapeutic target in multiple types of cancer. Cell Mol Life Sci. 2009;66:1326-36.
141. Thomas LW, Lam C, Edwards SW. Mcl-1; the molecular regulation of protein function. FEBS Lett. 2010;584:2981-9.
142. Dubrez L, Berthelet J, Glorian V. IAP proteins as targets for drug development in oncology. Onco Targets Ther. 2013;9:1285-304.
143. Shen DY, Zhang W, Zeng X, Liu CQ. Inhibition of Wnt/β-catenin signaling downregulates P-glycoprotein and reverses multi-drug resistance of cholangiocarcinoma. Cancer Sci. 2013;104:1303-8.
144. Wang W, Zhong W, Yuan J, Yan C, Hu S, Tong Y, Mao Y, Hu T, Zhang B, Song G. Involvement of Wnt/β-catenin signaling in the mesenchymal stem cells promote metastatic growth and chemoresistance of cholangiocarcinoma. Oncotarget. 2015;6:42276-89.
145. Wu WR, Zhang R, Shi XD, Zhu MS, Xu LB, Zeng H, Liu C. Notch1 is overexpressed in human intrahepatic cholangiocarcinoma and is associated with its proliferation, invasiveness and sensitivity to 5-fluorouracil in vitro. Oncol Rep. 2014;31:2515-24.

146. Kurita S, Mott JL, Almada LL, Bronk SF, Werneburg NW, Sun SY, Roberts LR, Fernandez-Zapico ME, Gores GJ. GLI3-dependent repression of DR4 mediates hedgehog antagonism of TRAIL-induced apoptosis. Oncogene. 2010;29:4848-58.
147. Razumilava N, Bronk SF, Smoot RL, Fingas CD, Werneburg NW, Roberts LR, Mott JL. miR-25 targets TNF-related apoptosis inducing ligand (TRAIL) death receptor-4 and promotes apoptosis resistance in cholangiocarcinoma. Hepatology. 2012;55:465-75.
148. Fingas CD, Mertens JC, Razumilava N, Sydor S, Bronk SF, Christensen JD, Rizvi SH, Canbay A, Treckmann JW, Paul A, Sirica AE, Gores GJ. Polo-like kinase 2 is a mediator of hedgehog survival signaling in cholangiocarcinoma. Hepatology. 2013;58:1362-74.
149. Marti P, Stein C, Blumer T, Abraham Y, Dill MT, Pikiolek M, Orsini V, Jurisic G, Megel P, Makowska Z, Agarinis C, Tornillo L, Bouwmeester T, Ruffner H, Bauer A, Parker CN, Schmelzle T, Terracciano LM, Heim MH, Tchorz JS. YAP promotes proliferation, chemoresistance, and angiogenesis in human cholangiocarcinoma through TEAD transcription factors. Hepatology. 2015;62:1497-510.
150. Lambert AW, Pattabiraman DR, Weinberg RA. Emerging Biological Principles of Metastasis. Cell. 2017;168:670-91.
151. Clark AG, Vignjevic DM. Modes of cancer cell invasion and the role of the microenvironment. Curr Opin Cell Biol. 2015;36:13-22.
152. Lamouille S, Xu J, Derynck R. Molecular mechanisms of epithelial-mesenchymal transition. Nat Rev Mol Cell Biol. 2014;15:178-96.
153. Gandalovičová A, Vomastek T, Rosel D, Brábek J. Cell polarity signaling in the plasticity of cancer cell invasiveness. Oncotarget. 2016;7:25022-49.

154. Vaquero J, Guedj N, Clapéron A, Nguyen Ho-Bouldoires TH, Paradis V, Fouassier L. Epithelial-mesenchymal transition in cholangiocarcinoma: From clinical evidence to regulatory networks. J Hepatol. 2017;66:424-41.
155. Yang LX, Gao Q, Shi JY, Wang ZC, Zhang Y, Gao PT, Wang XY, Shi YH, Ke AW, Shi GM, Cai JB, Liu WR, Duan M, Zhao YJ, Ji Y, Gao DM, Zhu K, Zhou J, Qiu SJ, Cao Y, Tang QQ, Fan J. Mitogen-activated protein kinase kinase kinase 4 deficiency in intrahepatic cholangiocarcinoma leads to invasive growth and epithelial-mesenchymal transition. Hepatology. 2015;62:1804-16.
156. Sato Y, Harada K, Itatsu K, Ikeda H, Kakuda Y, Shimomura S, Shan Ren X, Yoneda N, Sasaki M, Nakanuma Y. Epithelial-mesenchymal transition induced by transforming growth factor-β1/Snail activation aggravates invasive growth of cholangiocarcinoma. Am J Pathol. 2010;177:141-52.
157. Araki K, Shimura T, Suzuki H, Tsutsumi S, Wada W, Yajima T, Kobayahi T, Kubo N, Kuwano H. E/N-cadherin switch mediates cancer progression via TGF-β-induced epithelial-to-mesenchymal transition in extrahepatic cholangiocarcinoma. Br J Cancer. 2011;105:1885-93.
158. Duangkumpha K, Techasen A, Loilome W, Namwat N, Thanan R, Khuntikeo N, Yongvanit P. BMP-7 blocks the effects of TGF-β-induced EMT in cholangiocarcinoma. Tumour Biol. 2014;35:9667-76.
159. Chen Y, Ma L, He Q, Zhang S, Zhang C, Jia W. TGF-β1 expression is associated with invasion and metastasis of intrahepatic cholangiocarcinoma. Biol Res. 2015;48:26.

160. Huang CK, Aihara A, Iwagami Y, Yu T, Carlson R, Koga H, Kim M, Zou J, Casulli S, Wands JR. Expression of transforming growth factor β1 promotes cholangiocarcinoma development and progression. Cancer Lett. 2016;380:153-62.
161. Lee MJ, Yu GR, Yoo HJ, Kim JH, Yoon BI, Choi YK, Kim DG. ANXA8 down-regulation by EGF-FOXO4 signaling is involved in cell scattering and tumor metastasis of cholangiocarcinoma. Gastroenterology. 2009;137:1138-50.
162. Clapéron A, Guedj N, Mergey M, Vignjevic D, Desbois-Mouthon C, Boissan M, Saubaméa B, Paradis V, Housset C, Fouassier L. Loss of EBP50 stimulates EGFR activity to induce EMT phenotypic features in biliary cancer cells. Oncogene. 2012;31:1376-88.
163. Clapéron A, Mergey M, Nguyen Ho-Bouldoires TH, Vignjevic D, Wendum D, Chrétien Y, Merabtene F, Frazao A, Paradis V, Housset C, Guedj N, Fouassier L. EGF/EGFR axis contributes to the progression of cholangiocarcinoma through the induction of an epithelial-mesenchymal transition. J Hepatol. 2014;61:325-32.
164. Mon NN, Hasegawa H, Thant AA, Huang P, Tanimura Y, Senga T, Hamaguchi M. A role for focal adhesion kinase signaling in tumor necrosis factor-alpha-dependent matrix metalloproteinase-9 production in a cholangiocarcinoma cell line, CCKS1. Cancer Res. 2006;66:6778-84.
165. Itatsu K, Sasaki M, Yamaguchi J, Ohira S, Ishikawa A, Ikeda H, Sato Y, Harada K, Zen Y, Sato H, Ohta T, Nagino M, Nimura Y, Nakanuma Y. Cyclooxygenase-2 is involved in the up-regulation of matrix metalloproteinase-9 in cholangiocarcinoma induced by tumor necrosis factor-alpha. Am J Pathol. 2009;174:829-41.

166. Yamada D, Kobayashi S, Wada H, Kawamoto K, Marubashi S, Eguchi H, Ishii H, Nagano H, Doki Y, Mori M. Role of crosstalk between interleukin-6 and transforming growth factor-beta 1 in epithelial-mesenchymal transition and chemoresistance in biliary tract cancer. Eur J Cancer. 2013;49:1725-40.
167. Zhou QX, Jiang XM, Wang ZD, Li CL, Cui YF. Enhanced expression of suppresser of cytokine signaling 3 inhibits the IL-6-induced epithelial-to-mesenchymal transition and cholangiocarcinoma cell metastasis. Med Oncol. 2015;32:105.
168. Leelawat K, Leelawat S, Narong S, Hongeng S. Roles of the MEK1/2 and AKT pathways in CXCL12/CXCR4 induced cholangiocarcinoma cell invasion. World J Gastroenterol. 2007;13:1561-8.
169. Tan XY, Chang S, Liu W, Tang HH. Silencing of CXCR4 inhibits tumor cell proliferation and neural invasion in human hilar cholangiocarcinoma. Gut Liver. 2014;8:196-204.
170. Zhao S, Wang J, Qin C. Blockade of CXCL12/CXCR4 signaling inhibits intrahepatic cholangiocarcinoma progression and metastasis via inactivation of canonical Wnt pathway. J Exp Clin Cancer Res. 2014;33:103.
171. Leelawat K, Leelawat S, Tepaksorn P, Rattanasinganchan P, Leungchaweng A, Tohtong R, Sobhon P. Involvement of c-Met/hepatocyte growth factor pathway in cholangiocarcinoma cell invasion and its therapeutic inhibition with small interfering RNA specific for c-Met. J Surg Res. 2006;136:78-84.
172. Menakongka A, Suthiphongchai T. Involvement of PI3K and ERK1/2 pathways in hepatocyte growth factor-induced cholangiocarcinoma cell invasion. World J Gastroenterol. 2010;16:713-22.

173. Xu YF, Yang XQ, Lu XF, Guo S, Liu Y, Iqbal M, Ning SL, Yang H, Suo N, Chen YX. Fibroblast growth factor receptor 4 promotes progression and correlates to poor prognosis in cholangiocarcinoma. Biochem Biophys Res Commun. 2014 Mar 28;446(1):54-60.
174. El Khatib M, Bozko P, Palagani V, Malek NP, Wilkens L, Plentz RR. Activation of Notch signaling is required for cholangiocarcinoma progression and is enhanced by inactivation of p53 in vivo. PLoS One. 2013;8:e77433.
175. Zhou Q, Wang Y, Peng B, Liang L, Li J. The roles of Notch1 expression in the migration of intrahepatic cholangiocarcinoma. BMC Cancer. 2013;13:244.
176. Matsushima H, Kuroki T, Kitasato A, Adachi T, Tanaka T, Hirabaru M, Hirayama T, Kuroshima N, Hidaka M, Soyama A, Takatsuki M, Kinoshita N, Sano K, Nishida N, Eguchi S. Sox9 expression in carcinogenesis and its clinical significance in intrahepatic cholangiocarcinoma. Dig Liver Dis. 2015;47:1067-75.
177. Huang CK, Iwagami Y, Aihara A, Chung W, de la Monte S, Thomas JM, Olsen M, Carlson R, Yu T, Dong X, Wands J. Anti-Tumor Effects of Second Generation β-Hydroxylase Inhibitors on Cholangiocarcinoma Development and Progression. PLoS One. 2016;11:e0150336.
178. Pei T, Li Y, Wang J, Wang H, Liang Y, Shi H, Sun B, Yin D, Sun J, Song R, Pan S, Sun Y, Jiang H, Zheng T, Liu L. YAP is a critical oncogene in human cholangiocarcinoma. Oncotarget. 2015;6:17206-20.
179. Deng G, Zhu L, Huang F, Nie W, Huang W, Xu H, Zheng S, Yi Z, Wan T. SALL4 is a novel therapeutic target in intrahepatic cholangiocarcinoma. Oncotarget. 2015;6:27416-26.

180. Zhu L, Huang F, Deng G, Nie W, Huang W, Xu H, Zheng S, Yi Z, Wan T. Knockdown of Sall4 inhibits intrahepatic cholangiocarcinoma cell migration and invasion in ICC-9810 cells. Onco Targets Ther. 2016;9:5297-305.
181. Yang H, Lu X, Liu Z, Chen L, Xu Y, Wang Y, Wei G, Chen Y. FBXW7 suppresses epithelial-mesenchymal transition, stemness and metastatic potential of cholangiocarcinoma cells. Oncotarget. 2015;6:6310-25.

CHAPTER 2

Leukemia inhibitory factor protects cholangiocarcinoma cells from drug-induced apoptosis via a PI3K/AKT-dependent Mcl-1 activation

Stuart Duncan Morton[#1], Massimiliano Cadamuro[#1,2], **Simone Brivio**[2], Marta Vismara[2], Tommaso Stecca[3], Marco Massani[3], Nicolò Bassi[3,4], Alberto Furlanetto[5], Ruth Elizabeth Joplin[6], Annarosa Floreani[4], Luca Fabris[1,7], and Mario Strazzabosco[2,7]

[1]Department of Molecular Medicine, University of Padua, Padua, Italy
[2]Department of Surgery and Translational Medicine, University of Milan-Bicocca, Milan, Italy
[3]Fourth Surgery Division, Treviso Regional Hospital, Treviso, Italy
[4]Department of Surgical, Oncological and Gastroenterological Sciences, University of Padua, Padua, Italy
[5]Pathology Unit, Treviso Regional Hospital, Treviso, Italy
[6]School of Immunity and Infection, University of Birmingham, Birmingham, UK
[7]Section of Digestive Diseases, Yale University School of Medicine, New Haven, CT, USA
[#]these authors contributed equally to this article

***Published on**: Oncotarget, 2015 Sep 22;6(28):26052-64. doi: 10.18632/oncotarget.4482.*

ABSTRACT

Cholangiocarcinoma (CCA) is an aggressive, strongly chemoresistant liver malignancy. Leukemia inhibitory factor (LIF), an interleukin 6 family cytokine, promotes the progression of various carcinomas. To investigate the role of LIF in CCA, we first evaluated the expression of LIF and its receptor (LIFR) in human samples. LIF secretion and LIFR expression were then assessed in established and primary human CCA cell lines. In CCA cells, we tested the effects of LIF on proliferation, invasion, induction of a stem cell-like phenotype, and chemotherapy-induced (gemcitabine+cisplatin) apoptosis. To dissect the intracellular mechanisms activated in CCA cells in response to LIF, we evaluated the expression levels of pSTAT3, pERK1/2, and pAKT, as well as of pro-apoptotic (Bax) and anti-apoptotic (Mcl-1) proteins. LIF effect on chemotherapy-induced apoptosis was further evaluated after LIFR silencing and Mcl-1 inactivation. Results showed that LIF and LIFR expression were higher in neoplastic than in control cholangiocytes. Of note, LIF was also expressed by tumor stromal cells. LIF had no effects on CCA cell proliferation, invasion, and stemness signatures, but it effectively counteracted drug-induced apoptosis. Upon LIF stimulation, decreased apoptosis was associated with both AKT activation and Mcl-1 up-regulation, an effect abrogated by PI3K inhibition. LIFR silencing and Mcl-1 blockade restored drug-induced apoptosis. In conclusion, autocrine and paracrine LIF signaling promotes chemoresistance in CCA by up-regulating Mcl-1 via a novel

STAT3- and MAPK-independent, PI3K/AKT-dependent pathway. Targeting LIF signaling may increase CCA responsiveness to chemotherapy.

INTRODUCTION

Cholangiocarcinoma (CCA) is a highly aggressive cancer arising from epithelial cells lining intrahepatic (iCCA) or extrahepatic (eCCA) bile ducts. Although considered a rare tumor, incidence of CCA (particularly of iCCA) has steadily increased over the last few decades [1]. Despite this trend, treatment options remain limited to surgical resection and liver transplantation, and the overall survival beyond a year from diagnosis still remains less than 5% [1,2]. In fact, resection can only be offered to a minority of patients (20–40%) because of a propensity for early intrahepatic or lymph node metastatic dissemination, whereas liver transplant is available only for carefully selected cases in a few, highly-specialized liver centers [2,3]. Both procedures are further complicated by high rates of recurrence [2,3]. For patients ineligible for surgery, palliation including radiotherapy, photodynamic therapy or stenting to relieve biliary obstruction, may provide some benefit [2,4]. Notably, chemotherapy is recognized as largely ineffective, due to the high resistance of CCA cells to drug cytotoxicity [5]. A recent study shows that combined administration of gemcitabine (GEM) and cisplatin (CDDP) in the treatment of advanced

CCA increases patient overall survival of about four months compared with patients treated with GEM alone [6].

Although the mechanisms of chemoresistance in CCA are poorly understood, the extensive desmoplastic reaction typical of CCA has been suggested to play a role. In fact, the close interplay between the tumor epithelium and surrounding stromal cells, especially cancer-associated fibroblasts (CAF) and tumor-associated macrophages (TAM), may endow CCA cells with several malignant properties, including enhanced proliferation, motility, invasiveness, and resistance to apoptosis [7,8]. Among the cytokines released within the tumor microenvironment, interleukin (IL)-6 plays a pivotal role in CCA pathogenesis, as a potent stimulator of cancer growth [9,10].

Leukemia inhibitory factor (LIF) is a pleiotropic pro-inflammatory cytokine belonging to the IL-6 superfamily that is secreted by a variety of epithelial and stromal cells (e.g., fibroblasts, monocytes, macrophages, T-cells), albeit generally at very low levels [11]. However, LIF secretion may be potently stimulated by various pro-inflammatory cytokines, such as IL-6, IL-1 and tumor necrosis factor (TNF)-α, leading to elevated serum LIF levels in cancer patients [12,13]. LIF effects on cell functions are multifaceted, and still not extensively detailed. These effects closely depend on cell maturity and cell type, and may influence the balance between maintenance of pluripotency and differentiation, as well as the balance between proliferation and apoptosis [11,13,14]. Following LIF binding, the low-

affinity LIF receptor (LIFR) dimerizes with glycoprotein (gp)130 to form a high-affinity complex that transduces LIF signal through different intracellular pathways, in particular Janus kinase (JAK)-signal transducer and activator of transcription (STAT), mitogen-activated protein kinase (MAPK), and phosphatidylinositol-3 kinase (PI3K)/AKT pathways [15]. An increasing number of studies describe LIF as an important player in the pathogenesis and metastatic spread of various epithelial cancers [16-19]. Moreover, LIF and LIFR/gp130 were found to be expressed in the majority of 30 human carcinoma cell lines of different origin. However, LIF effects on cancer cell behavior were extremely variable, and often conflicting. For instance, LIF promoted proliferation in breast and pancreatic carcinomas, but triggered apoptosis in colon and gastric carcinomas. Of note, these effects were strictly influenced by the signaling pathways activated downstream of LIFR [20].

To date, very little is known about the role of LIF in CCA. Therefore, in this study, we evaluated: 1) the distribution of LIF, LIFR, and gp130 in human CCA liver tissue derived from surgical resection; 2) the secretion of LIF and the expression of LIFR in primary and established human CCA cell lines; 3) the functional effects of LIF on CCA cells with respect to: a) cell proliferation and invasion, b) cell viability and apoptosis in response to the chemotherapeutic agents currently used in CCA (GEM, CDDP), c) the induction of a stem cell-like

phenotype; d) the expression of pro- and anti-apoptotic proteins; and e) the downstream effectors of the signal transduction.

RESULTS

LIF, LIFR and gp130 were more extensively expressed by neoplastic bile ducts compared to peritumoral tissue. Analysis of histological sections from resected human CCA liver revealed a significantly more extensive immunoreactivity of LIF ($p<0.001$) and LIFR ($p<0.001$) (Table 1) on bile ducts in tumoral areas (Figure 1A, 1C) compared with matched, peritumoral tissue (Figure 1B, 1D). Bile ducts of peritumoral areas were LIF-negative in all 12 samples, whereas 17/19 (89%) of neoplastic tissue contained LIF-positive bile ducts of different degree (Table 1). Similarly, the tumor reactive stroma surrounding the neoplastic bile ducts showed more extensive LIF immunoreactivity than the peribiliary stroma in peritumoral tissue ($p<0.001$) (Table 1). Immunofluorescence studies revealed that in the tumor reactive stroma, LIF was expressed by inflammatory cells (CD45-positive), likely including macrophages, lymphocytes and neutrophils as evaluated by immunoperoxidase, as well as by CAF (alpha smooth muscle actin (α-SMA)-positive) (Figure 1G, 1H). Only 4/12 peritumoral samples (33%) had extensive (>30%) LIFR staining in bile ducts, whereas extensive LIFR positivity in neoplastic bile ducts was present in 17/19 (89%) CCA samples (Table 1). Gp130 expression on bile ducts in CCA and peritumoral tissue paralleled that of LIFR

(Figure 1E, 1F). By categorizing the CCA areas, a significantly higher extent of LIF staining in ductular-like than in mucin-producing tumoral bile ducts was determined (Supplementary Figure 1A, 1C); in contrast, no significant difference in the extent of LIFR staining was found between the two CCA subtypes (Supplementary Figure 1B, 1C).

LIF

	BILE DUCTS		STROMAL CELLS	
Score	**CCA**	**Peritumoral**	**CCA**	**Peritumoral**
0	2	12	1	7
1	7	0	8	4
2	9	0	8	1
3	1	0	2	0
Total	19	12	19	12

LIFR

	BILE DUCTS	
Score	**CCA**	**Peritumoral**
0	1	2
1	1	6
2	5	3
3	12	1
Total	19	12

Table 1. Extent of LIF-positive and LIFR-positive bile ducts/stromal cells in CCA and peritumoral areas of resected liver tissue sections. (0 = <5%; 1 = 5–30%; 2 = 30–70%; 3 = >70% area of positive ducts).

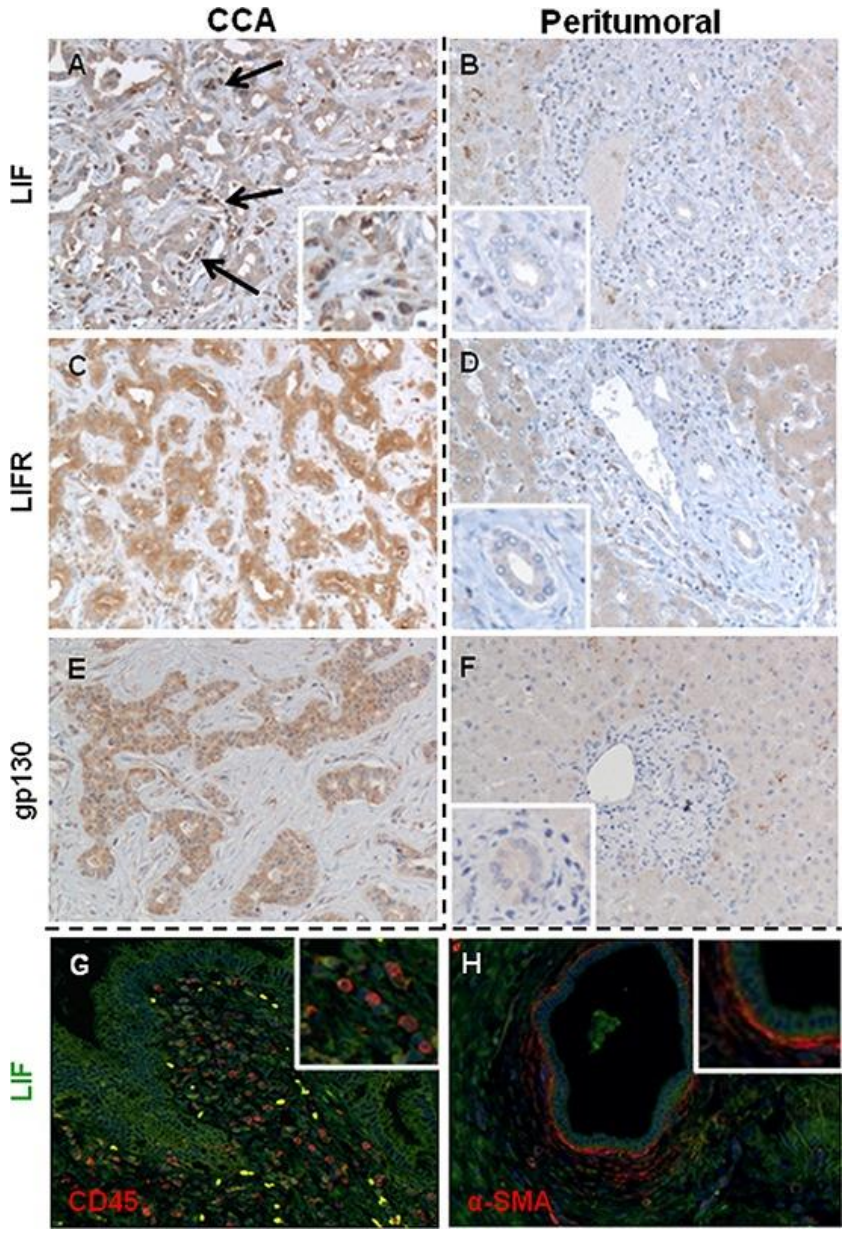

Figure 1. LIF, LIFR and gp130 immunohistochemical expression in CCA and peritumoral areas of human liver samples. In CCA bile ducts, the extensiveness of LIF (A) expression was heterogeneously distributed among samples, whereas the

staining of LIFR (C) and gp130 (E) was more homogeneous. In contrast, LIF (B), LIFR (D), and gp130 (F) immunoreactivity was significantly less in bile ducts of matched peritumoral tissues. By immunohistochemistry (A, black arrows and inset) and dual immunofluorescence (G and H), we demonstrated that LIF (green) was also extensively expressed by CD45-positive cells (red, G) and α-SMA-positive cells (red, H) that juxtaposed neoplastic biliary structures. Original magnification: A-H, 200×; insets, 400×.

LIFR protein expression was greater in CCA cells than in controls. Relative amounts of LIFR protein obtained from primary and established CCA cell lines and control cholangiocytes were evaluated by Western blotting (WB). Although LIFR protein expression levels were heterogeneous among CCA cells, the average level was 7 times greater than that of controls (1.05 ± 0.56 vs. 0.14 ± 0.03) (Figure 2A).

LIF secretion by cholangiocytes was variable. Using ELISA, no significant difference was found between the amount of LIF secreted by primary neoplastic or control cholangiocytes (29.9 ± 28.7 vs. 20.7 ± 0.3 pg/mL). However, the amount of LIF secreted by primary CCA cells was extremely variable, ranging from 0 to 95.7 pg/mL (Figure 2B). Among the established CCA cell lines, HuCCT-1 (iCCA) and TFK-1 (eCCA) cells expressed LIFR and secreted LIF (Figure 2A, 2B), as confirmed by immunofluorescence in cultured cells (Figure 2C, 2D). Therefore, these cell lines were selected for subsequent in vitro experiments. Data on LIFR expression and LIF secretion (obtained by WB analysis and ELISA, respectively) were further confirmed by real-

time PCR in established and primary CCA cell lines, as well as in control cholangiocytes (Supplementary Figure 2A, 2B).

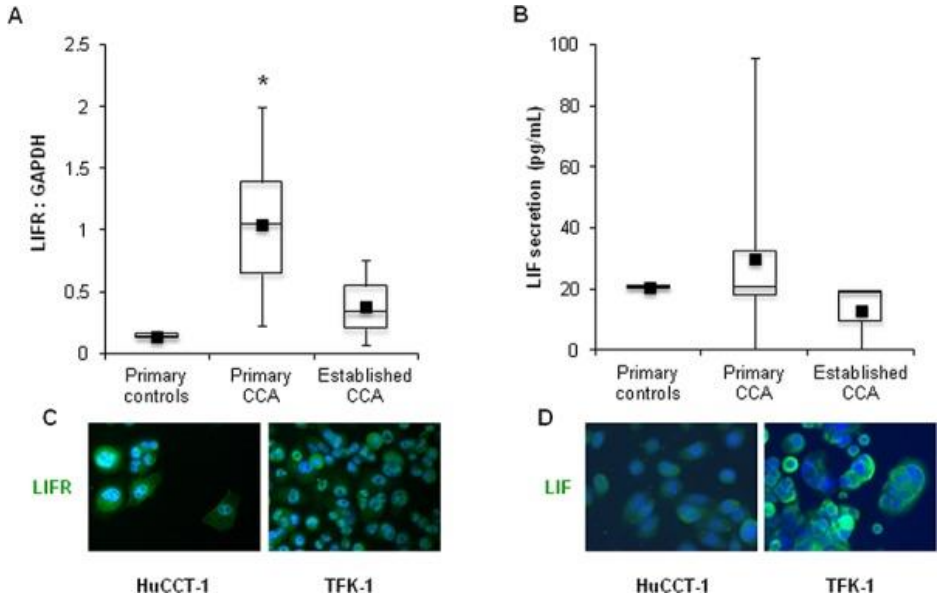

Figure 2. LIFR and LIF expression in human primary and established CCA cell lines. As evaluated by WB, LIFR protein levels were higher although variable in primary (n = 7) and established (n = 3) CCA cell lines compared with control cholangiocytes (n = 2) (A). Using ELISA, LIF was found to be secreted by both neoplastic and control cholangiocytes, though with a large variability (B). Among the established CCA cell lines, only HuCCT-1 and TFK-1 cells expressed LIFR (C) and LIF (D), as shown by immunocytochemistry. Original magnification: 200x; *p<0.05 vs. primary controls.

LIF did not promote proliferation and invasion of established CCA cell lines, but it protected them from apoptosis induced by chemotherapeutic agents. HuCCT-1 and TFK-1 cells challenged with increasing doses of recombinant human (rh)LIF did not show any

significant increase in the proliferative rate, except for a minimal change with the lowest dose in TFK-1 cells (Supplementary Figure 4A, 4B). Additionally, no change in invasive functions was observed with both CCA cell lines in response to rhLIF (Supplementary Figure 4E, 4F). To understand whether LIF may stimulate CCA cell proliferation in an autocrine fashion, thereby precluding further stimulation by exogenous LIF, we performed an MTS assay in CCA cells with genetic inactivation of LIFR. Upon transfection of 3 different siRNAs, the extent of the reduction in LIFR expression in HuCCT-1 and TFK-1 cells was evaluated by both real-time PCR and WB (Supplementary Figure 3). Using the 2 most effective siRNAs (siRNA1 and siRNA2), the effect of autocrine LIF on cell proliferation was evaluated by comparing silenced cells with scrambled controls in the absence of rhLIF treatment. No decrease in the proliferative rate was found in LIFR silenced cells compared with scrambled controls (Supplementary Figure 4C, 4D). We next turned at evaluating whether LIF can protect CCA cells from the cytotoxic effects of chemotherapeutic drugs currently used in the treatment of CCA. To this end, HuCCT-1 and TFK-1 cells were treated with CDDP, GEM, and GEM+CDDP after a pre-incubation with/without rhLIF, and their viability was then assessed by MTS. A drug-induced decrease in cell viability by 34–89% and 23–64% was observed in HuCCT-1 and TFK-1 cells, respectively (Table 2). This cytotoxic effect was significantly counteracted by rhLIF, which augmented cell viability by up to 69.0 ± 36.7% in HuCCT-1 (Figure 3A)

and 73.1 ± 17.7% in TFK-1 (Figure 3B) cells. To understand whether LIF-mediated cytoprotection relies on the ability of LIF to hinder apoptosis, we assessed the levels of active caspases 3/7, whose up-regulation is a hallmark of an ongoing apoptotic process. As expected, a marked increase in the activation of caspase 3/7 was observed in CCA cells exposed to GEM+CDDP. However, pre-treatment with rhLIF significantly reduced caspases 3/7 activity by 24% in HuCCT-1 and 22% in TFK-1 cells compared with cells challenged with GEM+CDDP in the absence of rhLIF pre-treatment (Figure 3C, 3D). The ability of LIF to exert anti-apoptotic effects in CCA was further confirmed in cells silenced for LIFR. Genetic inactivation of LIFR in cells exposed to rhLIF resulted in an increased drug-induced activation of caspases 3/7, comparable to that observed in cells without rhLIF pre-treatment (Figure 3C, 3D).

	GEM (30 µM)	CDDP (17 µM)	Mix
HuCCT-1	38.32 ± 2.40	65.66 ± 4.10	10.87 ± 1.07
TFK-1	62.03 ± 7.21	77.16 ± 4.54	35.79 ± 5.36

GEM, gemcitabine; CDDP, cisplatin; Mix, GEM + CDDP

Table 2. Percentage of viable CCA cells following a 24-hour treatment with chemotherapeutic drugs normalized to untreated cells (MTS assay).

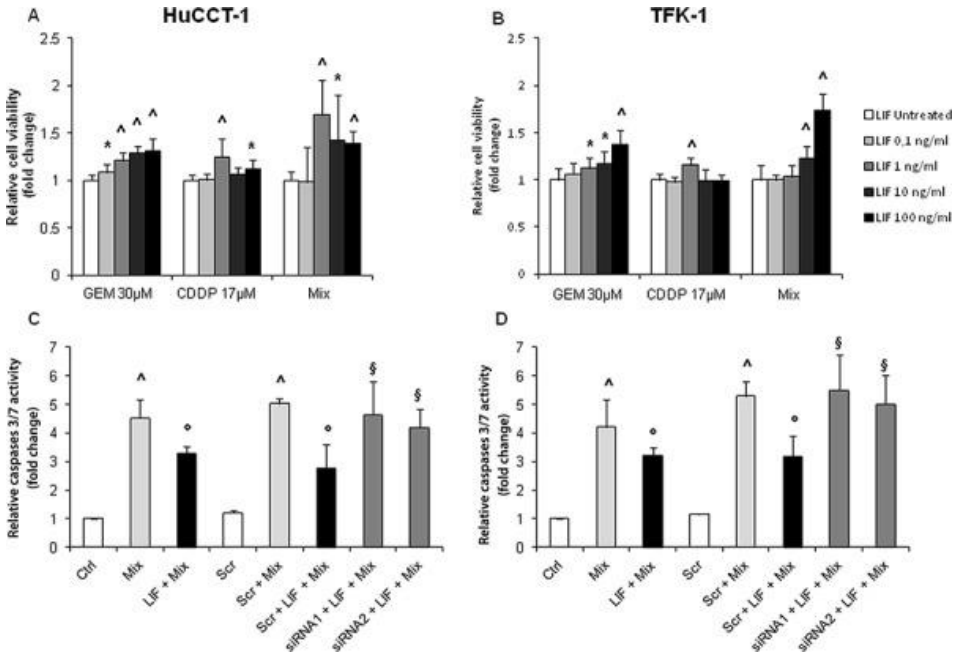

Figure 3. Effects of rhLIF on cell viability and apoptosis of CCA cells challenged with chemotherapeutic agents (GEM, CDDP, or GEM+CDDP). As evaluated by MTS assay, the pre-treatment of HuCCT-1 (A) and TFK-1 (B) cells with rhLIF was able to significantly counteract the cytotoxic effect of the chemotherapeutic agents, GEM, CDDP and GEM+CDDP (Mix). As assessed by caspase GLO 3/7 assay, the activation of caspases 3/7 in response to Mix in both CCA cell lines (C and D, pale gray columns) was significantly reduced by the pre-treatment with rhLIF (100 ng/mL) (C and D, black columns). In addition, the reduction of LIFR expression by two specific siRNAs was able to abolish the anti-apoptotic effects of rhLIF (C and D, dark gray columns). *p<0.05 vs. untreated; ^p<0.01 vs. untreated; °p<0.05 vs Mix treatment; §p<0.05 vs. Scr treated with Mix; n = minimum of 3 in duplicate.

LIF did not induce a stem cell-like phenotype in established CCA cell lines. To evaluate whether the anti-apoptotic functions of LIF are associated with the induction of a stem cell-like phenotype, as described for LIF in malignant melanoma [17], we evaluated the gene expression of two well-recognized stem cell markers, i.e. Nanog and

Oct4, following rhLIF stimulation. However, no significant up-regulation of either stem cell marker was detected in rhLIF-treated cells compared to untreated cells (Supplementary Figure 5A, 5B).

In CCA cells, LIF induced Mcl-1 up-regulation via PI3K/AKT, without activating STAT3 or ERK1/2. To dissect the intracellular signaling mediating the protective effect of LIF against drug-induced apoptosis in CCA cells, the relative expression levels of pBax (pro-apoptotic protein), Bcl-2, and Mcl-1 (anti-apoptotic proteins) were analyzed by WB in rhLIF-treated HuCCT-1 and TFK-1 cells. Compared with untreated cells, pBax levels remained unchanged (Supplementary Figure 6A, 6B), whereas Mcl-1 levels significantly increased in both CCA cell lines (Figure 4A, 4B). In contrast with pBax and Mcl-1, Bcl-2 was not expressed in either HuCCT-1 or TFK-1 cells (data not shown). rhLIF did not induce any significant changes in the phosphorylation levels of STAT3 (Figure 5A, 5B) or extracellular signal-regulated kinase (ERK)1/2 (or p44/42 MAPK) (Figure 5C, 5D), two well-known intracellular effectors of LIF [21], in either CCA cell line. In contrast, rhLIF potently stimulated the phosphorylation of AKT (Figure 5E, 5F). The key role of the PI3K/AKT axis in mediating LIF-induced Mcl-1 up-regulation was revealed by treating CCA cells with LY294002, a specific PI3K inhibitor, which significantly reduced Mcl-1 expression in rhLIF-treated HuCCT-1 and TFK-1 cells (Figure 4C, 4D).

In CCA cells, Mcl-1 inactivation abrogated the cytoprotective effects of LIF against chemotherapy-induced apoptosis. To understand whether Mcl-1 plays a central role in the LIF-dependent protection of CCA cells from the cytotoxic effects of chemotherapeutic drugs, we evaluated drug-induced apoptosis in HuCCT-1 and TFK-1 cells treated with the selective Mcl-1 inhibitor UMI-77. At our given dosage (10 μM) [22], UMI-77 did not induce any change in cell viability (data not shown), nor affect Mcl-1 expression in both cell lines (data not shown). By caspase 3/7 activation assay, we showed that the extent of apoptosis in GEM+CDDP-treated cells exposed to UMI-77 and rhLIF was comparable to that observed in GEM+CDDP-treated cells without rhLIF exposure (Figure 4C, 4D). Overall, these data point to a Mcl-1-mediated anti-apoptotic effect of LIF against chemotherapy toxicity in CCA, which occurs in a PI3K/AKT-dependent, STAT3- and MAPK-independent manner.

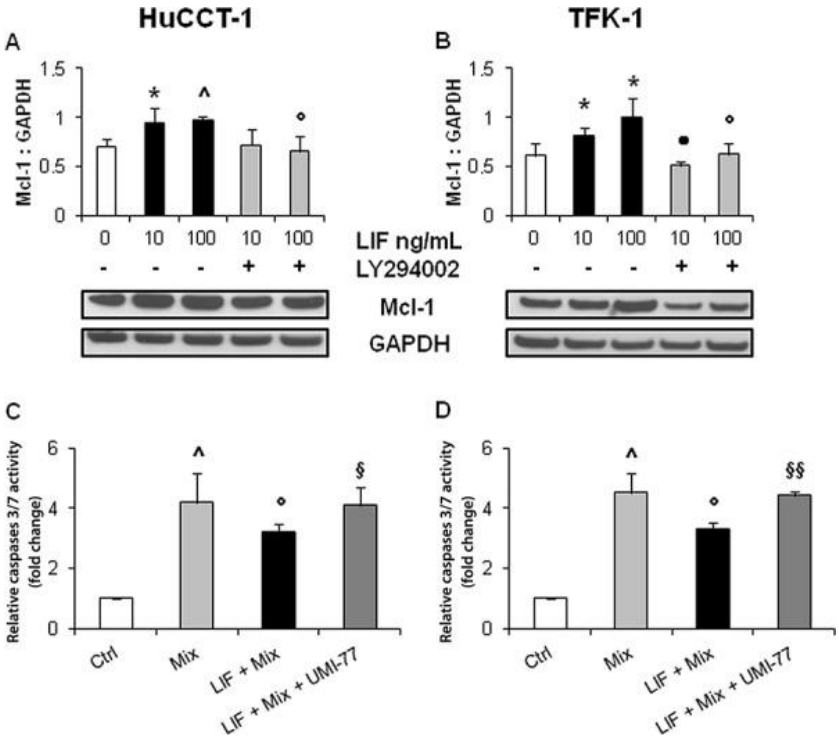

Figure 4. Mcl-1 up-regulation mediates the anti-apoptotic effects of rhLIF in CCA cells. By WB, we found that rhLIF induced a significant up-regulation of Mcl-1 (anti-apoptotic protein) (A and B, black columns) in both HuCCT-1 (A) and TFK-1 (B) cells compared with untreated cells. This effect was abrogated by the specific PI3K inhibitor LY294002 (A and B, gray columns). Representative blots are shown below each respective graph. Interestingly, the protective effect of rhLIF pre-treatment against GEM+CDDP (Mix) cytotoxicity (C and D, black columns) was abolished by UMI-77, a selective small molecule inhibitor of Mcl-1 (C and D, dark gray columns). *p<0.05 vs. untreated; ^p<0.01 vs. untreated; •p<0.01 vs. LIF 10 without LY294002; °p<0.05 vs. LIF 100; §p<0.05 vs Mix treatment; §§p < 0.01 vs Mix treatment; n = minimum of 3.

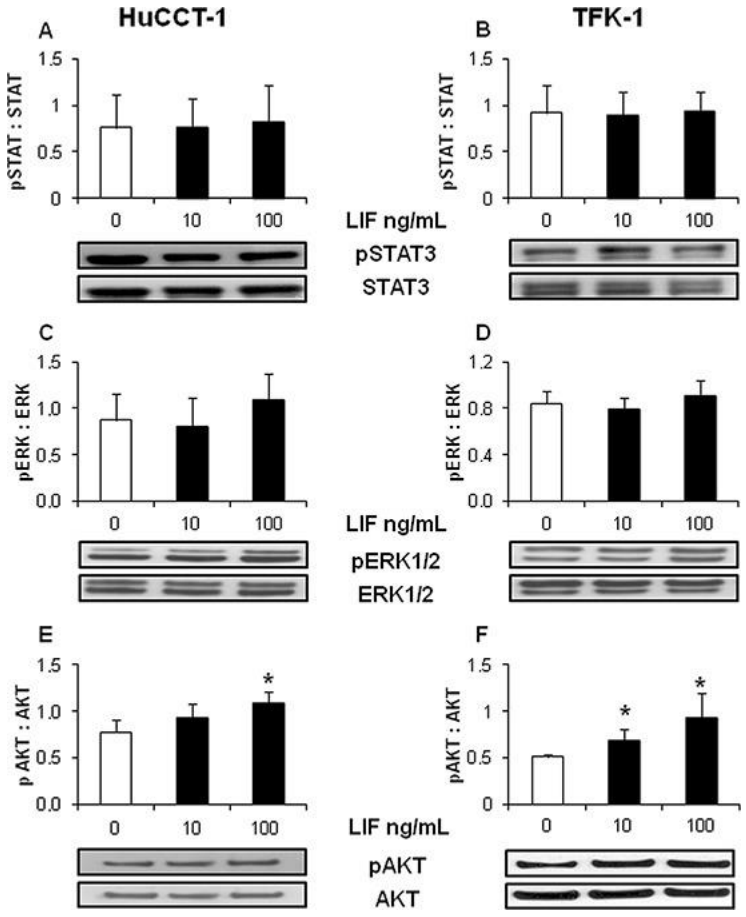

Figure 5. rhLIF acts through a STAT3- and ERK1/2-independent, AKT-dependent pathway. By WB, we showed that rhLIF did not modify the phosphorylation levels of STAT3 (A and B) or ERK1/2 (C and D) in either HuCCT-1 (A and C) or TFK-1 (B and D) cell lines, but it significantly promoted the phosphorylation of AKT (E and F) compared with untreated cells. Representative blots are shown below each respective graph. *p<0.05 vs. untreated; n = minimum of 3.

DISCUSSION

In this study, we investigated the role of LIF in CCA, a malignancy with extremely poor prognosis, with a view to unveiling

molecular mechanisms responsible for its peculiar aggressiveness, possibly amenable to therapeutic intervention. We demonstrated that in CCA, 1) LIF is de novo expressed both in the bile ducts (especially in the ductular-like rather than in the mucin-producing subtype) and in the stromal compartment; 2) its cognate receptor LIFR is selectively up-regulated in neoplastic cholangiocytes; 3) LIF aids neoplastic cholangiocytes to resist apoptosis induced by the chemotherapeutic agents GEM and CDDP, without affecting cell proliferation, invasion or the gain of stemness signatures; 4) anti-apoptotic effects of LIF are largely mediated by Mcl-1, through activation of the PI3K/AKT pathway, without the involvement of the conventional LIF downstream effectors STAT3 and ERK1/2.

In CCA tissue, both cholangiocytes and stromal cells (CAF and inflammatory cells) proved to be a source of LIF. Conversely, LIF was not expressed by bile ducts in the peritumoral regions. In tumor epithelia, LIF expression was heterogeneous, with a greater extensiveness in areas exhibiting a ductular phenotype. These findings are consistent with a recent study showing that LIF is overexpressed in CCA in conjunction with oncostatin M, another IL-6 family member that is closely related to LIF, with pleiotropic functions in cell differentiation, proliferation and invasion [23]. In culture conditions, we could confirm that LIF was variably secreted by CCA cells, in keeping with the heterogeneous distribution observed in histological specimens. Interestingly, LIF secretion may be induced by pro-

inflammatory cytokines typically released by macrophages and activated T-cells populating the local inflammatory microenvironment, such as TNF-α, IL-6, IL-1β and transforming growth factor (TGF)-β, [12,13,25], as well as by hypoxia, which is a typical feature of CCA [17]. Once secreted, LIF itself may induce the expression of LIFR by malignant cells, thus stimulating a positive loop [12,17]. Indeed, our immunohistochemical, WB, and real-time PCR data showed that LIFR was selectively up-regulated in CCA bile ducts. Of note, LIF receptor complex also consists of gp130, which, unlike LIFR, can be expressed by every cell type within the human body [26]. Nevertheless, we verified the expression of gp130, and found that it displayed a profile similar to LIFR. Overall, the de novo expression of LIF and the up-regulation of its receptor in neoplastic bile ducts, along with LIF overexpression in the tumor reactive stroma, indicate the presence of autocrine and paracrine LIF-mediated mechanisms in CCA. Znoyko et al. suggested that an autocrine LIF/LIFR axis is also active in reactive ductules of cirrhotic livers, likely acting as an important signal for ductular reaction [27]. It is interesting to note that in our CCA series, LIF expression was more prevalent in the tumoral areas characterized by a ductular-like appearance, rather than by a mucin-producing phenotype. These two specific iCCA phenotypes have been recently proposed to originate from topographically distinct cholangiocyte subpopulations, i.e. the major hilar ducts for the mucin-producing form, and the smaller ducts associated with hepatic

progenitor cells for the ductular-like variant [28]. Further studies are warranted to understand whether LIF expression may indeed represent a signature of an iCCA subtype arising from hepatic progenitor cells.

Despite the observation that LIF was prevalently expressed in the ductular-like areas of CCA, we found that LIF did not exert any proliferative or pro-invasive effects in CCA cells. The effects of LIF on neoplastic cells are highly variable, and its failure to stimulate proliferation or invasiveness has been already reported in other epithelial cancers [20]. The nature of the functional effects of LIF in different cancer cell types is actually dependent upon the signal transduction pathways that may be activated downstream of its receptor [11]. Our data illustrate that LIF enabled CCA cells to overcome apoptosis induced by GEM and CDDP, which have been recently proposed in the treatment of advanced CCA [6]. In CCA cells that were exposed to GEM+CDDP, LIF could enhance their viability by up to 73% compared with LIF-untreated cells. In accordance with these findings, LIF was able to hamper the increase of active caspases 3/7 induced by GEM+CDDP by 22–24% in both CCA cells. Of note, activation of caspase 3/7 is a fundamental step initiating the cascade of events ultimately leading to apoptotic cell death. The relevance of LIF signaling in conferring anti-apoptotic properties upon CCA cells was confirmed by the restoration of GEM+CDDP cytotoxicity when LIFR was silenced.

To study the mechanisms underlying the resistance to drug-induced apoptosis mediated by LIF, we first evaluated the possible involvement of LIF in inducing a stem cell-like phenotype in CCA cells. Cancer stem cells have an unlimited capacity for self-renewal, and an impressive capacity for drug resistance. Therefore, their activation in CCA may largely account for the failure of current chemotherapies. LIF has been recently reported to regulate the expression of stemness-related transcription factors, including Nanog and Oct4, in malignant melanoma [17]. Importantly, Nanog and Oct4 are recognized as inducers of a stem cell-like phenotype in multiple types of human cancer, and their expression was found to correlate with resistance to gemcitabine or cisplatin treatment [29,30]. However, in our experimental conditions, LIF failed to modulate their gene expression levels, implying that its anti-apoptotic functions are unlikely to be related to a dedifferentiation of CCA cells to a cancer stem cell phenotype. Therefore, we turned to study the balance between pro-apoptotic and anti-apoptotic proteins of the Bcl-2 family. The anti-apoptotic Bcl-2 family member Mcl-1 is known to act as a critical survival factor in both hematogenous and solid tumors, and is currently regarded as a major oncogene [31]. Importantly, its expression has been widely documented in both normal and malignant cholangiocytes [32]. In this study, we demonstrated that Mcl-1 expression by CCA cells can be further augmented by LIF treatment, whereas the expression of the pro-apoptotic protein pBax remained

unchanged, suggesting that this dysregulation may be responsible for apoptosis evasion induced by LIF. JAK/STAT3, MAPK and PI3K are common downstream effectors of LIFR [15,16,33], and they have all been reported to mediate the IL-6-induced Mcl-1 up-regulation in CCA cells [9,10,33]. In our model, LIF was unable to significantly alter the levels of either pSTAT3 or pERK1/2. Conversely, LIF stimulation increased the expression of pAKT in both CCA cell lines, and treatment of CCA cells with LY294002, a specific PI3K inhibitor, effectively prevented LIF from up-regulating Mcl-1. This demonstrates that the positive modulation of Mcl-1 expression in CCA cells is dependent upon PI3K/AKT activation, as reported in breast cancer [16], nasopharyngeal carcinoma [18], and rhabdomyosarcoma cells [34]. Pro-survival effects of LIF have also been reported in colorectal cancer cells, where LIF can negatively regulate the tumor suppressor p53 through a STAT3-dependent pathway [35]. In our experimental conditions, Mcl-1 inactivation by UMI-77 restored the sensitivity of CCA cells challenged with LIF to chemotherapeutic agents. This finding is in accordance with recent data indicating that maritoclax, a similar selective inhibitor of Mcl-1 triggering its proteosomal degradation, is able to enhance apoptosis induction by the small-molecule Bcl-2 inhibitor ABT-737 in melanoma cells [36].

Overall, our results indicate that in CCA, LIF signaling may be a critical mechanism promoting cancer growth and progression. In fact, LIF is able to protect CCA cells from chemotherapy-induced apoptosis,

via a STAT3- and MAPK-independent, PI3K/AKT-dependent Mcl-1 up-regulation. The pro-oncogenic effects of LIF rely on its broad secretion by both cancer and reactive stromal cells, as well as on the aberrant expression of its receptor by neoplastic bile ducts (Figure 6). In particular, these pro-oncogenic effects are prominent in the ductular-like areas of iCCA. Importantly, LIF-mediated paracrine effects highlight the ability of the tumor reactive stroma to promote therapeutic resistance in epithelial cancers with abundant desmoplasia. Since our histological samples were obtained from patients undergoing surgical resection, and in our center chemotherapy is only reserved for those with advanced CCA (which generally do not perform histological evaluation), correlating LIF/LIFR expression with clinical data was not possible in the present study. However, we demonstrated that the downstream effectors of LIF signaling could represent innovative molecular targets amenable to therapeutic modulation, with a view to increasing CCA responsiveness to conventional chemotherapy.

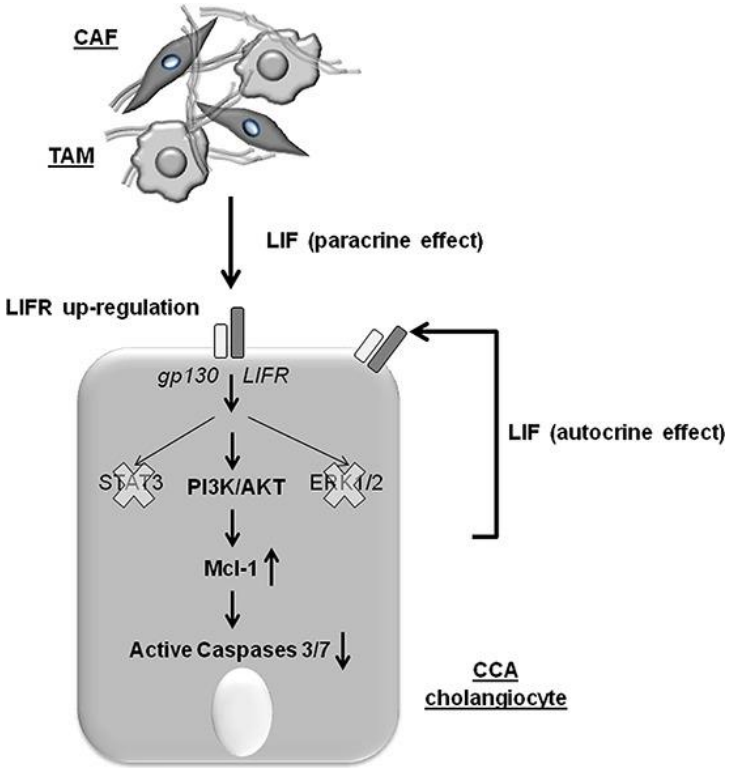

Figure 6. The working model illustrating the molecular mechanisms underlying the protective effects of LIF against chemotherapy in neoplastic cholangiocytes. In CCA cells, LIFR is up-regulated under the influence of LIF released by both neoplastic cholangiocytes themselves (autocrine loop) and reactive stromal cells, such as CAF and TAM (paracrine loop). When LIFR dimerizes with gp130, LIF signaling is transduced through the PI3K/AKT pathway to increase the expression levels of the anti-apoptotic protein Mcl-1, which confers resistance against chemotherapeutic agents by hampering the activation of caspases 3/7.

Conflicts of interest: All authors have no conflict of interest regarding this study to declare.

Financial support: Progetto di Ricerca Ateneo 2011 (grant #CPD113799/11) to LF, MC and SDM. Associazione Scientifica Gastroenterologica di Treviso (ASGET, "associazione di promozione sociale senza scopo di lucro") to LF and SDM. Associazione Chirurgica Tarvisium to NB, MM and TS. NIH Grant DK079005, Silvio O. Conte Digestive Diseases Research Core Centers – 5P30DK034989", grant from "PSC

partners for a care", projects CARIPLO 2011–0470 and PRIN 2009ARYX4T_005 to MS.

MATERIALS AND METHODS

Tissue samples. Formalin-fixed, paraffin-embedded sections of surgically resected CCA liver from 19 patients were included in the immunohistochemical study and compared with the corresponding peritumoral areas where available (n = 12). The patients were predominantly male (12/19), with a median age of 64 years (min 35; max 81), and 63% (12/19) were iCCA. CCA areas were then categorized as ductular-like or mucin-producing according to Komuta [28].

Cell lines. Three established human CCA cell lines were used: EGI-1, TFK-1 (both eCCA, purchased from Deutsche Sammlung von Mikroorganismen und Zellkulturen, DSMZ, Germany), and HuCCT-1 (iCCA, from Health Science Research Resource Bank, HSRRB, Japan), along with primary biliary cell preparations obtained from surgically resected human iCCA liver samples (n = 7), as previously described [37]. Human cholangiocytes isolated from liver explants of alcoholic liver cirrhosis (n = 2) served as controls. All specimens were reviewed by the same dedicated pathologist (AF) to confirm diagnosis. Local regional ethical committee approval was obtained for tissue collection and cell preparations.

LIF, LIFR and gp130 expression in tissues. By immunohistochemistry, we evaluated the expression of LIF, LIFR and gp130 in bile ducts and the stroma, in both neoplastic and matched peritumoral areas. Further details are provided in the supplementary section. The extent of immunoreactivity was scored by two independent observers (SDM, MC) as: 0 = < 5%; 1 = 5–30%; 2 = 30–70%; 3 = > 70% area of positive cells, as previously reported [38]. In selected tissue specimens, dual immunofluorescence for LIF and α-SMA (myofibroblast marker) or CD45 (inflammatory cell marker) was performed to assess the specific contribution of different stromal cell types to LIF production.

LIF and LIFR expression in cells. To evaluate whether immunohistochemical findings were consistent with in vitro data, LIF and LIFR expression was then assessed in cultured cholangiocytes by immunocytochemistry. LIFR protein expression was also assessed by WB in both established and primary CCA cell lines. Furthermore, gene expression of LIF and LIFR in CCA cell lines was evaluated by real-time PCR. Further details are provided in the supplementary section.

LIF secretion by cultured cholangiocytes. The supernatants of CCA and control cholangiocytes cultured for 24 h at a density of 5×10^4 were analyzed for the presence of secreted LIF using an ELISA kit, according

to the supplier's instructions (Raybiotech, Milan). For each experiment, a LIF standard curve was generated.

Cell proliferation. HuCCT-1 and TFK-1 cells were cultured at a density of 1×10^4 for 48 h with/without exposure to increasing doses (0.1, 1, 10, 100 ng/mL) of recombinant human LIF (rhLIF, R&DSystems). Proliferation activity was assessed by MTS assay according to the supplier's instructions (CellTiter 96 AQueous One Solution Cell Proliferation Assay, Promega).

Cell viability. MTS assay was also used to assess whether LIF (24 h pre-treatment at 0.1, 1, 10, 100 ng/mL) affected the viability of HuCCT-1 and TFK-1 cells in response to a 24 h treatment with cisplatin, 17 μM (CDDP; Sigma-Aldrich) [39] and gemcitabine, 30 μM (GEM; Sigma-Aldrich) [40], either alone or in combination (GEM+CDDP).

Stem cell-like phenotyping. Real-time PCR was used to assess LIF effect (100 ng/mL) on Nanog and Oct4 gene expression. RNA was isolated from cultured cells, as previously described [41]. Further details are available in the supplementary section.

Cell invasiveness. The invasiveness of HuCCT-1 and TFK-1 cells was assessed by Boyden chamber assay, as previously described [42]. Methodology is detailed in the supplementary section.

Downstream effectors of LIF signaling in CCA cells. After exposure of HuCCT-1 and TFK-1 cells to rhLIF (10, 100 ng/mL) for 15 min (STAT3, pSTAT3, ERK1/2, pERK1/2, AKT, pAKT) or 24 h (Bax, pBax, Bcl-2 and Mcl-1), the expression level of different proteins of interest was evaluated by WB (see the supplementary section). To unravel the pathway regulating Mcl-1 expression, its protein expression was also measured in CCA cells pre-treated with the PI3K chemical inhibitor LY294002 (10 μM, Sigma) [43] for 10 mins, and then treated with rhLIF plus LY294002 for 24 h.

Activation of caspases 3/7. HuCCT-1 and TFK-1 cells were seeded into a 96-well plate at a density of 1×10^4 per well with/without rhLIF (100 ng/mL) for 24 h, prior to treatment with GEM+CDDP for 12 h. The luminescence-based solution Caspase-Glo 3/7 (Promega) was then used to assess activation of caspases 3/7. Luciferase reaction was evaluated using a microplate reader (BMG Labtech).

Mcl-1 inactivation. Apoptotic response following GEM+CDDP treatment, assessed as described above (i.e., activation of caspases 3/7), was also evaluated upon Mcl-1 inhibition in HuCCT-1 and TFK-1 cells. We used a novel, selective, small molecule inhibitor of Mcl-1, UMI-77 (10 μM), for 24 h [22]. Antagonism of Mcl-1 by UMI-77 does not rely on the down-regulation of its expression, but on the ability of UMI-77 to block the heterodimerization of Mcl-1 with pro-apoptotic

members of the Bcl-2 family, including Bax and Bak [22, 44]. Specifically, the inhibitory effect of UMI-77 is related to its binding to the BH3-binding groove of Mcl-1.

Silencing of LIFR. Gene silencing was performed using commercially available siRNAs against LIFR, and scramble RNA was used as a control (Life Technologies). HuCCT-1 and TFK-1 cell lines were transfected using Lipofectamine 2000 transfection reagent (Life Technologies). Further details are provided in the supplementary section.

Statistical analyses. Results are shown as the mean ± standard deviation. Statistical comparisons were made using Student's t-test. Statistical analyses were performed using SPSS 20.0 software (IBM Corp.). A p value < 0.05 was considered significant.

REFERENCES

1. Bragazzi M, Cardinale V, Carpino G, Venere R, Semeraro R, Gentile R, Gaudio E, Alvaro D. Cholangiocarcinoma: Epidemiology and risk factors. Transl Gastrointest Cancer. 2011;1:21–32.

2. Razumilava N, Gores GJ. Classification, Diagnosis, and Management of Cholangiocarcinoma. Clin Gastroenterol Hepatol. 2013;11:13–21.

3. Bridgewater J, Galle PR, Khan SA, Llovet JM, Park JW, Patel T, Pawlik TM, Gores GJ. Guidelines for the diagnosis and management of intrahepatic cholangiocarcinoma. J Hepatol. 2014;60:1268–1289.

4. Quyn AJ, Ziyaie D, Polignano FM, Tait IS. Photodynamic therapy is associated with an improvement in survival in patients with irresectable hilar cholangiocarcinoma. HPB (Oxford) 2009;11:570–577.
5. Gatto M, Bragazzi MC, Semeraro R, Napoli C, Gentile R, Torrice A, Gaudio E, Alvaro D. Cholangiocarcinoma: update and future perspectives. Dig Liver Dis. 2010;42:253–260.
6. Valle J, Wasan H, Palmer DH, Cunningham D, Anthoney A, Maraveyas A, Madhusudan S, Iveson T, Hughes S, Pereira SP, Roughton M. Cisplatin plus gemcitabine versus gemcitabine for biliary tract cancer. N Engl J Med. 2010;362:1273–1281.
7. Rizvi S, Gores GJ. Pathogenesis, diagnosis, and management of cholangiocarcinoma. Gastroenterology. 2013;145:1215–1229.
8. Zabron A, Edwards RJ, Khan SA. The challenge of cholangiocarcinoma: dissecting the molecular mechanisms of an insidious cancer. Dis Model Mech. 2013;6:281–292.
9. Meng F, Yamagiwa Y, Ueno Y, Patel T. Over-expression of interleukin-6 enhances cell survival and transformed cell growth in human malignant cholangiocytes. J Hepatol. 2006;44:1055–1065.
10. Kobayashi S, Werneburg NW, Bronk SF, Kaufmann SH, Gores GJ. Interleukin-6 contributes to Mcl-1 up-regulation and TRAIL resistance via an Akt-signaling pathway in cholangiocarcinoma cells. Gastroenterology. 2005;128:2054–2065.
11. Mathieu ME, Saucourt C, Mournetas V, Gauthereau X, Theze N, Praloran V, Thiébaud P, Bœuf H. LIF-dependent signaling: new pieces in the Lego. Stem cell reviews. 2012;8:1–15.
12. Kamohara H, Ogawa M, Ishiko T, Sakamoto K, Baba H. Leukemia inhibitory factor functions as a growth factor in pancreas carcinoma cells:

Involvement of regulation of LIF and its receptor expression. Int J Oncol. 2007;30:977–983.
13. McKenzie RC, Szepietowski J. Cutaneous leukemia inhibitory factor and its potential role in the development of skin tumors. Dermatol Surg. 2004;30:279–290.
14. Gadient RA, Patterson PH. Leukemia inhibitory factor, Interleukin 6, and other cytokines using the GP130 transducing receptor: roles in inflammation and injury. Stem cells. 1999;17:127–137.
15. Zouein FA, Kurdi M, Booz GW. LIF and the heart: just another brick in the wall? Eur Cytokine Netw. 2013;24:11–19.
16. Li X, Yang Q, Yu H, Wu L, Zhao Y, Zhang C, Yue X, Liu Z, Wu H, Haffty BG, Feng Z, Hu W. LIF promotes tumorigenesis and metastasis of breast cancer through the AKT-mTOR pathway. Oncotarget. 2014;5:788–801.
17. Kuphal S, Wallner S, Bosserhoff AK. Impact of LIF expression in malignant melanoma. Exp Mol Pathol. 2013;95:156–165.
18. Liu SC, Tsang NM, Chiang WC, Chang KP, Hsueh C, Liang Y, Juang JL, Chow KP, Chang YS. Leukemia inhibitory factor promotes nasopharyngeal carcinoma progression and radioresistance. J Clin Invest. 2013;123:5269–5283.
19. Kellokumpu-Lehtinen P, Talpaz M, Harris D, Van Q, Kurzrock R, Estrov Z. Leukemia-inhibitory factor stimulates breast, kidney and prostate cancer cell proliferation by paracrine and autocrine pathways. Int J Cancer. 1996;66:515–519.
20. Kamohara H, Sakamoto K, Ishiko T, Masuda Y, Abe T, Ogawa M. Leukemia inhibitory factor induces apoptosis and proliferation of human carcinoma cells through different oncogene pathways. Int J Cancer. 1997;72:687–695.

21. Heinrich PC, Behrmann I, Haan S, Hermanns HM, Muller-Newen G, Schaper F. Principles of interleukin (IL)-6-type cytokine signaling and its regulation. The Biochem J. 2003;374:1–20.
22. Abulwerdi F, Liao C, Liu M, Azmi AS, Aboukameel A, Mady AS, Gulappa T, Cierpicki T, Owens S, Zhang T, Sun D, Stuckey JA, Mohammad RM, et al. A novel small-molecule inhibitor of mcl-1 blocks pancreatic cancer growth in vitro and in vivo. Mol Cancer Ther. 2014;13:565–575.
23. Kang MJ, Kim J, Jang JY, Park T, Lee KB, Kim SW. 22q11-q13 as a hot spot for prediction of disease-free survival in bile duct cancer: integrative analysis of copy number variations. Cancer Genet. 2014;207:57–69.
24. Clark EA, Golub TR, Lander ES, Hynes RO. Genomic analysis of metastasis reveals an essential role for RhoC. Nature. 2000;406:532–535.
25. Albrengues J, Bourget I, Pons C, Butet V, Hofman P, Tartare-Deckert S, Feral CC, Meneguzzi G, Gaggioli C. LIF mediates proinvasive activation of stromal fibroblasts in cancer. Cell Rep. 2014;7:1664–1678.
26. Wolf J, Rose-John S, Garbers C. Interleukin-6 and its receptors: A highly regulated and dynamic system. Cytokine. 2014;70:11–20.
27. Znoyko I, Sohara N, Spicer SS, Trojanowska M, Reuben A. Expression of oncostatin M and its receptors in normal and cirrhotic human liver. J Hepatol. 2005;43:893–900.
28. Komuta M, Govaere O, Vandecaveye V, Akiba J, Van Steenbergen W, Verslype C, Laleman W, Pirenne J, Aerts R, Yano H, Nevens F, Topal B, Roskams T. Histological diversity in cholangiocellular carcinoma reflects the different cholangiocyte phenotypes. Hepatology. 2012;55:1876–1888.
29. Lu Y, Zhu H, Shan H, Lu J, Chang X, Li X, Lu J, Fan X, Zhu S, Wang Y, Guo Q, Wang L, Huang Y, et al. Knockdown of Oct4 and Nanog expression inhibits the stemness of pancreatic cancer cells. Cancer Lett. 2013;340:113–123.

30. Noh KH, Kim BW, Song KH, Cho H, Lee YH, Kim JH, Chung JY, Kim JH, Hewitt SM, Seong SY, Mao CP, Wu TC, Kim TW. Nanog signaling in cancer promotes stem-like phenotype and immune evasion. J Clin Invest. 2012;122:4077–4093.

31. Beroukhim R, Mermel CH, Porter D, Wei G, Raychaudhuri S, Donovan J, et al. The landscape of somatic copy-number alteration across human cancers. Nature. 2010;463:899–905.

32. Okaro AC, Deery AR, Hutchins RR, Davidson BR. The expression of antiapoptotic proteins Bcl-2, Bcl-X(L), and Mcl-1 in benign, dysplastic, and malignant biliary epithelium. J Clin Pathol. 2001;54:927–932.

33. Isomoto H, Kobayashi S, Werneburg NW, Bronk SF, Guicciardi ME, Frank DA, Gores GJ. Interleukin 6 upregulates myeloid cell leukemia-1 expression through a STAT3 pathway in cholangiocarcinoma cells. Hepatology. 2005;42:1329–1338.

34. Wysoczynski M, Miekus K, Jankowski K, Wanzeck J, Bertolone S, Janowska-Wieczorek A, Ratajczak J, Ratajczak MZ. Leukemia inhibitory factor: a newly identified metastatic factor in rhabdomyosarcomas. Cancer Res. 2007;67:2131–2140.

35. Yu H, Yue X, Zhao Y, Li X, Wu L, Zhang C, Liu Z, Lin K, Xu-Monette ZY, Young KH, Liu J, Shen Z, Feng Z, et al. LIF negatively regulates tumor-suppressor p53 through Stat3/ID1/MDM2 in colorectal cancers. Nat Commun. 2014;5:5218.

36. Pandey MK, Gowda K, Doi K, Sharma AK, Wang H-G, Amin S. Proteosomal degradation of Mcl-1 by maritoclax induces apoptosis and enhance the efficacy of ABT-737 in melanoma cells. PloS One. 2013;8:e78570.

37. Massani M, Stecca T, Fabris L, Caratozzolo E, Ruffolo C, Furlanetto A, Morton S, Cadamuro M, Strazzabosco M, Bassi N. Isolation and characterization of biliary epithelial and stromal cells from resected human

cholangiocarcinoma: a novel in vitro model to study tumor-stroma interactions. Oncol Rep. 2013;30:1143–1148.

38. Fabris L, Cadamuro M, Moserle L, Dziura J, Cong X, Sambado L, Nardo G, Sonzogni A, Colledan M, Furlanetto A, Bassi N, Massani M, Cillo U, et al. Nuclear expression of S100A4 calcium binding protein increases cholangiocarcinoma invasiveness and metastasization. Hepatology. 2011;54:890–899.

39. Chattopadhyay S, Machado-Pinilla R, Manguan-García C, Belda-Iniesta C, Moratilla C, Cejas P, Fresno-Vara JA, de Castro-Carpeño J, Casado E, Nistal M, Gonzalez-Barón M, Perona R. MKP1/CL100 controls tumor growth and sensitivity to cisplatin in non-small-cell lung cancer. Oncogene. 2006;25:3335–3345.

40. Shord SS, Camp JR, Young LA. Paclitaxel decreases the accumulation of gemcitabine and its metabolites in human leukemia cells and primary cell cultures. Anticancer Res. 2005;25:4165–4171.

41. Spirli C, Locatelli L, Morell CM, Fiorotto R, Morton SD, Cadamuro M, Fabris L, Strazzabosco M. PKA dependent p-Ser- beta-catenin, a novel signaling defect in a mouse model of Congenital Hepatic Fibrosis. Hepatology. 2013;58:1713–1723.

42. Cadamuro M, Nardo G, Indraccolo S, Dall'olmo L, Sambado L, Moserle L, Franceschet I, Colledan M, Massani M, Stecca T, Bassi N, Morton S, Spirli C, et al. Platelet-derived growth factor-D and Rho GTPases regulate recruitment of cancer-associated fibroblasts in cholangiocarcinoma. Hepatology. 2013;58:1042–1053.

43. Spirli C, Okolicsanyi S, Fiorotto R, Fabris L, Cadamuro M, Lecchi S, Tian X, Somlo S, Strazzabosco M. Mammalian target of rapamycin regulates vascular

endothelial growth factor-dependent liver cyst growth in polycystin-2-defective mice. Hepatology. 2010;51:1778–1788.

44. Mohammad RM, Muqbil I, Lowe L, Yedjou C, Hsu HY, Lin LT, Siegelin MD, Fimognari C, Kumar NB, Dou QP, Yang H, Samadi AK, Russo GL, et al. Broad targeting of resistance to apoptosis in cancer. Semin Cancer Biol. 2015 in press.

SUPPLEMENTARY MATERIALS AND METHODS

Immunohistochemistry and immunofluorescence. For immunohistochemical staining, after deparaffinization, sections were rehydrated in alcohol and endogenous peroxidase activity was quenched with methanol containing 3% H_2O_2 for 30 mins. Antigen retrieval was performed by steam-heating the slides for 20 mins in either 10 mmol/L citrate buffer (pH 6) for LIF or 1.27 mM ethylenediaminetetraacetic acid buffer (pH 8) for LIFR and gp130. Blocking was achieved using UltraVision protein block (ThermoScientific) for 8 mins. The sections were incubated with primary antibodies against LIF (1:50, Santa Cruz), LIFR (1:80, Santa Cruz) and gp130 (1:25, Santa Cruz) overnight at 4°C. After rinsing with phosphate-buffered saline 1M (PBS) supplemented with 0.05% Tween20 (PBS-T; both Sigma), slides were incubated for 30 mins at room temperature with EnVision horseradish peroxidase (HRP)-conjugated secondary antibody (DAKO). All antibodies were diluted in PBS. Specimens were developed using 3,3-diaminobenzedine tetrahydrochloride 0.04 mg/mL (Sigma) with H_2O_2 0.01% diluted in

PBS and counterstained with Gill's Hematoxylin N°2 (Sigma). Specimens were analyzed with an Eclipse E800 microscope (Nikon) and LuciaG 5.0 software (Nikon), and images were collected with a digital camera (Nikon, DS-U1). For immunofluorescence, sections were deparaffinized and rehydrated as described above. Antigen retrieval was performed as above using 10 mmol/L citrate buffer (pH 6). Blocking was achieved as above. The sections were incubated with primary antibodies against LIF (1:50, Santa Cruz), and CD45 (1:300, DAKO) or α-SMA (1:100, DAKO) overnight at 4°C. Slides were then incubated for 30 mins at room temperature with the respective secondary Alexa Fluor 488- or 594-conjugated antibody (1:500, Life Technologies) and mounted with Vectastain + DAPI (Vector Laboratories).

Immunocytochemistry. After fixation with 4% paraformaldehyde (Carlo Erba), cells were incubated overnight at 4°C with primary antibodies against LIF (1:100), and LIFR (1:100). After washing with PBS-T, the cells were incubated for 30 mins at room temperature with the appropriate Alexa Fluor 488 secondary antibody (1:500, Life Technologies) and then mounted with Vectastain + DAPI.

ELISA for LIF quantification. Cells were seeded into a 24-well plate at 5×10^4 per well. After 24 h, supernatants were harvested, stored at

-80°C and then the ELISA was developed according to the supplier (RayBiotech). A calibration curve was generated for each experiment.

Western blotting (WB). Equal concentrations of total lysate obtained from cultured cells were electrophoresed on a 4-12% NuPAGE® Novex Bis-Tris gel (Life Technologies) and proteins were transferred to a nitrocellulose membrane (Life Technologies). The membrane was then blocked with 5% non-fat dry milk (Euroclone) in Tris-buffered saline (TBS) supplemented with 0.1% Tween-20 (TBS-T) for 1 hour and then incubated overnight at 4°C with rabbit anti-LIFR (1:1000, Santa Cruz), rabbit anti-Bax (1:500, Santa Cruz), rabbit anti-phosphorylated Bax (pBax) (1:1000; Bioss), rabbit anti-B-cell lymphoma (Bcl)-2 (1:500, Santa Cruz), rabbit anti-myeloid cell leukemia (Mcl)-1 (1:1000, Cell Signaling), rabbit anti-STAT3, rabbit anti-phosphorylated STAT3 (pSTAT3) (both 1:1000, Cell Signaling), rabbit anti-AKT (1:1000, Cell Signaling), rabbit anti-phosphorylated AKT 1/2/3 (pAKT) (1:1000, Santa Cruz), rabbit anti-ERK1/2 (1:1000, Cell Signaling), and rabbit anti-phosphorylated ERK1/2 (pERK1/2) (1:1000, Cell Signaling). As a reference protein, mouse anti-GAPDH (1:10000, Santa Cruz) was used. The membrane was washed 3 times with TBS-T before incubation with goat anti-mouse (1:2000, Sigma) or goat anti-rabbit (1:2000, Bio-Rad) HRP-conjugated secondary antibodies for 1 hour. Proteins were visualized using enhanced chemiluminescence (SuperSignal West Pico, Thermo Scientific).

Stem cell-like phenotyping. Briefly, untreated and rhLIF-treated (100 ng/mL for 24 hours) HuCCT-1 and TFK-1 cells were homogenized in 1 mL TRIzol® Reagent (Life Technologies). Template complementary DNA was obtained by reverse transcription using 0.5 μg of total RNA, Superscript II reverse transcriptase (Life Technologies), random hexamers (50 pmol), and oligo-dT primers (100 pmol) (Promega). Relative transcript levels were quantified using Taqman gene expression probes for human Nanog and Oct4 (Life Technologies) and the real-time PCR was performed on an ABI 7500 thermocycler (Applied Biosystems). The relative expression of each gene was normalized against that of GAPDH.

Gene expression of LIF and LIFR. Using the same approach described for stem-cell phenotyping, we quantified the relative expression levels of LIF and LIFR in established and primary CCA cell lines using specific Taqman gene expression commercially available probes (Life Technologies).

Cell invasiveness. Briefly, 5×10^4 cells were re-suspended in serum-free medium and seeded over a polyvinylpyrrolidone-free polycarbonate, 8 μm-pore membrane (Transwell, Costar) coated with 50 μg/mL Matrigel, within a Boyden microchamber. The lower chambers contained serum-free medium with/without rhLIF (10, 100 ng/mL). After 48 h, cells on the upper surface of the membrane were

removed with a cotton swab whilst cells that adhered to the lower surface were fixed and stained using a Diff-Quick Staining Set (Medion Diagnostics); ten random fields of each membrane were photographed to count the number of clearly discernible nuclei.

Silencing of LIFR. Gene silencing of LIFR was performed using commercially available siRNAs against LIFR; scramble RNA served as a control (both Life Technologies). HuCCT-1 and TFK-1 cell lines were transfected using 20 pM of siRNA and Lipofectamine 2000 transfection reagent (Life Technologies) 24 h after plating. Transfection efficiency was assessed by WB and real-time PCR for LIFR.

SUPPLEMENTARY FIGURES

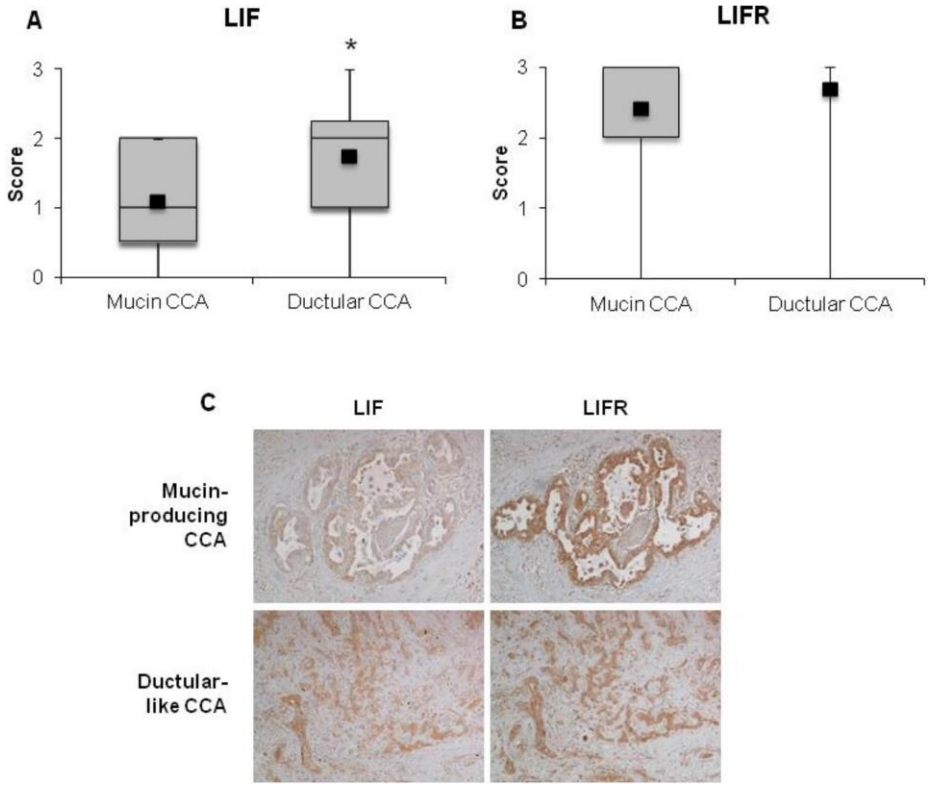

Supplementary Figure 1. Extensiveness of LIF and LIFR expression in ductular-like and mucin-producing areas of CCA. LIF expression was more extensive in ductular-like than in mucin-producing CCA bile ducts (A), whereas no significant difference in LIFR staining was observed between the two CCA phenotypes (B). Representative micrographs illustrating LIF and LIFR staining in sequential sections of mucin-producing (upper panels) and ductular-like (lower panels) CCA areas are shown (C). Original magnification: 200x; *p<0.05.

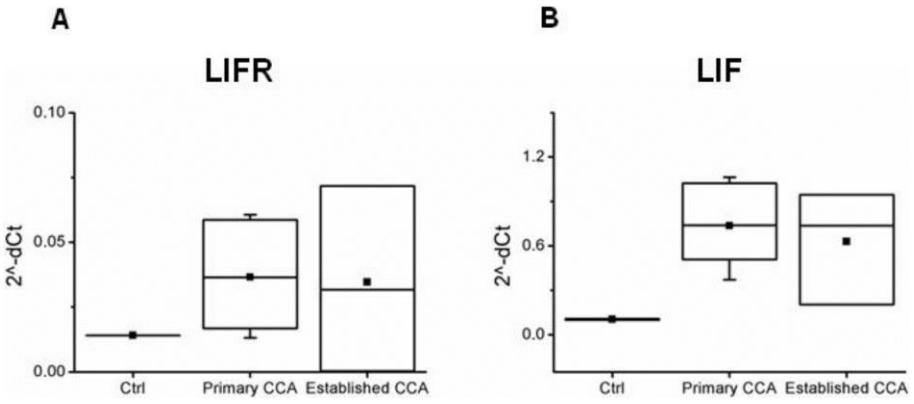

Supplementary Figure 2. LIFR and LIF gene expression quantification in human primary control and neoplastic cholangiocytes, and established CCA cell lines. To confirm data obtained by WB and ELISA, the gene expression of LIFR (A) and LIF (B) was assessed in primary (n = 7) and established (n = 3) CCA cell lines, and in control cholangiocytes (n = 2) by real-time PCR. The results show increased mRNA levels for both receptor and ligand in CCA cells compared with controls.

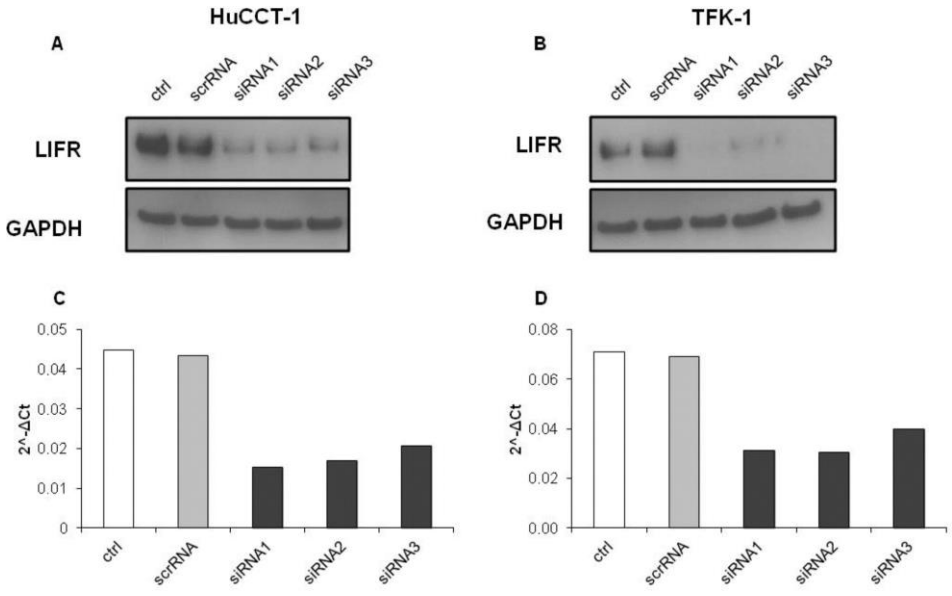

Supplementary Figure 3. Effects of siRNA on LIFR expression in CCA cells. The ability of three different siRNAs (siRNA1, siRNA2, and siRNA3) to suppress LIFR expression was evaluated by both WB and real-time PCR in HuCCT-1 (A and C) and TFK-1 (B and D) cells. All siRNAs induced a pronounced reduction in protein (A and B) and mRNA levels (C and D) of LIFR. Therefore, siRNA1 and siRNA2 were selected for the experiments on cell proliferation (shown in Supplementary Figure 4C, 4D) and drug-induced cytotoxicity (shown in Figure 3C, 3D).

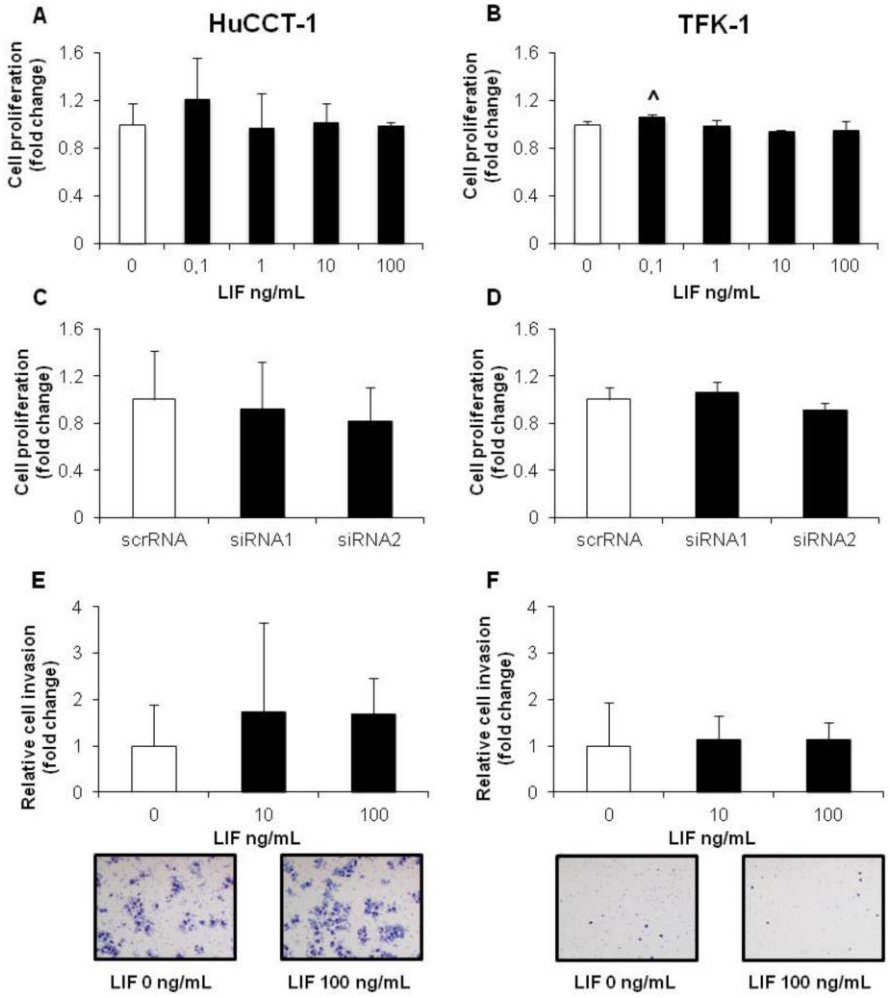

Supplementary Figure 4. LIF did not affect cell proliferation and invasion of HuCCT-1 and TFK-1 cells. By MTS assay, we found that HuCCT-1 (A) and TFK-1 (B) cells challenged with rhLIF at increasing doses did not show any relevant change in cell proliferation, except for a minimal increase with the lowest dose in TFK-1 (^p<0.01 vs. LIF 0; n = 3 in duplicate). Interestingly, in the absence of rhLIF stimulation, LIFR silencing did not reduce cell proliferation of HuCCT-1 (C) and TFK-1 (D) cells compared with scrambled cells, thus ruling out a possible constitutive activation of cell proliferation triggered by autocrine LIF. Additionally, no effects were observed on cell invasion with either HuCCT-1 (E) or TFK-1 (F) cells upon LIF stimulation, as assessed in Boyden chamber assays (n = minimum of 3). Micrographs of representative fields of invaded cells in response to medium alone or LIF supplementation are illustrated. Original magnification: 100×.

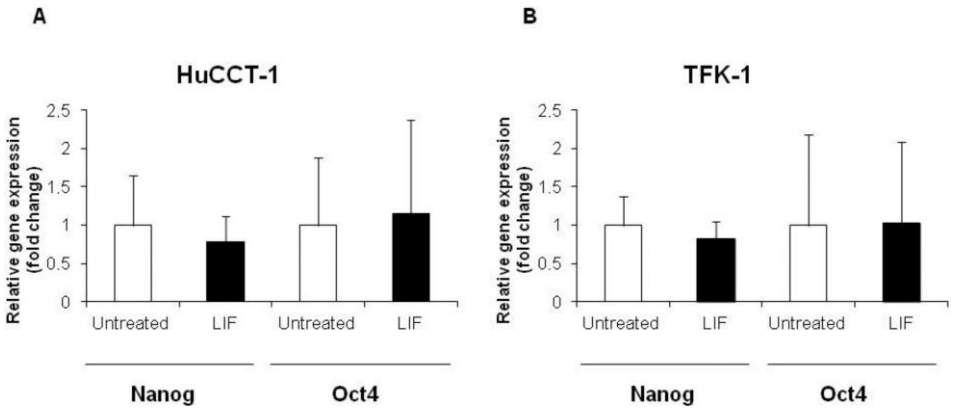

Supplementary Figure 5. rhLIF did not increase gene expression of Nanog and Oct4 in HuCCT-1 and TFK-1 cells. By real-time PCR, we found that rhLIF stimulation (100 ng/mL) was unable to change Nanog and Oct4 mRNA levels in HuCCT-1 (A) and TFK-1 (B) cells (n = 3).

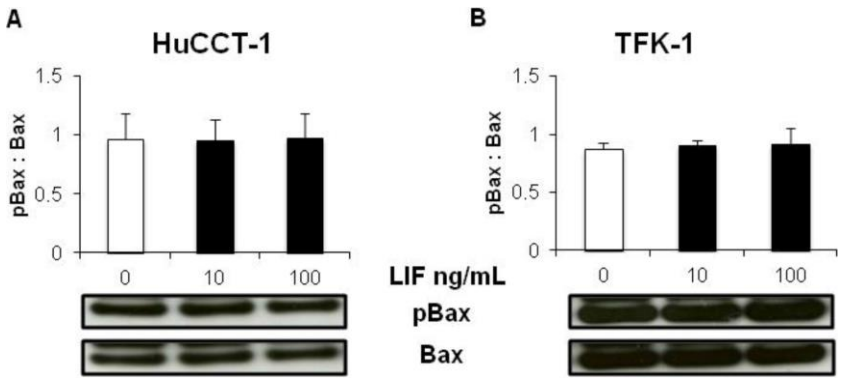

Supplementary Figure 6. Effects of rhLIF on Bax phosphorylation in CCA cells. By WB, we showed that rhLIF did not modify pBax:Bax ratio (pro-apoptotic) in either HuCCT-1 (A) or TFK-1 (B) cells compared with untreated cells. Representative blots are shown below each respective graph (n = 3).

CHAPTER 3

Low-Dose Paclitaxel Reduces S100A4 Nuclear Import to Inhibit Invasion and Hematogenous Metastasis of Cholangiocarcinoma

Massimiliano Cadamuro[1,2], Gaia Spagnuolo[1], Luisa Sambado[3], Stefano Indraccolo[4], Giorgia Nardo[4], Antonio Rosato[4,5], **Simone Brivio**[1], Chiara Caslini[1], Tommaso Stecca[6], Marco Massani[6], Nicolò Bassi[5,6], Eugenio Novelli[7], Carlo Spirli[2,8], Luca Fabris[2,8,9,*], and Mario Strazzabosco[1,2,8,*]

[1]School of Medicine and Surgery, University of Milan-Bicocca, Italy
[2]International Center for Digestive Health (ICDH), University of Milan-Bicocca
[3]Metabolism, Disease and Clinical Nutrition Unit, Treviso Regional Hospital, Italy
[4]Veneto Institute of Oncology IOV – IRCCS, Padua, Italy
[5]Dep. of Surgery, Oncology and Gastroenterology, University of Padua School of Medicine, Italy
[6]4th Surgery Division, Treviso Regional Hospital
[7]Biostatistics Unit, Clinica San Gaudenzio, Novara, Italy
[8]Section of Digestive Diseases, Yale University School of Medicine, New Haven (CT), USA
[9]Dep. of Molecular Medicine (DMM), University of Padua School of Medicine
*these authors contributed equally to this article

***Published on**: Cancer Research, 2016 Aug 15;76(16):4775-4784. doi: 10.1158/0008-5472.CAN-16-0188.*

ABSTRACT

Nuclear expression of the calcium-binding protein S100A4 is a biomarker of increased invasiveness in cholangiocarcinoma (CCA), a primary liver cancer with scarce treatment opportunities and dismal prognosis. In this study, we provide evidence that targeting S100A4 nuclear import by low dose paclitaxel (PTX), a microtubule stabilizing agent, inhibits CCA invasiveness and metastatic spread. Administration of low dose PTX to established (EGI-1) and primary (CCA-TV3) CCA cell lines expressing nuclear S100A4 triggered a marked reduction in nuclear expression of S100A4 without modifying its cytoplasmic levels, an effect associated with a significant decrease in cell migration and invasiveness. While low dose PTX did not affect cellular proliferation, apoptosis or cytoskeletal integrity, it significantly reduced SUMOylation of S100A4, a critical posttranslational modification that directs its trafficking to the nucleus. This effect of lose dose PTX was reproduced by ginkolic acid, a specific SUMOylation inhibitor. Downregulation of nuclear S100A4 by low dose PTX was associated with a strong reduction in RhoA and Cdc42 GTPase activity, MT1-MMP expression and MMP-9 secretion. In a SCID mouse xenograft model, low dose metronomic PTX treatment decreased lung dissemination of EGI-1 cells without significantly affecting their local tumor growth. In the tumor mass, nuclear S100A4 expression by CCA cells was significantly reduced, whereas rates of proliferation and apoptosis were unchanged. Overall, our findings

highlight nuclear S100A4 as a candidate therapeutic target in CCA and establish a mechanistic rationale for the use of low dose PTX in blocking metastatic progression of cholangiocarcinoma.

INTRODUCTION

Cholangiocarcinoma (CCA), a malignancy arising from either the intrahepatic or the extrahepatic bile ducts, still carries a severe prognosis. CCA is responsible for the 10–20% of deaths related to primary liver tumors [1]. In the Western countries, its incidence is steadily increasing in the last decades [1,2], but, unfortunately, the prognosis of CCA has not changed, with less than 5% of patients surviving up to 5 years from diagnosis [1]. At the time of diagnosis, less than 30% of patients are eligible for surgical resection or liver transplantation, the only potentially curative strategies. Thus, in 70% of patients the stage is advanced, because of the tumor invasiveness and early extrahepatic dissemination. Furthermore, success of curative treatments is hindered by the high rate of recurrence, with a 5-year survival after resection around 20–40% [3]. Combined cisplatin and gemcitabine therapy, the current standard of care for advanced CCA, increases patient's overall survival by less than four months with respect to gemcitabine alone [4]. The lack of effective treatments reflects the deep gap in knowledge on the molecular mechanisms underlying CCA invasiveness. Better understanding of these

mechanisms is needed to predict the invasiveness of the individual tumor and to devise molecular targeted therapy [5].

Among the biomarkers of increased tumour invasiveness, S100A4 has drawn particular attention in the last few years. S100A4, a low molecular weight, cytoskeleton-associated calcium-binding protein, is normally expressed by mesenchymal (mostly fibroblasts and macrophages), but not by epithelial cells. S100A4 may handle different functions depending upon its cellular localization. When localized in the cytoplasm, it may interact with cytoskeleton and plasma membrane proteins (including actin, non-muscle myosin-IIA and -IIB, p53, liprin-β1, methionine aminopeptidase-2) [6], thereby contributing to the regulation of cell proliferation, survival, differentiation, as well as cell reshaping and cytoskeletal rearrangement. When translocated to the nucleus, S100A4 may act as transcription factor for several genes, including those encoding adherence junction proteins, thus controlling cell motility [7]. A number of studies have shown that S100A4 is a marker of poor prognosis in breast and colon cancers [7,8]. We have shown that in CCA patients undergoing surgical resection, nuclear expression of S100A4 in tumor cells is a strong, independent prognostic marker of poor outcome in terms of both metastasization and tumor-related death [9]. Furthermore, S100A4 lentiviral silencing significantly reduced motility and invasive capabilities of CCA cells [9], suggesting that nuclear expression of S100A4 is not merely a marker of cancer

invasiveness, but is a key determinant of the metastatic phenotype of CCA.

Aim of this study was to understand the mechanisms by which nuclear S100A4 induces an invasive phenotype in CCA and the mechanism regulating nuclear translocation of S100A4. Unfortunately, mechanisms governing S100A4 expression in the nucleus remain elusive, and there are no strategies to selectively target S100A4 nuclear import. In planning our experiments, we came across studies from the early '90s showing that paclitaxel (PTX) was able to reduce the expression of S100A4 in the B16 murine melanoma cells [10,11]. PTX is a semisynthetic derivative of taxol, a natural diterpene alkaloid, isolated from the bark of Taxus brevifolia. Because of its anti-proliferative and pro-apoptotic effects, PTX is currently used in chemotherapy protocols for the treatment of ovary, lung, thyroid and breast carcinomas [12]. Our study shows that low dose PTX inhibits tumor invasiveness and hematogenous metastases by blocking SUMOylation-dependent S100A4 nuclear import in CCA.

MATERIALS AND METHODS

Human established and primary CCA cell lines. The S100A4-expressing established CCA cell lines, EGI-1 (both in the nucleus and in the cytoplasm) and TFK-1 (only in the cytoplasm), both obtained from extrahepatic CCA [9], were purchased from Deutsche Sammlung von Mikroorganismen und Zellkulturen (DSMZ, Germany). The primary

CCA cell line CCA-TV3 was isolated from a human sample derived from surgical resection of an intrahepatic mass-forming CCA, histologically categorized as cholangiocellular carcinoma (grading G3), performed in Treviso Regional Hospital (MM, TS) as described [13]. Local regional ethical committee approval was obtained for tissue collection and cell preparation. Cultured cells were grown in RPMI1680 supplemented with 10% FBS and 1% penicillin at 37°C in a 5% CO2 atmosphere, and then frozen at low passages (<5). After any resuscitation, cell authentication was performed by checking morphology and by evaluating their immunophenotype as characterized by our previous studies [9,13], including cytokeratin (K)-7, K19, EpCAM (clone HEA125), E-cadherin, β-catenin and S100A4. Following experiments were run in cultured cells with <20 passages. Mycoplasma contamination was excluded using a specific biochemical test (Lonza).

Treatment with PTX. In all experiments, cultured CCA cells were seeded and grown for 24h (otherwise differently indicated) before exposure for 24h to PTX at low doses (1.5 and 15nM, diluted in DMSO, Sigma), except for assessment of cell proliferation, viability, apoptosis and cytoskeletal integrity, where high doses (150 and 1500nM) were further tested. Untreated CCA cells served as controls.

Expression of S100A4. Differential expression of S100A4 was evaluated in cytoplasmic and nuclear cell fractions by Western blotting

(WB) using the same primary antibody (DAKO, 1:2000) and the NePer Kit (Pierce) as detection system, as already performed by us [9,13].

Membrane-type 1 (MT1) matrix metalloproteinase (MMP) expression. MT1-MMP expression was evaluated by WB in total lysate of EGI-1 before and after PTX treatment using an anti-MT1-MMP monoclonal antibody (Millipore, 1:500). The membrane expression levels of MT1-MMP were then evaluated by assessing the fluorescence intensity profile on cultured cells in five random fields for each experiment [14]. See supplemental section for details.

Cell proliferation and cell viability. They were evaluated by BRDU (GE healthcare) and MTS (Promega) respectively, while cell apoptosis was assessed by immunofluorescence for cleaved caspase-3 (Cell Signaling). See supplemental section for details.

Cytoskeletal integrity assessment. In PTX-treated CCA cells, actin filaments were stained by Alexa Fluor 488-conjugated phalloidin (Invitrogen), and then the percentage of cells showing a damaged cytoskeleton on the total cultured cells, was evaluated [15]. In additional experiments, we assessed the expression of β-tubulin by WB in EGI-1 cells before and after exposure to PTX at different doses, in microtubule fractions purified by ultracentrifugation (Cytoskeleton Inc).

Cell migration (wound healing) assay. See supplemental materials for details.

Cell invasion (Boyden chamber) assay. It was performed as previously described [9,13].

Rho-A, Rac-1 and Cdc-42 GTP levels. See supplemental section for details.

MMP-9 secretion. Since ELISA assessed both pro and active MMP-9 forms (RayBiotech), we performed gelatin zymography in EGI-1 with and without PTX treatment to see whether MMP-9 was actually active. See supplement for details.

SUMOylation assay. CCA cells were seeded in a 6-well plate and let to grow until confluence, before exposure to PTX. Cell lysates were prepared using Cellytic (Sigma) and 200µl (1mg/ml) were loaded into column coated with VIVAbind SUMO matrix (VivaBioscience), to capture SUMOylated proteins. SUMOylated protein fraction was then eluted and analyzed by WB (1:1000). Amount of SUMOylated S100A4 was then related to that of total S100A4 (flow through) and compared with controls.

SUMO E1, E2, and E3 enzyme expression. In CCA cells cultured and exposed to PTX as before, expression levels of the three enzymatic subunits, E1 (activating enzyme), E2 (conjugating enzyme) and E3 (ligase), involved in SUMO modification, were measured by Real-Time PCR using specific probes (LifeTechnologies) and compared to untreated cells.

Effects of ginkolic acid (GA) on S100A4 nuclearization, and on CCA cell viability and migration. Selected effects of GA, a well-established SUMOylation inhibitor, on nuclearization of S100A4 (by WB), cell viability (by MTS assay) and migration (by wound healing assay) of CCA cells were studied and compared with PTX. Given the toxicity of GA, a preliminary dose-response experiment of cell viability was run treating EGI-1 with increasing concentrations of GA (1, 10, 100μM) for 72h [16].

Xenotransplantation experiments in severe combined immune-deficient (SCID) mice. EGI-1 (500.000 cells suspended in PBS 100μl) were injected into the spleen of SCID mice (6–8 weeks old; Charles River Laboratories), after transduction with a lentiviral vector encoding the firefly luciferase gene to enable detection of tumor engraftment by in vivo bioluminescence imaging. Tumor engraftment was checked at weekly intervals using the Living Image® software (Xenogen), and considered positive when reaching an average of at

least 10^3 p/sec/cm^2/sr, according to our previous studies [9,13]. CCA cells injected intrasplenically are delivered straight into the liver through the portal venous axis, giving rise to orthotopic CCAs. Procedures involving animals and their care were conform to the institutional guidelines that comply with national and international laws and policies (EEC Council Directive 86/609, OJ L 358, December 12, 1987), and approved by the Ethical Committee of the University of Padua.

Low dose metronomic (LDM) PTX treatment of SCID mice xenotransplanted with human EGI-1 cells. Once tumor engraftment was confirmed by bioluminescence imaging (time 0), we started metronomic infusion of PTX (diluted in a 50%/50% solution of Cremophor EL (BASF) and ethanol (Carlo Erba) (vehicle)) for 2 weeks at the dosage of 2.6mg/kg/die by i.p. injection using micro-osmotic pumps (Alzet 1004, Durec). Mice were randomly divided into 2 experimental groups: a) controls (vehicle only, n=14); b) LDM PTX (n=10). After the first week of treatment, mice were checked by bioluminescence imaging (time 1) to detect metastatic spread, as previously performed [9,13]. At the end of treatment (time 2), after a further bioluminescence analysis, mice were anesthetized and sacrificed for necroscopic examination and sample harvesting from spleen (to evaluate the tumor mass at the site of injection) and lungs (to evaluate hematogenous metastases). Tissue samples were fixed in

buffered formalin and embedded in paraffin for immunohistochemical analysis. The xenograft model is illustrated in Supplementary Fig. 1A.

Assessment of the tumor growth in the site of engraftment. The tumor growth in the site of injection was evaluated in paraffin-embedded sections obtained from the tumor-bearing spleen, collected at the time of sacrifice. The tumor mass area was measured using an electronic caliper and expressed in mm^2.

Metastasis analysis. Serial sections from 10 different cutting plans at a 200μm-interval were taken from lungs of sacrificed mice and stained by H&E (Supplementary Fig. 1B). In the same section, immunohistochemistry for human mitochondria (1:100, Millipore) was performed to detect two different types of metastatic invasion, isolated tumor cells (ITC), represented by single cells or small clumps up to 5 cells, and micro metastases (MM), larger clusters containing more than 5 cells [17-19]. Immunohistochemistry for human mitochondria provides a useful tool to improve human cancer cell detection in xenograft models. The metastases were expressed as total number of human mitochondria-expressing cells in the 10 cutting plans.

Immunohistochemistry for S100A4, p-Hist3 and CC3 in SCID mice spleen specimens. See supplemental section for details.

Statistical analysis. In vitro experiments. Results were shown as the mean ± standard deviation (SD). Statistical comparisons were made using Student's t-test. Statistical analyses were performed using SPSS 20.0 software (IBM Corp.). A 2-tailed p value <0.05 was considered significant. In vivo experiments. Continuous data were shown as mean±SD, and categorical data as counts and percentages. Distributions of tumor size, number of MM and ITC in lung samples were graphically displayed by box plots and scatter dot plots comparing the two groups (PTX vs vehicle). One-sample Kolmogorov-Smirnov test was used to check distributions for normality, while Levene's statistic for homogeneity of variances. Mean differences between the two groups were analyzed with the two independent samples t-test or Welch's test, according to distributions characteristics. Welch's t-test is an adaptation of Student's t-test and is more reliable when the two samples have unequal variances and unequal sample sizes. Data were collected and reviewed in Microsoft Excel, and statistical analysis was performed using SPSS 20.0 software. All 2-tailed p<0.05 were considered statistically significant.

RESULTS

Low dose PTX decreased expression of S100A4 in the nucleus but not in the cytoplasm of EGI-1 and primary CCA cell lines. As previously shown [9], EGI-1 cells constitutively expressed S100A4 in the nucleus, and therefore represent a good model to study the effects

of its nuclear down-modulation. Treatment with low dose PTX (1.5 and 15nM) induced a significant and marked reduction in S100A4 nuclear expression (of about 60 and 80%, with respect to controls, respectively) (Fig. 1A), without modifying its cytoplasmic expression (Fig. 1B). This finding was further confirmed in primary CCA cell lines (CCA-TV3) obtained from a surgical sample similarly expressing S100A4 in the nucleus; PTX induced a dose-dependent reduction in the nuclear levels of S100A4 of 38% (1.5nM) and 62% (15nM) as compared with controls, again without affecting the cytoplasmic fraction (Fig. 1C,D).

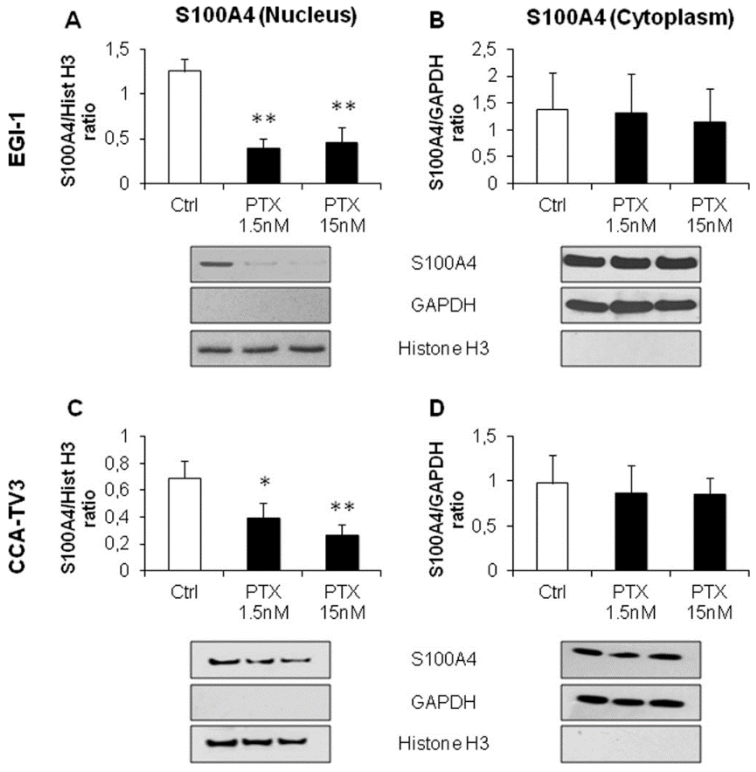

Figure 1. Low dose PTX reduced nuclear but not cytoplasmic S100A4 expression in established (EGI-1) and primary (CCA-TV3) CCA cell lines. Treatment with PTX at low doses (1.5, 15nM) induced a significant reduction in the nuclear (A and C) but not in the cytoplasmic S100A4 content (B and D), with respect to controls, in both cell lines. Below each column plot, representative blots of S100A4 together with histone H3 and GAPDH (markers of nuclear and cytoplasmic fractions, respectively), are shown (n=5 for EGI-1; n=3 for CCA-TV3). *p<0.05 vs Ctrl, **p<0.01 vs Ctrl.

Low dose PTX reduced cell motility and invasiveness of EGI-1 and primary CCA cell lines, without affecting cell proliferation, cell viability and apoptosis. Following exposure to PTX at 1.5 and 15nM, both EGI-1 (Fig. 2A) and CCA-TV3 cells (Supplementary Fig. 2A) showed a significant dose-dependent reduction in cell motility, compared with controls. Cell motility and cell invasiveness of EGI-1 and CCA-TV3 were also significantly reduced in a dose-dependent manner by low dose PTX (Fig. 2B and Supplementary Fig. 2B, respectively). Interestingly, by comparing PTX 1.5 and 15nM effects on CCA cells, we found that the degree of cell motility inhibition paralleled the extent of S100A4 nuclear reduction (Fig. 2A–B). In contrast, low dose PTX did not induce significant change in cell proliferation (Fig. 3A for EGI-1, Supplementary Fig. 3A for CCA-TV3), cell viability (Fig. 3B for EGI-1, Supplementary Fig. 3B for CCA-TV3) and apoptosis (Fig. 3C for EGI-1, Supplementary Fig. 3C for CCA-TV3). Cell proliferation, viability and apoptosis were instead strongly affected by high dose PTX (Fig. 3A–C, Supplementary Fig. 3A–C) in both CCA cell lines. These data indicate that in CCA cells, nuclear expression of S100A4 exerts

clear pro-motile and pro-invasive effects, without influencing the proliferation/apoptosis balance.

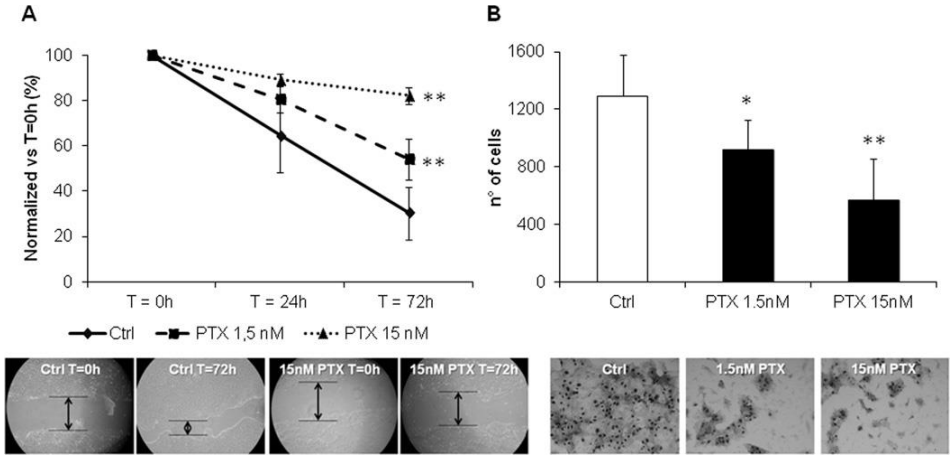

Figure 2. Low dose PTX reduced motility and invasiveness of EGI-1 cells. In the wound healing assay, cell motility of EGI-1 significantly decreased in a dose-dependent fashion, following PTX 1.5 (dotted line) and 15nM (dashed line) exposure, compared with controls (continue line) (n=12) (A). In Boyden chambers coated with Matrigel, the same PTX dose regimens significantly attenuated the invasive properties of EGI-1, with respect to controls (n=6) (B). Representative images of scratch and transwell filter are shown below their respective plot. *p<0,05 vs Ctrl; **p<0.01 vs Ctrl.

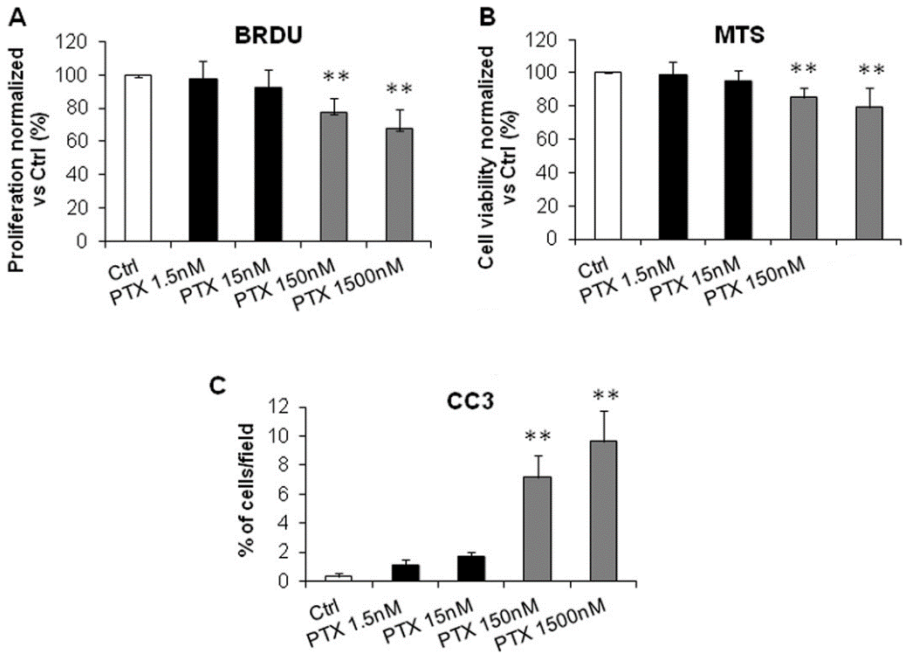

Figure 3. In contrast with high doses, low dose PTX did not affect cell proliferation, viability, and apoptosis of EGI-1 cells. Effects of low dose PTX (1.5, 15nM) on cell proliferation (BRDU incorporation, A), viability (MTS assay, B), and apoptosis (CC3 immunofluorescence, C) were evaluated in EGI-1 and compared with effects of higher doses (150, 1500nM) and with untreated cells. In contrast with the highest doses, these cell activities were not affected by low dose PTX (n=6 in all experiments). **p<0.01 vs Ctrl.

Low dose PTX reduced Rho-A and Cdc-42 activation and MMP-9 secretion in EGI-1 cells. To better understand the mechanisms promoting cell motility and invasiveness dependent upon S100A4 nuclearization, we turned to study the effects of low dose PTX on the activity of small Rho GTPases, the expression of MT1–MMP and the secretion of MMP-9. Small Rho GTPases are key effectors of cell motility by inducing the formation of stress fibers (Rho-A),

lamellipodia (Rac-1) and filopodia (Cdc-42) [20]. MMP-9 on the other hand, is a proteolytic enzyme secreted by many cancer cell types: it potently stimulates matrix degradation, facilitating the invasive migration of tumoral cells from the primary site of growth [21]. Its activation depends upon the expression of membrane-anchored MMP, particularly of MT1-MMP, whose expression at the surface of cancer cells is critical for breaking the basement membrane [22]. Since EGI-1 phenocopied the behavior of primary CCA-TV3 cell line, the following experiments were performed in EGI-1 only. As compared with controls, EGI-1 treated with low dose PTX showed a significant reduction in Rho-A (Fig. 4A) and Cdc-42 (Fig. 4B) GTP levels, but not in Rac-1 (Supplementary Fig. 4). As evaluated by WB and immunofluorescence on cultured EGI-1, MT1-MMP expression significantly decreased after PTX treatment (inhibition of 40 and 46% with 1.5, and of 50 and 49% with 15nM, for WB and immunofluorescence, respectively) (Fig. 4C–D). Similarly, MMP-9 secretion and activation were inhibited by challenging CCA cell cultures with PTX, as shown by ELISA (inhibition of 57% with 1.5, and of 72% with 15nM) and gel zymography (Fig. 4E–F).

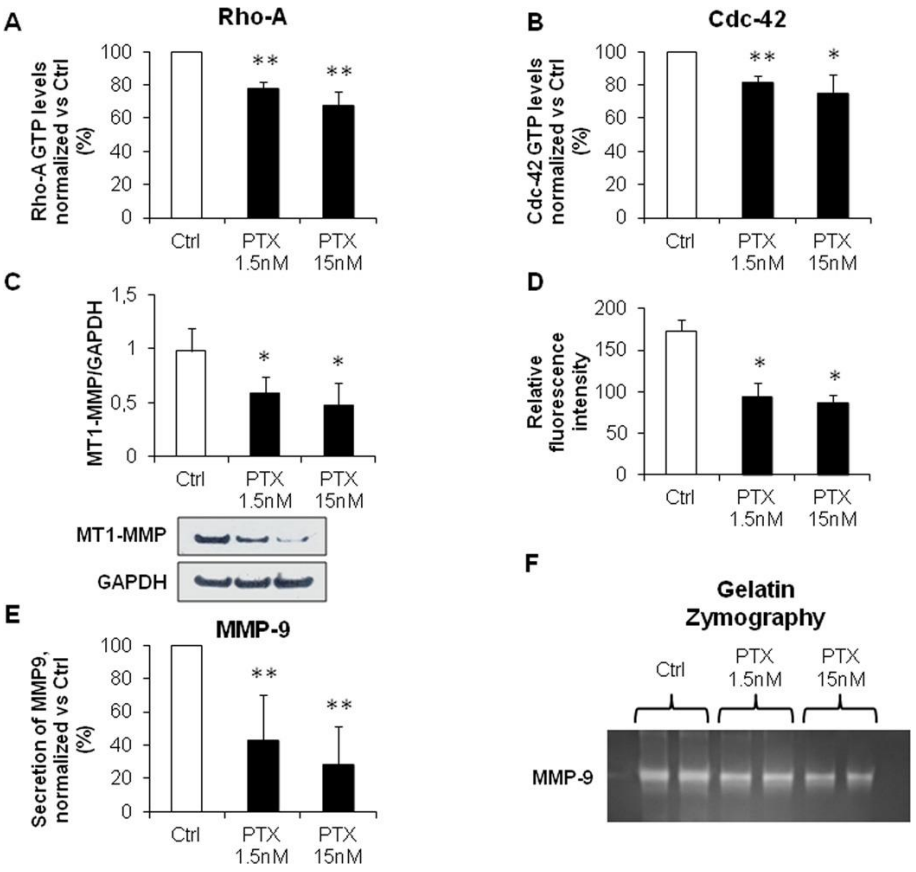

Figure 4. Low dose PTX inhibited Rho-A and Cdc-42 GTP levels, together with MT1-MMP expression and MMP-9 secretion. By G-LISA assay, low dose PTX (1.5, 15nM) significantly reduced Rho-A (A) and Cdc-42 (B) GTP levels in EGI-1, with respect to controls (n=3, in duplicate). Low dose PTX strongly inhibited MT1-MMP expression (WB, C), specifically on its membrane localization (fluorescence intensity profile, D) (n=3, for both experiments). Low dose PTX blunted both secretion (ELISA, E) (n=5, in duplicate) and activation (gelatin zymography, F) of MMP-9. *p<0.05 vs Ctrl, **p<0.01 vs Ctrl.

Low dose PTX did not induce cytoskeletal damage in EGI-1 cells. S100A4 is normally associated to cytoskeletal fibers. To study if low dose PTX altered cytoskeletal integrity, we performed phalloidin

fluorescence in dose-dependent experiments, ranging from 1.5–15nM to 150–1500nM. In contrast with high dose PTX, which induced actin fiber changes (shortening, thickening, fragmentation often leading to dense coiling, accumulating in the perinuclear area) in 16% (150nM) and 32% (1500nM) of cultured EGI-1, more than 90% of cells treated with low dose PTX showed preserved cytoskeletal structure (Supplementary Fig. 5). These data indicate that effects of low dose PTX on cell motility and invasiveness are not due to a cytoskeletal damage. Next, we sought to understand the mechanisms regulating the nuclear import of S100A4.

PTX selectively reduced the SUMOylation fraction of S100A4, a critical mechanism for cell invasiveness of EGI-1 cells. Post-translational modification by small ubiquitin-like modifier (SUMO) of target proteins is an important mechanism directing their intracellular shuttling. We showed that EGI-1 contained much higher amounts of SUMOylated S100A4 than TFK-1, a CCA cell line expressing S100A4 only in the cytoplasm, where instead un-SUMOylated S100A4 was detected (Supplementary Fig. 6A). Furthermore, after treatment with low dose PTX, EGI-1 showed a marked reduction selectively in the SUMOylated fraction of S100A4 as compared with controls, whereas the S100A4 unSUMOylated levels remained unchanged (Fig. 5A). SUMO inhibition by PTX was not associated with decreased mRNA expression levels of the three SUMO E components of the SUMOylating

complex (Supplementary Fig. 6B–D). To study if inhibition of SUMOylation halted cell invasive capabilities, EGI-1 were treated with GA, a specific natural inhibitor of the E1 subunit. Preliminary dose-response experiments to assess toxicity levels of GA on EGI-1 cells identified 1μM as the dose devoid of effects on cell viability (not shown), and therefore used onwards. Consistent with our hypothesis, GA significantly reduced cell motility of EGI-1 with respect to controls (Fig. 5B), an effect associated with a significant reduction (37%) in the nuclear expression of S100A4 of an extent comparable to PTX 1.5nM, without affecting the cytoplasmic levels of S100A4 (Fig. 5C,D).

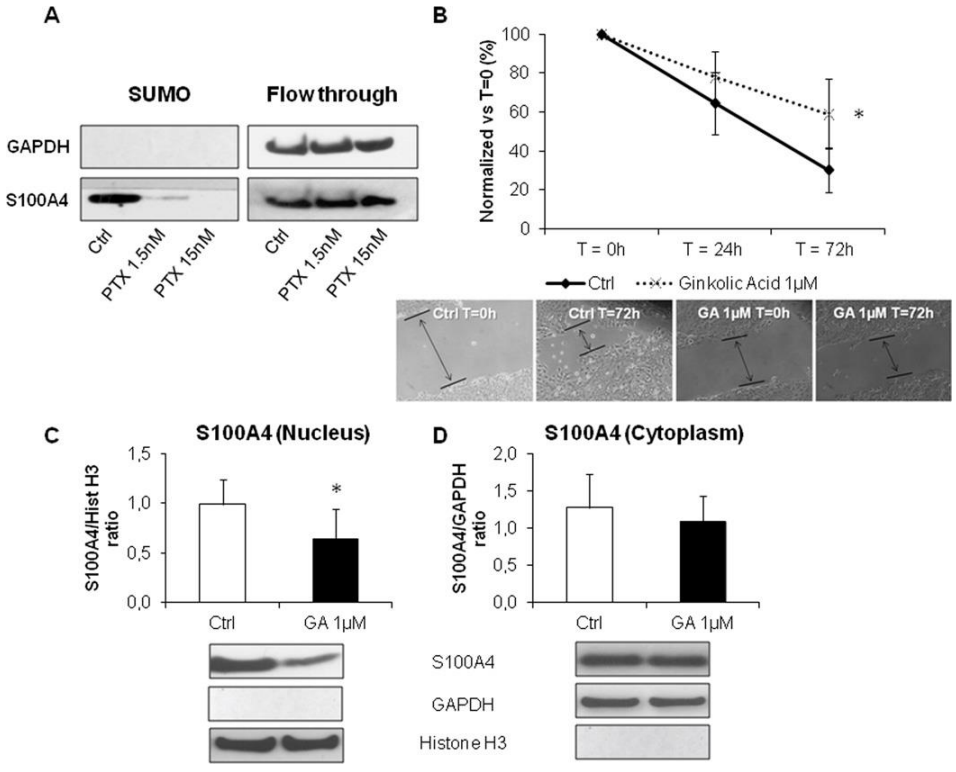

Figure 5. SUMOylation of S100A4 was modulated by low dose PTX and led motility and S100A4 nuclear import in EGI-1 cells. By SUMOylation assay, EGI-1 exposed to PTX 1.5 and 15nM showed a stark reduction in the amount of SUMOylated S100A4 compared with controls, without changes in the total amount of un-SUMOylated S100A4 protein (flow through) (A). PTX effects were reproduced by ginkolic acid (GA, 1μM), a specific SUMOylation inhibitor, which significantly reduced EGI-1 cell migration (B, dotted line, n=12). This effect was associated with a significant decrease in the nuclear S100A4 (C) compared with controls, whilst the cytoplasmic fraction was unaffected (D). Below each column plot, representative blots of S100A4 together with histone H3 (nuclear marker) and GAPDH (cytoplasmic marker), are shown (n=6). *p<0.05 vs Ctrl.

PTX treatment reduced lung metastasization but not the tumor growth at the site of injection in the experimental model of CCA. Altogether, the in vitro data suggest that the SUMOylation-dependent nuclear import of S100A4 is indeed a mechanistic determinant of the invasive phenotype of CCA cells, which can be inhibited by PTX at nM doses without altering the cytoskeletal integrity, as well as the proliferation and/or apoptosis activities. To test in vivo whether targeting nuclear S100A4 by low dose PTX is therapeutically relevant to reduce CCA invasiveness, we moved to the experimental model of CCA generated by EGI-1 cell xenotransplantation in the SCID mouse [9,13]. To reproduce the small nM doses of PTX able to hamper S100A4 nuclear entry in CCA cells in vitro, a low dose metronomic regimen was chosen for drug infusion in xenografted mice (LDM PTX). To assess specific effects on cancer invasiveness, the treatment was started upon successful EGI-1 cell engraftment as confirmed by bioluminescence imaging (on average 29.75±4.53 days after intrasplenic injection).

Notably, before starting LDM PTX, the levels of photon emission were comparable between the two groups. With respect to control animals, LDM PTX did not significantly reduce neither photon emission from the spleen through the treatment time (Supplementary Fig. 7A,B), nor the size of the splenic tumor mass at the time of sacrifice (Supplementary Fig. 7C). Immunohistochemistry in tissue sections obtained from the tumor mass confirmed that LDM PTX was effective in decreasing S100A4 expression in the nucleus of engrafted EGI-1 cells compared with controls (Fig. 6A), however, the expression of p-Hist3 (proliferation marker) and CC3 (apoptosis marker) did not significantly differ between LDM PTX-treated and control mice (Fig. 6B,C). These findings indicate that LDM PTX reproduces the down-modulating effects on S100A4 nuclear expression by EGI-1 shown in vitro, without causing a dysregulation in the proliferation/apoptosis balance of CCA cells. In contrast, LDM PTX significantly halted metastatic dissemination. Immunohistochemistry for human mitochondria revealed that both ITC and MM in the lung were significantly reduced by PTX treatment (Fig. 7A,B). These data further prove the functional impact of S100A4 nuclear expression on CCA biology as mechanism specifically driving hematogenous metastasization, without stimulating tumorigenesis.

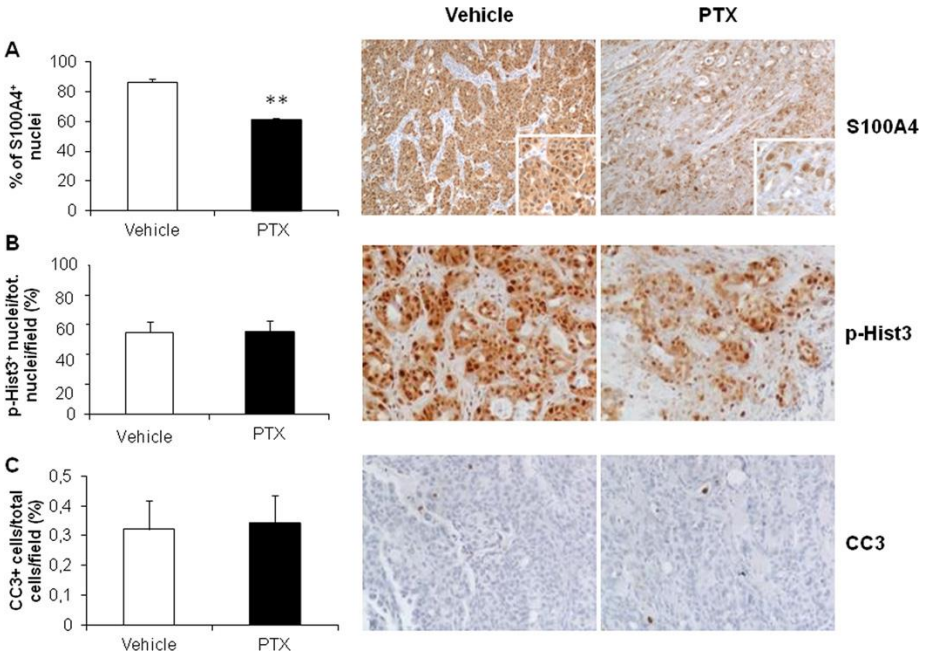

Figure 6. LDM PTX reduced nuclear S100A4 expression without affecting proliferation and apoptosis of xenotransplanted EGI-1 cells, in vivo. Nuclear immunoreactivity for S100A4 was significantly reduced in the tumor mass at the site of injection (spleen) of LDM PTX-treated mice (n=10) with respect to vehicle-treated controls (n=14) (A). Conversely, LDM PTX did not modify neither cell proliferation (immunohistochemistry for p-Hist3, B) nor apoptosis (immunohistochemistry for CC3, C) in the splenic mass compared with controls. Representative micrographs of spleen sections immunostained for S100A4, p-Hist3 and CC3 are shown in the right side of the plot (immunoperoxidase; A, M=100×; B, C, M=200×; insets, M=200×). **p<0.01 vs Ctrl.

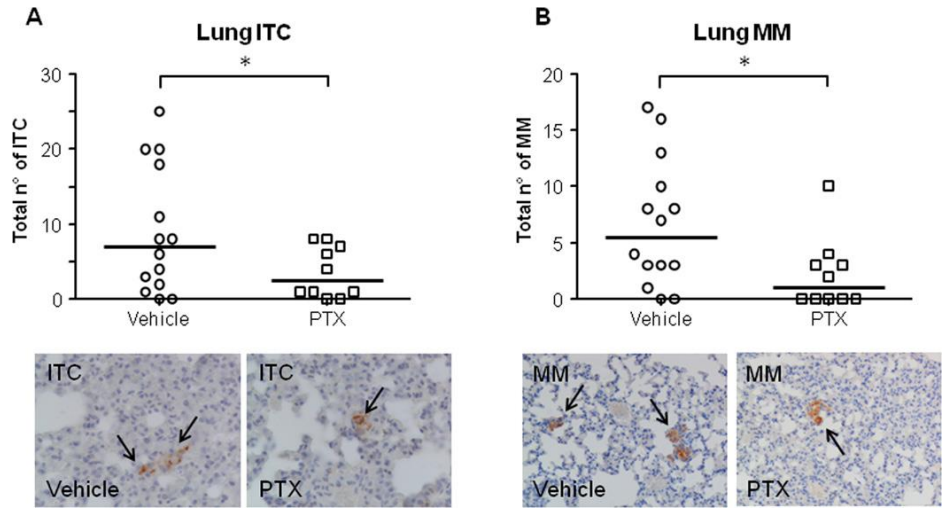

Figure 7. LDM PTX inhibited lung metastatic colonization of EGI-1 cells, in vivo. A significant reduction in the number of both ITC (A) and MM (B) was found in treated mice (n=10) with respect to controls (n=14). Representative micrographs of ITC and MM (black arrows) derived from EGI-1 cell dissemination to the lung parenchyma after xenograft in SCID mice undergoing LDM PTX and in controls, identified by the specific immunoreactivity for human mitochondria, are shown below their respective dot plot. *p<0.05 vs Ctrl; Immunoperoxidase; original magnification, M=400× (ITC), M=200× (MM).

DISCUSSION

An unmet need in CCA, as in other malignancies whose dismal prognosis relates to limited therapeutic approaches, is the development of biomarkers able to identify patients most likely to take advantage of curative treatments. Biomarkers may also represent disease-relevant targets for therapeutic interventions [9]. Our previous studies showed that nuclear expression of S100A4 in cancer cells of resected CCA (nearly a half) identified a more invasive clinical phenotype, characterized by increased metastasization and reduced

survival after surgery [9]. Of note, a worse prognosis after surgery was still observed even when S100A4 nuclear expression was scattered, limited to less than 30% of the neoplastic ducts [9]. The aim of the present study was to understand the mechanisms by which nuclear expression of S100A4 promotes cancer invasiveness, and to elucidate the mechanism regulating nuclear translocation of S100A4. We also wanted to understand if these mechanisms are putative target for therapeutic intervention.

We initially found that PTX given in vitro at low doses (1.5 and 15nM) was able to effectively and selectively down-regulate S100A4 expression in the nucleus of CCA cells, leaving cytoplasmic expression unaffected. Then, by combining in vitro and in vivo techniques, we showed that: a) PTX-induced down-regulation of nuclear S100A4 was associated with a reduction in motility and invasiveness of CCA cells, in activity of Rho-A and Cdc-42, and in secretion of MMP-9; b) at the doses able to down-regulate nuclear expression of S100A4, PTX did not affect cell proliferation, apoptosis, and cytoskeletal architecture; c) the nuclear translocation of S100A4 was regulated by SUMOylation, a post-translational mechanism that was affected by PTX; d) in SCID mice xenografted with human nuclear S100A4-expressing CCA cells, down-regulation of nuclear S100A4 by LDM PTX was associated with a reduction in hematogenous metastasization.

The biological functions of S100A4 are largely unknown. They depend on its interacting partners, which are mainly located in the

cytoplasm, where S100A4 is commonly expressed. In the nucleus, interacting partners have not been characterized yet, opening the possibility that nuclear S100A4 may act independently as transcription factor [7].

Earlier studies showed that in mouse melanoma cells, taxol at conventional doses, reduced the total amount of S100A4, an effect associated with maintenance in the G0 phase of the cells and increased expression of p53 [10,11]. We initially found that in CCA cells, low doses of PTX (1.5–15nM) induced a marked reduction in S100A4 selectively in the nucleus, without altering its cytoplasmic expression. This effect, obtained in an established CCA cell line (EGI-1) was reproduced in a primary CCA cell line derived from a patient undergoing surgical resection. The nuclear down-regulation of S100A4 was biologically relevant since it associated with a strong inhibition of the motile and invasive properties displayed by CCA cells in culture. Interestingly, at the same small doses, PTX did not exert anti-proliferative and pro-apoptotic functions, nor it affected cell viability or the integrity of the actin cytoskeletal filaments of cultured CCA cells. All these cytotoxic effects were instead induced by PTX at higher doses (150–1500nM), coupled with pronounced anti-proliferative and pro-apoptotic activities, in line with the mechanism of action supporting the current indications of PTX for the chemotherapeutic treatment of several aggressive carcinomas, from ovary, to breast and thyroid cancer [23,24]. The lack of pro-

proliferative stimuli when S100A4 translocates into the nucleus has been recently shown also in colorectal cancer cells [25]. In this study, although S100A4 translocated into the nucleus in a cell cycle-dependent fashion, being most prominent in the G2/M phase, lentiviral silencing of nuclear S100A4 did not induce changes in cell proliferation. Our findings are consistent with these observations, and confirm that nuclear S100A4 confers specific pro-invasive functions.

Among putative molecular players mediating the effects of nuclear S100A4 on cell motility and invasiveness, we focused on the small G proteins (GTPases) belonging to the Rho family and on matrix metalloproteinases (MMPs). The small Rho GTPases are recognized as key effectors able to activate invasion and metastasis programs [20,26]. In EGI-1 cells, inhibition of S100A4 nuclear import by low dose PTX significantly reduced the activation of Rho-A and Cdc-42. In cancer cells, Cdc-42 is one of the factors involved in the formation of specialized plasma-membrane actin-based microdomains combining adhesive properties with matrix degrading activities, called invadopodia, which support cancer invasion by dismantling the basement membrane and then by invading the stromal environment mostly composed of fibrillar type I collagen. A main component of invadopodia is the transmembrane metalloproteinase MT1-MMP, whose function is essential for the in situ to invasive carcinoma transition in breast cancer [14]. MT1-MMP promotes the activation of several soluble MMPs, such as MMP-2 and MMP-9. Our data indicate

that EGI-1 cells constitutively expressed MT1-MMP and MMP-9, but not MMP-2, and when exposed to low dose PTX, they showed a significant dose-dependent reduction in the surface expression of MT1-MMP along with the ability to secrete MMP-9. Interestingly, the interplay between Rho-A and Cdc-42 regulates the delivery and accumulation of MMPs at the invading surface [27]. Furthermore, since MMP-9 secretion can be also modulated by the activation of the Rho-A/ROCK signaling [21], and the membrane translocation of MT1-MMP is directly regulated by Cdc-42 [28], we suggest the cooperation of Rho-A/MMP-9 and Cdc-42/MT1-MMP pathways to form invadopodia activated by nuclear S100A4.

Cytoskeletal damages induced by PTX, a well-established depolymerizing agent [29], could in theory influence the nuclear translocation of S100A4. From this point of view, it is important to underline that structural cytoskeleton alterations were absent with low dose PTX, in contrast with what coherently observed with high dose PTX. The mechanisms regulating S100A4 entry into the nucleus remain enigmatic. Notably, S100A4 does not possess nuclear docking sites or nuclear import sequences. In human chondrocytes, nuclearization of S100A4 was induced by IL-1β through a SUMOylation-dependent mechanism [30]. SUMOylation is a post-translational mechanism similar to ubiquitination, operated by SUMO proteins, and involved in several biological functions, including protein stability, DNA repair, cell cycle regulation, apoptosis, nuclear

transport and gene transcription [31]. The SUMOylation processes are catalyzed by three enzymes, SUMO E1, E2 and E3, acting as pacemaker of the cascade reaction leading to the modification of their substrate protein [32]. Components of the SUMOylation machinery have been found deregulated in several human cancers, and are emerging as relevant players in tumour invasiveness and in epithelial-mesenchymal transition [33]. We found that EGI-1 (expressing S100A4 the nucleus) contained higher amounts of SUMOylated S100A4 with respect to TFK-1 (expressing S100A4 only in the cytoplasm). Then, in EGI-1 treated with low dose PTX, down-regulation of nuclear S100A4 was associated with a significant, dose-dependent reduction in the S100A4 SUMOylated fraction, without changes in the un-SUMOylated subset. These effects occurred without affecting the expression levels of E1, E2, E3 subunits of the SUMOylating complex, thus suggesting a functional inhibitory mechanism, similar to GA. GA is a natural compound derived from Gingko biloba that specifically inhibits the first step of the SUMOylation reaction by directly binding E1 and inhibiting the formation of the E1-SUMO intermediate [16]. Of note, also the reduction in nuclear levels of S100A4 induced by GA significantly inhibited EGI-1 cell motility, to an extent comparable to PTX. This observation confirms the relevance of SUMOylation in mediating the pro-oncogenic functions of S100A4 when translocated into the nucleus.

To translate the results of the in vitro experiments, we turned to an experimental model of CCA generated by xenotransplantation of human EGI-1 cells into the spleen of SCID mice, as we performed in previous studies [9,13]. Because of its short half-life [34], PTX was administered to xenografted SCID mice with a LDM infusion. Continuous delivery of PTX by LDM ensured the achievement of constant low concentrations of PTX comparable with the small doses used for the in vitro experiments [34]. To evaluate specific effects on tumor invasion, LDM PTX was started only after human CCA cell engraftment was confirmed by bioluminescence imaging. At the end of treatment, histological evaluation of the splenic tumor showed in the LDM PTX-treated group, a significant reduction in the amount of nuclear S100A4-expressing EGI-1 cells. In line with what observed in vitro, down-regulation of S100A4 was not associated with reduced tumour cell proliferation (p-Hist3) or with increased apoptosis (CC3) of CCA cells. Therefore, our experimental model is ideal to study if pharmacologic targeting of nuclear S100A4 is a useful strategy to inhibit invasiveness and metastasization. We found that LDM PTX did not affect the growth of the tumor at the site of injection, but caused a significant reduction in both ITC and MM in the lungs, where EGI-1 cells metastatise following a hematogenous route through the portal vein and the hepatic veins. This finding is of great clinical value, because the lung is the site most frequently involved in the

extrahepatic progression of CCA, fostered by a specific mechanism of vascular encasement by tumor cells [5].

It is important to underline that PTX may exert additional functions not related to modulation of S100A4 nuclear transport that potentially may contribute to its anti-invasive effects. These are largely dependent upon PTX ability to promote microtubule polymerization and stabilization, which inhibits mitosis and leads to apoptosis. While these mechanisms of action are well evident at the conventional doses, at the much lower doses used in the current study, they do not seem to occur. Recent studies performed in ovarian carcinoma cells indicate that alternatively, PTX may inhibit the expression of other critical molecular factors of tumor progression, such as hypoxia-inducible factor-1α and vascular endothelial growth factor [35].

In conclusion, this study unveils a specific role of SUMOylation-dependent nuclear import of S100A4 in CCA on hematogenous metastasization. The small GTPases Cdc-42 and Rho-A, in concert with MT1-MMP and MMP-9, are the molecular effectors mediating the pro-invasive functions promoted by S100A4 nuclearization. Bearing in mind the potential toxic effects of PTX in patients with overt cirrhosis and cholestasis [36], these mechanisms represents a promising therapeutic target aimed at preventing metastatic dissemination after detection of the tumor.

Conflict of interest: All authors have no conflict of interest regarding this study to declare.

Financial support: Progetto di Ricerca Ateneo 2011 (Grant #CPD113799/11) to L. Fabris and M. Cadamuro. Grant Associazione Chirurgica Tarvisium to M. Massani, T. Stecca and N. Bassi. Grant Associazione Italiana Ricerca sul Cancro (AIRC) #IG14295 to S. Indraccolo. Projects CARIPLO 2011-0470 and PRIN 2009ARYX4T_005 to M. Strazzabosco. NIH Grants DK079005 to M. Strazzabosco, RO1DK 101528 to C. Spirli, and DK034989 Silvio O. Conte Digestive Diseases Research Core Centers to M. Strazzabosco and C. Spirli.

REFERENCES

1. Blechacz B, Gores GJ. Cholangiocarcinoma: advances in pathogenesis, diagnosis, and treatment. Hepatology. 2008;48:308–321.

2. Khan SA, Thomas HC, Davidson BR, Taylor-Robinson SD. Cholangiocarcinoma. Lancet. 2005;366:1303–1314.

3. Sempoux C, Jibara G, Ward SC, Fan C, Qin L, Roayaie S, et al. Intrahepatic cholangiocarcinoma: new insights in pathology. Semin Liver Dis. 2011;31:49–60.

4. Valle J, Wasan H, Palmer DH, Cunningham D, Anthoney A, Maraveyas A, et al. Cisplatin plus gemcitabine versus gemcitabine for biliary tract cancer. N Engl J Med. 2010;362:1273–1281.

5. Fabris L, Alvaro D. The prognosis of peri-hilar cholangiocarcinoma after radical treatments. Hepatology. 2012;56:800–802.

6. Boye K, Maelandsmo GM. S100A4 and metastasis: a small actor playing many roles. Am J Pathol. 2010;176:528–535.

7. Saleem M, Kweon MH, Johnson JJ, Adhami VM, Elcheva I, Khan N, et al. S100A4 accelerates tumorigenesis and invasion of human prostate cancer through the transcriptional regulation of matrix metalloproteinase 9. Proc Natl Acad Sci U S A. 2006;103:14825–14830.

8. Gongoll S, Peters G, Mengel M, Piso P, Klempnauer J, Kreipe H, et al. Prognostic significance of calcium-binding protein S100A4 in colorectal cancer. Gastroenterology. 2002;123:1478–1484.
9. Fabris L, Cadamuro M, Moserle L, Dziura J, Cong X, Sambado L, et al. Nuclear expression of S100A4 calcium-binding protein increases cholangiocarcinoma invasiveness and metastasization. Hepatology. 2011;54:890–899.
10. Lakshmi MS, Parker C, Sherbet GV. Metastasis associated MTS1 and NM23 genes affect tubulin polymerisation in B16 melanomas: a possible mechanism of their regulation of metastatic behaviour of tumours. Anticancer Res. 1993;13:299–303.
11. Parker C, Lakshmi MS, Piura B, Sherbet GV. Metastasis-associated mts1 gene expression correlates with increased p53 detection in the B16 murine melanoma. DNA Cell Biol. 1994;13:343–351.
12. Horwitz SB. Taxol (paclitaxel): mechanisms of action. Ann Oncol. 1994;5:S3–S6.
13. Cadamuro M, Nardo G, Indraccolo S, Dall'olmo L, Sambado L, Moserle L, et al. Platelet-derived growth factor-D and Rho GTPases regulate recruitment of cancer-associated fibroblasts in cholangiocarcinoma. Hepatology. 2013;58:1042–1053.
14. Lodillinsky C, Infante E, Guichard A, Chaligné R, Fuhrmann L, Cyrta J, et al. p63/MT1-MMP axis is required for in situ to invasive transition in basal-like breast cancer. Oncogene. 2016;35:344–357.
15. Rozelle AL, Machesky LM, Yamamoto M, Driessens MH, Insall RH, Roth MG, et al. Phosphatidylinositol 4,5-bisphosphate induces actin-based movement of raft-enriched vesicles through WASP-Arp2/3. Curr Biol. 2000;10:311–320.

16. Fukuda I, Ito A, Hirai G, Nishimura S, Kawasaki H, Saitoh H, et al. Ginkgolic acid inhibits protein SUMOylation by blocking formation of the E1-SUMO intermediate. Chem Biol. 2009;16:133–140.
17. Hermanek P, Hutter RV, Sobin LH, Wittekind C. International Union Against Cancer. Classification of isolated tumor cells and micrometastasis. Cancer. 1999;86:2668–2673.
18. Amin BD, Hoda SA. Minimal metastatic disease in sentinel lymph nodes in breast carcinoma: some modest proposals to refine criteria for "isolated tumor cells". Adv Anat Pathol. 2006;13:185–189.
19. Zhang ZY, Ge HY. Micrometastasis in gastric cancer. Cancer Lett. 2013;336:34–45.
20. Raftopoulou M, Hall A. Cell migration: Rho GTPases lead the way. Developmental Biology. 2004;265:23–32.
21. Turner NA, O'Regan DJ, Ball SG, Porter KE. Simvastatin inhibits MMP-9 secretion from human saphenous vein smooth muscle cells by inhibiting the RhoA/ROCK pathway and reducing MMP-9 mRNA levels. FASEB J. 2005;19:804–806.
22. Gialeli C, Theocharis AD, Karamanos NK. Roles of matrix metalloproteinases in cancer progression and their pharmacological targeting. FEBS J. 2011;278:16–27.
23. Cresta S, Sessa C, Catapano CV, Gallerani E, Passalacqua D, Rinaldi A, et al. Phase I study of bortezomib with weekly paclitaxel in patients with advanced solid tumours. Eur J Cancer. 2008;44:1829–1834.
24. Ain KB, Egorin MJ, DeSimone PA. Treatment of anaplastic thyroid carcinoma with paclitaxel: phase 2 trial using ninety-six-hour infusion. Collaborative Anaplastic Thyroid Cancer Health Intervention Trials (CATCHIT) Group. Thyroid. 2000;10:587–594.

25. Egeland EV, Boye K, Pettersen SJ, Haugen MH, Øyjord T, Malerød L, et al. Enrichment of nuclear S100A4 during G2/M in colorectal cancer cells: possible association with cyclin B1 and centrosomes. Clin Exp Metastasis. 2015;32:755–767.

26. Franco-Barraza J, Valdivia-Silva JE, Zamudio-Meza H, Castillo A, García-Zepeda, Benítez-Bribiesca L, et al. Actin Cytoskeleton Participation in the Onset of IL-1β Induction of an Invasive Mesenchymal-like Phenotype in Epithelial MCF-7 Cells. Archives of Medical Research. 2010;41:170–181.

27. Spuul P, Ciufici P, Veillat V, Leclercq A, Daubon T, Kramer IJ, et al. Importance of RhoGTPases in formation, characteristics, and functions of invadosomes. Small GTPases. 2014;5:e28195.

28. Ispanovic E, Serio D, Haas TL. Cdc42 and RhoA have opposing roles in regulating membrane type 1-matrix metalloproteinase localization and matrix metalloproteinase-2 activation. Am J Physiol Cell Physiol. 2008;295:C600–C610.

29. Zhang Y, Zang H, Zang F, Liu S, Wang R, Sun Y, et al. Folate-targeted paclitaxel-conjugated polymeric micelles inhibits pulmonary metastatic hepatoma in experimental murine H22 metastasis model. Int J Nanomed. 2014;9:2019–2030.

30. Miranda KJ, Loeser RF, Yammani RR. SumoylSUMOylation and nuclear translocation of S100A4 regulate IL-1beta-mediated production of matrix metalloproteinase-13. J Biol Chem. 2010;285:31517–31524.

31. Pichler A, Melchior F. Ubiquitin-related modifier SUMO1 and nucleocytoplasmic transport. Traffic. 2002;3:381–387.

32. Johnson ES. Protein modification by SUMO. Annu Rev Biochem. 2004;73:355–382.

33. Bogachek MV, De Andrade JP, Weigel RJ. Regulation of epithelial-mesenchymal transition through SUMOylation of transcription factors. Cancer Res. 2015;75:11–15.
34. Stearns ME. Taxol reduces circulating tumor cells to prevent bone metastases in SCID mice. Invasion Metastasis. 1995;15:232–241.
35. Kim BR, Yoon K, Byun HJ, Seo SH, Lee SH, Rho SB. The anti-tumor activator sMEK1 and paclitaxel additively decrease expression of HIF-1α and VEGF via mTORC1-S6K/4E-BP-dependent signaling pathways. Oncotarget. 2014;5:6540–6551.
36. Xie JD, Huang Y, Chen DT, Pan JH, Bi BT, Feng KY, et al. Fentanyl Enhances Hepatotoxicity of Paclitaxel via Inhibition of CYP3A4 and ABCB1 Transport Activity in Mice. PLoS One. 2015;10:e0143701.

SUPPLEMENTARY MATERIALS AND METHODS

Cell apoptosis. Since in some treatments with rapid cytotoxicity, reduction in mitochondrial activity does not affect cell survival and therefore, analysis of cell viability by MTS might underestimate the number of dead cells, cell apoptosis was assessed by immunofluorescence for cleaved caspase 3 (CC3, 1:500, rabbit, Cell Signaling) and then developed. Results were expressed as percentage of cells with positive cytoplasmic staining for CC3 on the total number of cells, in 20 random fields taken at 200x magnification, by two independent observers (MC, LS) as previously described [9].

Cell migration (wound healing) assay. CCA cell lines were seeded in a 6-well plate, grown until confluence, and then starved for 24h. Each cell monolayer was scratched three times with a sterile p200 tip, and three micrographs were taken at t=0h for each wound. Then, on the same scratched area, micrographs were taken again at 24h and 72h to measure the distance between the wound margins using LuciaG 5.0 software (Nikon), and expressed by normalizing each time point to t=0h [9,13].

Membrane-type 1 (MT1) matrix metalloproteinase (MMP) expression. To assess the membrane expression levels of MT1-MMP, immunofluorescence staining was analyzed using the LuciaG 5.0 software (Nikon). After selecting a region of interest between two adjacent tumor cells, the relative labeling intensity was evaluated on either red (MT1-MMP, red line) or blue (DAPI, nuclei, blue line) channels, and the higher peak of red fluorescence was measured (Supplemental Fig. 4B).

Activity of Rho-A, Rac-1 and Cdc-42 GTPase. CCA cells were seeded and cultured for three days to reach at least the 70% of confluence to assess Rho-A and Rac-1 GTP levels, and the 20-30% of confluence for Cdc-42 GTP levels. Then, confluent cells were exposed to PTX, and proteins were extracted to perform the G-LISA assay according to the supplier (Cytoskeleton Inc.).

MMP-9 secretion. Fifty-thousand cells were seeded on a 24-well plate and then treated with PTX. Supernatant was harvested, stored at -80°C, and ELISA performed to quantify both the pro and the active MMP-9 forms (RayBiotech).

Gelatin zymography assay. One hundred μg of total protein lysate was loaded on each well of a 10% Tris-Glycine + 0.1% Gelatin gel (LifeTechnologies) and proteins were run for 90mins using a Tris-Glycine Buffer. Gels were then incubated with renaturing buffer for 30min at room temperature (LifeTechnologies), and incubated in developing buffer (LifeTechnologies) for 4h at 37°C. Finally, gels were stained for 30min with Coomassie Brilliant blue (Bio-Rad) and pictures were taken using the Gel Logic 100 Imaging System (Kodak).

Immunohistochemistry for S100A4, p-Hist3 and CC3 in SCID mice spleen specimens. The sections derived from spleen were immunostained for S100A4 (1:400), p-Hist3 (1:50, rabbit, Cell Signaling), and CC3 (1:300), developed with DAB and H_2O_2 0.01% and counterstained with Gill's Haematoxylin N°2 (Sigma). All antibodies were diluted in PBS 1M, and supplemented with 1% BSA and 0.05% Tween20 (Sigma). Results were expressed as percentage of positive cells/field at 200x in 10 randomly taken fields, as previously performed [9]. Positive staining for S100A4 and p-Hist3 was considered as expression of intense brown staining in the nucleus,

whereas positivity for CC3 was represented by granular brown staining in the cytoplasm of EGI-1 cells.

SUPPLEMENTARY FIGURES

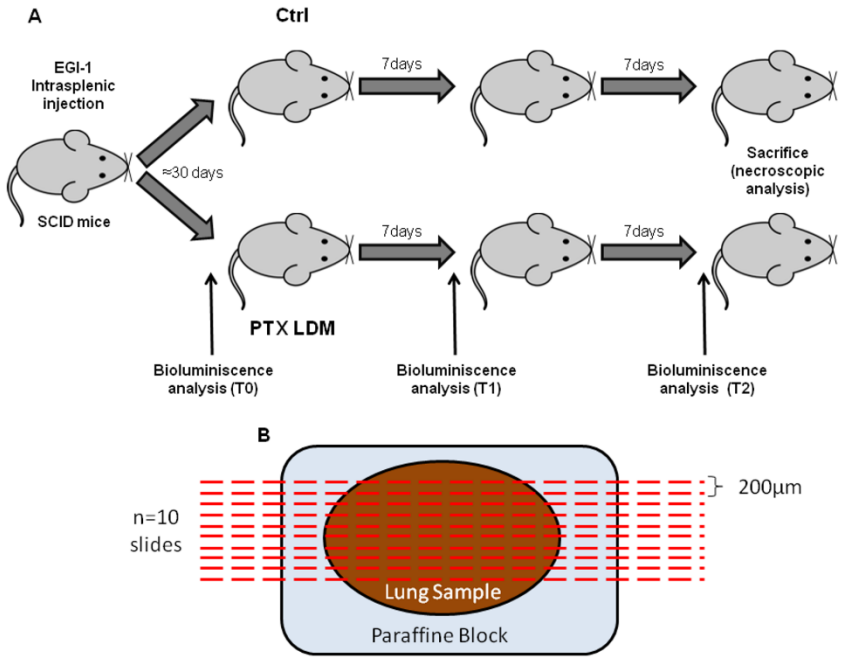

Supplementary Figure 1. Schedule of treatment with low dose metronomic PTX and assessment by bioluminescence analysis in SCID mice xenografted with EGI-1 cells. See text for detail.

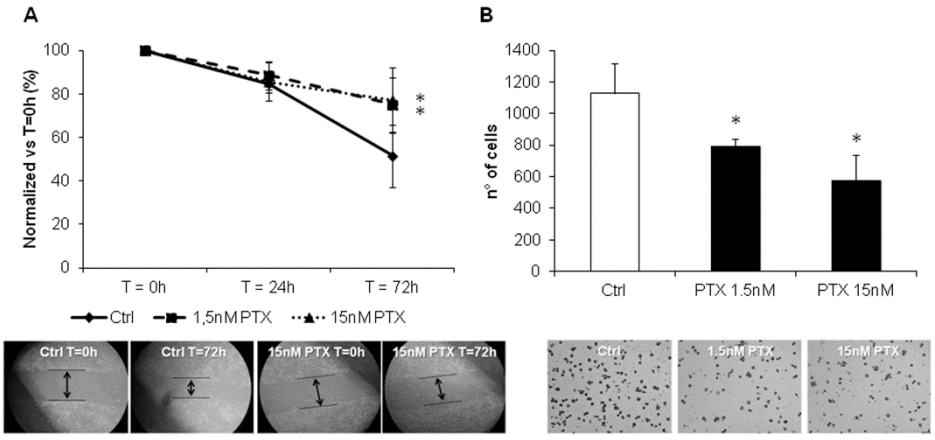

Supplementary Figure 2. Low dose PTX reduced motility and invasiveness of CCA-TV3 cells. Consistent with data obtained with EGI-1 cells, by wound-healing assay, cell motility of CCA-TV3 cells significantly decreased, in a dose-dependent fashion, following PTX 1.5 (dotted line) and 15nM (dashed line) exposure compared with untreated controls (continue line) (n=4) (A). Similar to EGI-1 cells, the same PTX dose regimens significantly blunted the invasive abilities of CCA-TV3 cells, with respect to controls in Boyden chambers coated with Matrigel, (n=3) (B). Representative images of scratch and transwell filter are shown below their respective plot. *p<0,05 vs Ctrl; **p<0.01 vs Ctrl.

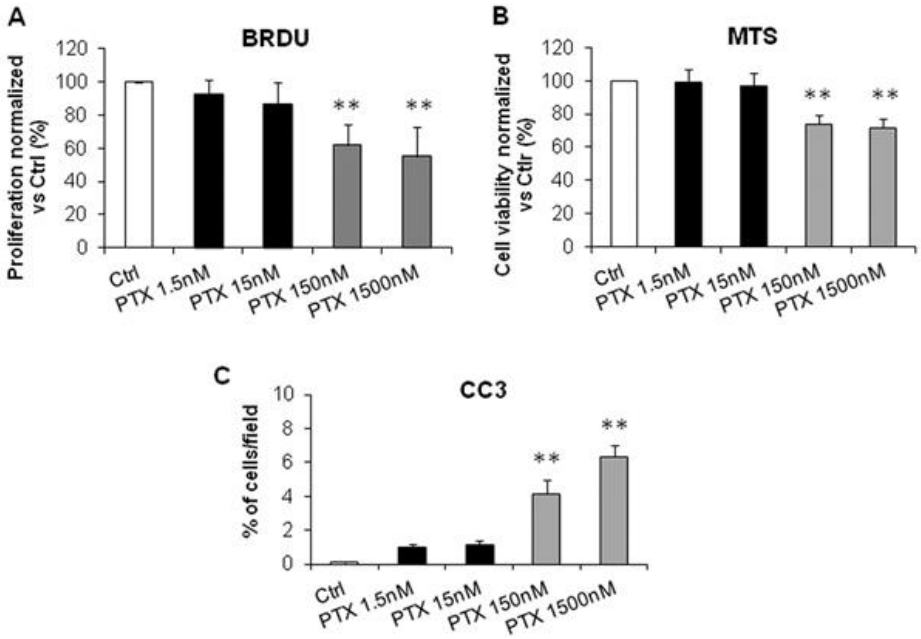

Supplementary Figure 3. In contrast with high doses, low dose PTX did not affect cell proliferation, viability, and apoptosis of CCA-TV3 cells. Concomitant effects of low dose PTX (1.5 and 15nM) on cell proliferation (BRDU incorporation, A), viability (MTS assay, B), and apoptosis (CC3 immunofluorescence in cultured cells, C) were also evaluated in CCA-TV3 cells and compared with the effects of higher doses (150 and 1500nM) and with untreated controls. In contrast with high doses, these cell activities were not affected by low dose PTX (n=3 in all experiments), in accordance with what observed in EGI-1 cells. **p<0.01 vs Ctrl.

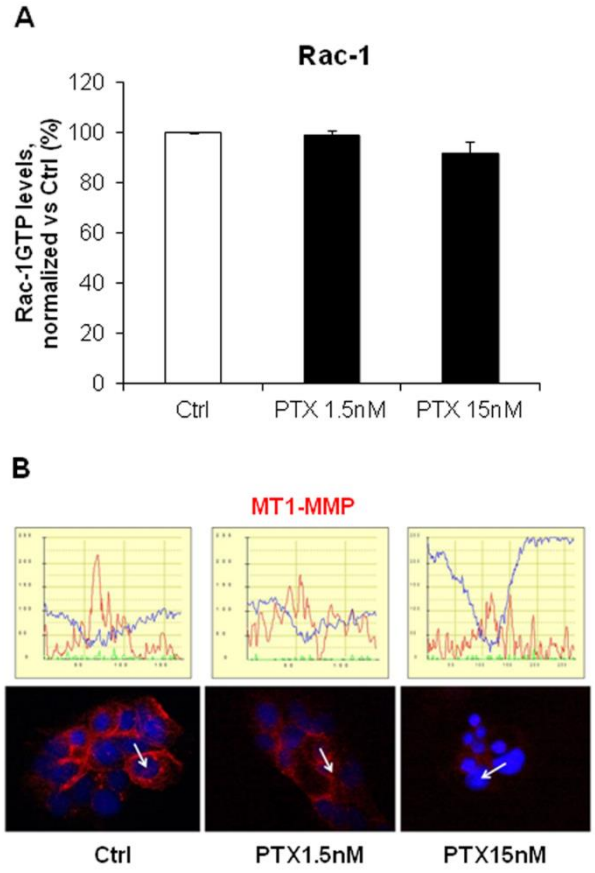

Supplementary Figure 4. Low dose PTX did not affect Rac-1 GTP levels, while it reduced the MT1-MMP membrane expression. By G-LISA assay, low dose PTX (1.5 and 15nM) did not modify Rac-1 GTP levels in EGI-1 cells, with respect to untreated controls (A, n=3, in duplicate). In contrast, the same PTX doses significantly blunted the expression of MT1-MMP (red) at the membrane level of EGI-1 cells, as shown by immunofluorescence analysis of cultured cells; representative plots are given above each micrograph. Red line depicts the fluorescence intensity profile of MT1-MMP through the cell area, while blue line represents the intensity of nuclear staining (DAPI); peak of red line corresponds to the lowest level of blue staining, according to a membrane localization of MT1-MMP. Original magnification: 400x (B).

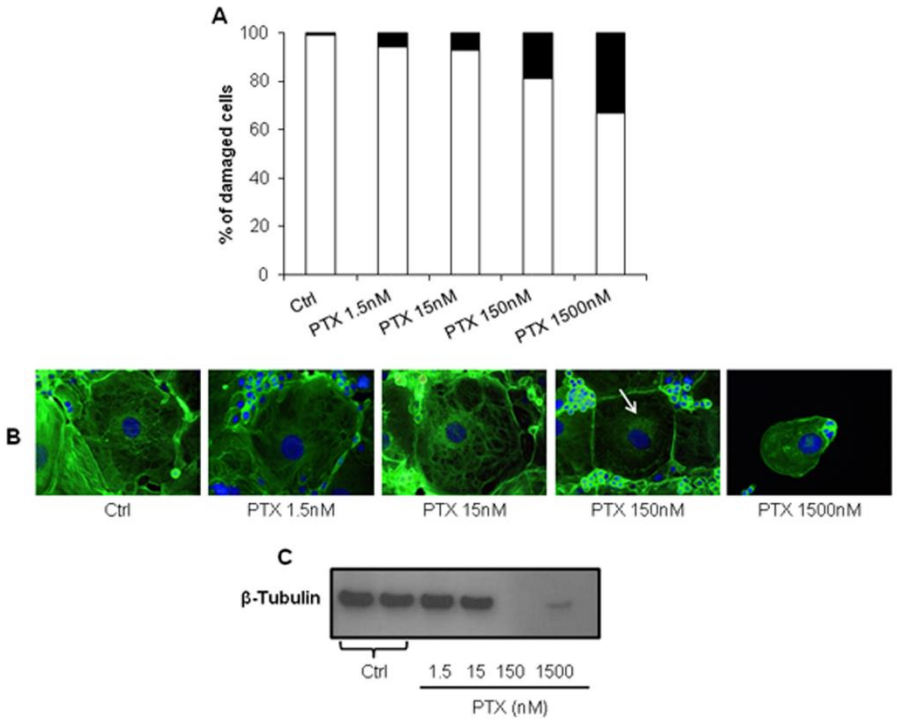

Supplementary Figure 5. Low dose PTX did not affect cytoskeletal integrity of EGI-1 cells. By phalloidin staining, only a small percentage of EGI-1 cells challenged with low dose PTX (1.5, 15nM), displayed structural alterations of the actin filaments, which instead were observed in a larger subset of EGI-1 cells exposed to high dose PTX (150, 1500nM). No differences in damaged cells between low dose PTX and untreated cells could be observed (n=3, percentage of apoptotic cells expressed as black area of the column) (A). Representative immunofluorescence for FITC-conjugated phalloidin (green) in cultured cells treated with increasing doses of PTX are shown below each column plot; perinuclear condensation, a hallmark of cytoskeletal disaggregation, is clearly observed in single cells treated with PTX 150nM (white arrow), whereas cytoplasm shrinkage is evident in cells treated with PTX 1500nM. Original magnification, M=400x (B). WB for β-tubulin in microtubule fractions purified by ultracentrifugation shows lack of expression indicating cytoskeletal damage in cells exposed to PTX 150 e PTX 1500nM (C).

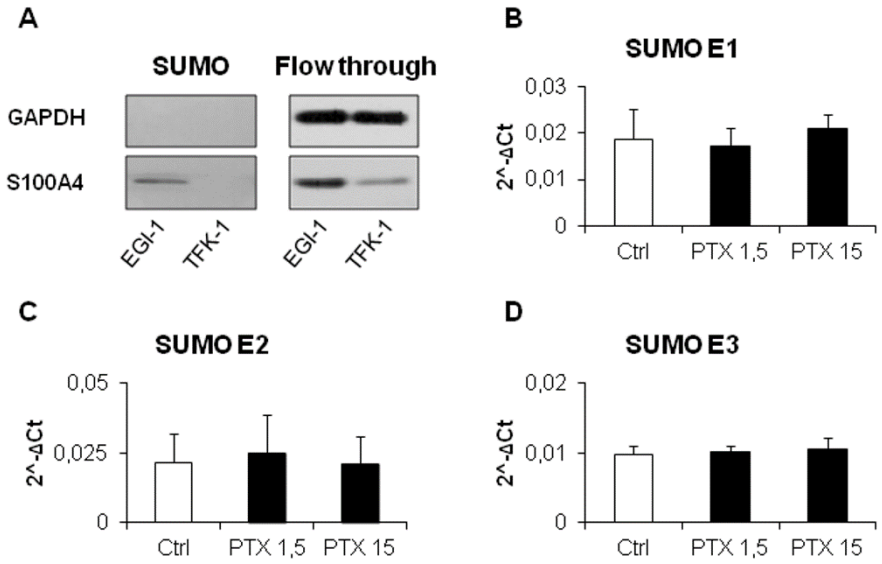

Supplementary Figure 6. EGI-1 cells but not TFK-1 cells contained SUMOylated S100A4; inhibitory effects of low dose PTX on SUMOylating complex did not associate with any deregulation of SUMO E subunits. By SUMOylation assay, SUMOylated S100A4 could be detected only in EGI-1 cells (expressing S100A4 in the nucleus), whereas it was absent in TFK-1 cells, a CCA cell line where S100A4 expression is limited to the cytoplasm. Accordingly, un-SUMOylated S100A4 could be detected in either cell lines, as shown by the band present in the flow through fraction (A). By Real time PCR, mRNA expression levels of each SUMOylating complex subunit in EGI-1 cells (B, E1; C, E2; D, E3) were not affected by treatment with low dose PTX.

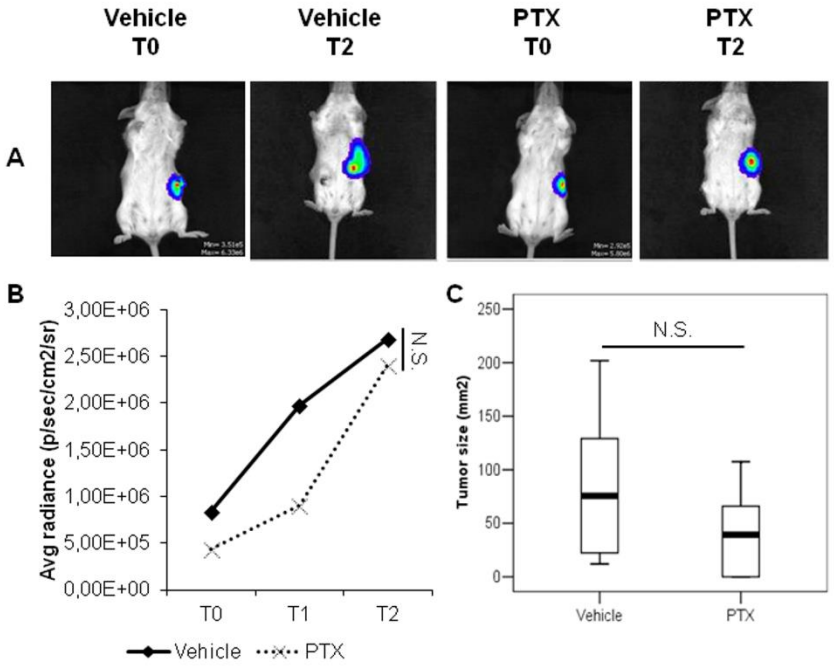

Supplementary Figure 7. LDM PTX did not affect the splenic tumor mass in SCID mice xenotransplanted with EGI-1 cells, in vivo. SCID mice xenografted by intrasplenic injection of EGI-1 cells transduced with a lentiviral vector encoding the firefly luciferase gene were treated with LDM PTX or vehicle after confirming tumor engraftment by bioluminescence imaging. No statistically significant differences between LDM PTX treated mice and controls were observed both in the level of photon emission (A, representative images taken at the beginning (T0) and at the end (T2) of treatment; B, bioluminescence curve during the treatment) and in the size of the splenic tumor mass measured at necroscopic examination (C).

CHAPTER 4

Platelet-derived growth factor D enables cancer-associated fibroblasts to promote tumor lymphangiogenesis in cholangiocarcinoma

Massimiliano Cadamuro[1,2], **Simone Brivio**[1], Marta Vismara[1], Joachim Mertens[3,4], Anja Moncsek[3,4], Chiara Milani[1], Maria Cristina Malerba[1], Tommaso Stecca[5], Marco Massani[6], Valeria Mariotti[7], Carlo Spirli[8], Romina Fiorotto[8], Stefano Indraccolo[9], Giorgia Nardo[9], Mario Strazzabosco[#1,2,8], and Luca Fabris[#2,7,8]

[1]School of Medicine and Surgery, University of Milan-Bicocca, Monza, Italy
[2]International Center for Digestive Health, University of Milan-Bicocca, Monza, Italy
[3]Division of Gastroenterology and Hepatology, University Hospital Zürich, Zürich, Switzerland
[4]Swiss HPB Center, University Hospital Zürich, Zürich, Switzerland
[5]Department of Surgical Oncological and Gastroenterological Sciences, University of Padua, Padua, Italy
[6]Department of Surgery, IV unit, Regional Hospital Ca' Foncello, Treviso, Italy
[7]Department of Molecular Medicine, University of Padua, Padua, Italy
[8]Liver Center, School of Medicine Section of Digestive Diseases, Yale University, New Haven, Connecticut, USA
[9]Immunology and Molecular Oncology Unit, Veneto Institute of Oncology IRCCS, Padua, Italy
[#]these authors contributed equally to this article

Unpublished data

ABSTRACT

Background and aims. In cholangiocarcinoma (CCA), early metastatic spreading via lymphatic vessels often precludes curative surgery. CCA invasiveness is fostered by the strong stromal reaction, enriched in cancer-associated fibroblasts (CAF) and lymphatic endothelial cells (LEC). Since platelet-derived growth factor (PDGF)-D secreted by CCA cells recruits CAF, here we investigated its role in promoting CCA-associated lymphangiogenesis. **Methods.** Human CCA specimens were immunostained for D2-40 (LEC marker), α-SMA (CAF), and for vascular endothelial growth factors (VEGF-A and VEGF-C), and their cognate receptors VEGFR2 and VEGFR3 (lymphangiogenesis). VEGF-A and VEGF-C secretion (ELISA) was evaluated in human fibroblasts challenged with PDGF-D, with or without inhibitors of PDGFRβ (imatinib). Using human LEC exposed to conditioned medium from PDGF-D-stimulated fibroblasts (with/without imatinib), we assessed migration (Boyden chambers), 3D vascular assembly (AngioTool), trans-endothelial electric resistance and trans-endothelial migration of CCA cells (EGI-1). **Results.** In CCA specimens, CAF and LEC laid closely adjacent, reciprocally expressing VEGF-A/VEGF-C (CAF), and VEGFR2/VEGFR3 (LEC). Upon stimulation with PDGF-D, fibroblasts secreted increased levels of VEGF-A and VEGF-C. PDGF-D-stimulated fibroblasts induced LEC recruitment and 3D vascular assembly, increased LEC monolayer permeability, and promoted trans-endothelial migration of CCA cells,

all effects suppressed by imatinib. In a syngeneic rat model of CCA, CAF depletion induced by navitoclax was associated to a markedly decreased lymphatic vascularization. **Conclusion.** PDGF-D secreted by CCA enables CAF to produce VEGF-A and VEGF-C, thus promoting the expansion of the lymphatic vasculature and tumor cell intravasation, likely responsible for the early metastatic dissemination observed in CCA, which may eventually be blocked by inducing CAF apoptosis or by inhibiting PDGFRβ signalling.

INTRODUCTION

Cholangiocarcinoma (CCA), originating from the intrahepatic or extrahepatic bile ducts, is one of the epithelial malignancy with the worst outcome worldwide [1]. Although the epidemiological impact of CCA has become stronger in the last decade, effective treatments are still scarce and limited to surgical resection and, in a few cases, liver transplant [1-3]. However, only less than one third of patients are actually eligible for curative surgery at the time of diagnosis, due to a proclivity for early lymph node metastatization [1,4]. Although mechanisms promoting CCA invasiveness are still unclear [5], the lymphatic vasculature developing within the tumor microenvironment provides an important initial route of metastatic dissemination. Indeed, several lines of evidence indicate that the expansion of the lymphatic bed correlates with both increased metastatization and poor prognosis in CCA patients [6-8].

Tumor-associated lymphangiogenesis is driven by a number of soluble mediators, including vascular endothelial growth factor (VEGF)-A, VEGF-C, VEGF-D, angiopoietin (Ang)-1 and Ang-2, together with their cognate receptors VEGFR2 (for VEGF-A, VEGF-C and VEGF-D), VEGFR3 (for VEGF-C and VEGF-D), and Tie2 (for angiopoietins) [9,10]. Although VEGF ligands can be expressed by the cancer cells themselves, inflammatory cells and fibroblasts accumulating nearby the tumor represent the main source of VEGF [11]. In fact, as in other ductal carcinomas with pronounced invasiveness (e.g., breast and pancreatic cancer) [12,13], the neoplastic growth of bile ducts occurs in close contiguity with a rich stromal reaction, termed tumor reactive stroma, mainly composed of cancer-associated fibroblasts (CAF), tumor-associated macrophages, and lymphatic endothelial cells (LEC) [14-16].

Within the tumor reactive stroma, a multitude of paracrine signals is mutually exchanged between the cancer and stromal compartment, aimed at fostering local invasiveness and metastatic spread of the epithelial counterpart [5,11,17]. CAF are the most represented cell type in the tumor reactive stroma. Recently, we demonstrated that in CCA, they are locally recruited by malignant cholangiocytes via the secretion of platelet-derived growth factor (PDGF)-D [18]. In fact, PDGF-D is specifically produced by CCA cells upon hypoxic stimulus, and can bind to its cognate receptor PDGFRβ expressed by CAF [18]. The concept that CAF are essential drivers of

CCA aggressiveness has been highlighted by the finding that in a syngeneic rat model of CCA, selective CAF depletion achieved by navitoclax (i.e., a specific inhibitor of the anti-apoptotic proteins Bcl-2, Bcl-w and Bcl-xL) markedly suppressed tumor growth and improved host survival [19].

In the present study, we hypothesized that, in addition to inducing CAF accumulation within the tumor stroma, PDGF-D may stimulate their pro-lymphangiogenic abilities, eventually promoting the chemotaxis of LEC, and their assembly in a proper vascular system favoring CCA cell intravasation. Furthermore, we tested the hypothesis that depletion of CAF by navitoclax would lead to a reduction in the lymphatic vascularization of the tumor mass, *in vivo*.

MATERIALS AND METHODS

Cell lines. Human fibroblasts, obtained from liver explants of primary sclerosing cholangitis, as previously published [18], and the commercially available human lymphatic endothelial cells (LEC, purchased from ScienCell™) and EGI-1 cells (PDGF-D expressing extrahepatic CCA cell line, purchased from Deutsche Sammlung von Mikroorganismen und Zellkulturen) were used. Phenotypic characterization of cultured fibroblasts reproduced that of CAF, as they expressed alpha-smooth muscle actin (α-SMA), fibroblast specific protein-1 (FSP-1), vimentin and PDGFRβ, consistent with an activated phenotype. See Supplemental Materials for details.

Human tissue samples and immunohistochemistry. Paraffin-embedded histological samples of surgically resected intrahepatic CCA (n=6) and hepatocellular carcinoma (HCC) (n=6) were obtained from archival tissues from Ca' Foncello Regional Hospital (Treviso, Italy). Local regional ethical committee approval was obtained for tissue collection. Tissue specimens were immunostained for D2-40 (lymphatic vessel marker) and CD34 (blood vessel marker), to evaluate lymphatic microvessel density (LMVD) and blood microvessel density (BMVD), respectively. In CCA slides, double immunostaining for D2-40 and α-SMA (CAF marker) was performed to evaluate the spatial relationship between CAF and LEC, whereas dual immunofluorescence, with antibodies against VEGF-A, VEGF-C, VEGFR2, or VEGFR3, matched with D2-40, α-SMA, or cytokeratin (K)19 antibodies, was performed to assess expression of lymphangiogenesis growth factors and receptors. Further details are given in Supplementary Methods and Supplementary Table 1.

Syngeneic rodent model of CCA. To evaluate whether targeting CAF affects tumor lymphangiogenesis *in vivo*, we used the syngeneic rat model of CCA, generated by intrahepatic transplantation of neoplastic cholangiocytes (BDEneu rat cells) into Fischer 344 male rats, where CAF were selectively depleted by navitoclax [19]. 8μm-cut cryostat liver sections obtained from rats harboring syngeneic CCA, with (n=6) and without (n=6) treatment with navitoclax, were studied by

immunohistochemistry and dual immunofluorescence for PDGF-D, α-SMA, and Lyve-1 (LEC marker in rat) (same protocol as above) to evaluate whether, in conditions of PDGF-D expression by CCA cells, CAF reduction was associated to a decreased LMVD. See details in Supplemental Materials.

Lymphangiogenic growth factors quantification. ELISA was performed in fibroblast supernatant following exposure to recombinant human (rh) PDGF-D (100ng/ml, 24h, R&D Systems) to assess the secretion of lymphangiogenic growth factors VEGF-A, VEGF-C, VEGF-D, Ang-1 or Ang-2. The intracellular pathway activated by PDGF-D was dissected by assessing the secretory levels before and after inhibition of PDGFRβ (imatinib mesylate, IM), and its intracellular transducers, i.e., extracellular-regulated kinase (ERK) (U0126) and c-Jun N-terminal kinase (JNK) (SP600125). See Supplemental Material for details.

Western blotting (WB). WB was performed to assess the directionality of the PDGF-D-induced cross talk involving CAF and LEC, by evaluating PDGFRβ, VEGFR2 and VEGFR3 expression in LEC and fibroblasts. Details of WB experiments are described in Supplementary Methods and Supplementary Table 1.

***In vitro* assessment of lymphangiogenesis.** The effects of conditioned medium harvested from PDGF-D-stimulated fibroblasts on **LEC migration** and **3D tube formation** were studied as reported in Supplemental Materials, with/without antagonism of PDGFRβ (on fibroblasts), VEGFR2 and VEGFR3 (on LEC). VEGF-A and VEGF-C served as positive controls.

***In vitro* assessment of lymphatic intravasation by CCA cells.** Under the same conditions reported above, we evaluated the **transendothelial resistance (TEER)** of LEC monolayers, and the **transendothelial migration (TrEM)** of EGI-1 cells transduced with a lentiviral vector encoding EGFP reporter gene, as previously performed [18]. See Supplementary Methods.

MTS assay. See Supplementary Methods.

Statistical Analysis. Results are shown as the mean ± standard deviation. Statistical comparisons were performed using Student's t-test. A p value <0.05 was considered significant.

RESULTS

Lymphatic Microvascular Density (LMVD) rather than Blood Microvascular Density (BMVD) is increased in CCA compared with HCC. To evaluate the extent of tumor-associated

lymphangiogenesis and angiogenesis, we quantified the density of D2-40$^+$ lymphatic vessels (LMVD) and CD34$^+$ blood vessels (BMVD) in human specimens of CCA and HCC, a primary liver malignancy characterized by a rich blood vascularization. With respect to HCC, where high BMVD was associated with negligible LMVD, CCA showed a marked increase in LMVD, but a lower BMVD (Fig. 1A,B). Specifically, in CCA samples, LMVD was comparable to BMVD, thus confirming that the expansion of the lymphatic vasculature is a defining feature of desmoplastic CCA, in contrast with the scarcity of lymphatic vessels observed in HCC.

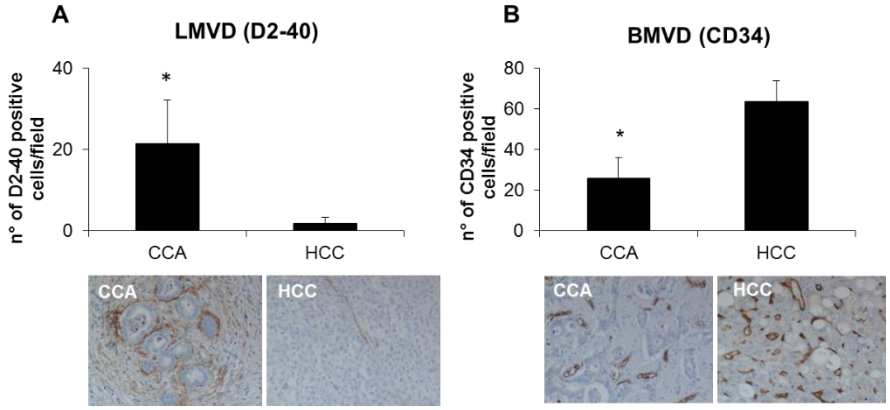

Figure 1. In CCA, lymphatic microvascular density (LMVD) is much more preponderant than in HCC, at variance with blood microvascular density (BMVD). In human archival paraffin sections, LMVD was more extensively represented in CCA with respect to HCC, as shown by IHC for D2-40 (lymphatic endothelial cell marker) (A). On the contrary, BMVD, evaluated as number of CD34$^+$ (blood endothelial cell marker) cells, was increased in HCC samples (B). Below the plots, representative pictures of D2-40$^+$ (A), and CD34$^+$ (B) structures are shown for CCA and HCC. n=6; *p<0.01; Original magnification: 200x.

In human CCA specimens, CAF and LEC are in close vicinity and reciprocally express VEGF ligands and receptors. We then investigated the spatial relationship between the prominent lymphatic vasculature and CAF in CCA. Double immunostaining for α-SMA (CAF marker) and D2-40 (LEC marker) revealed that CAF and LEC laid in close vicinity within the tumor reactive stroma of human CCA (Fig. 2A). By dual immunofluorescence, we further observed that CAF expressed VEGF-A and VEGF-C, whereas their cognate receptors VEGFR2 and VEGFR3 were reciprocally expressed by LEC (Fig. 2B-E). Some extra-CAF immunostaining for VEGF-A and VEGF-C could be observed in inflammatory cells populating the tumor stroma. However, in neoplastic bile ducts, VEGF-A expression was scattered, whereas VEGF-C was consistently negative (Fig. 2F,G). Overall, these data are consistent with the hypothesis that a paracrine mechanism directed from CAF to LEC is responsible for the development of a rich lymphatic plexus within the tumor microenvironment.

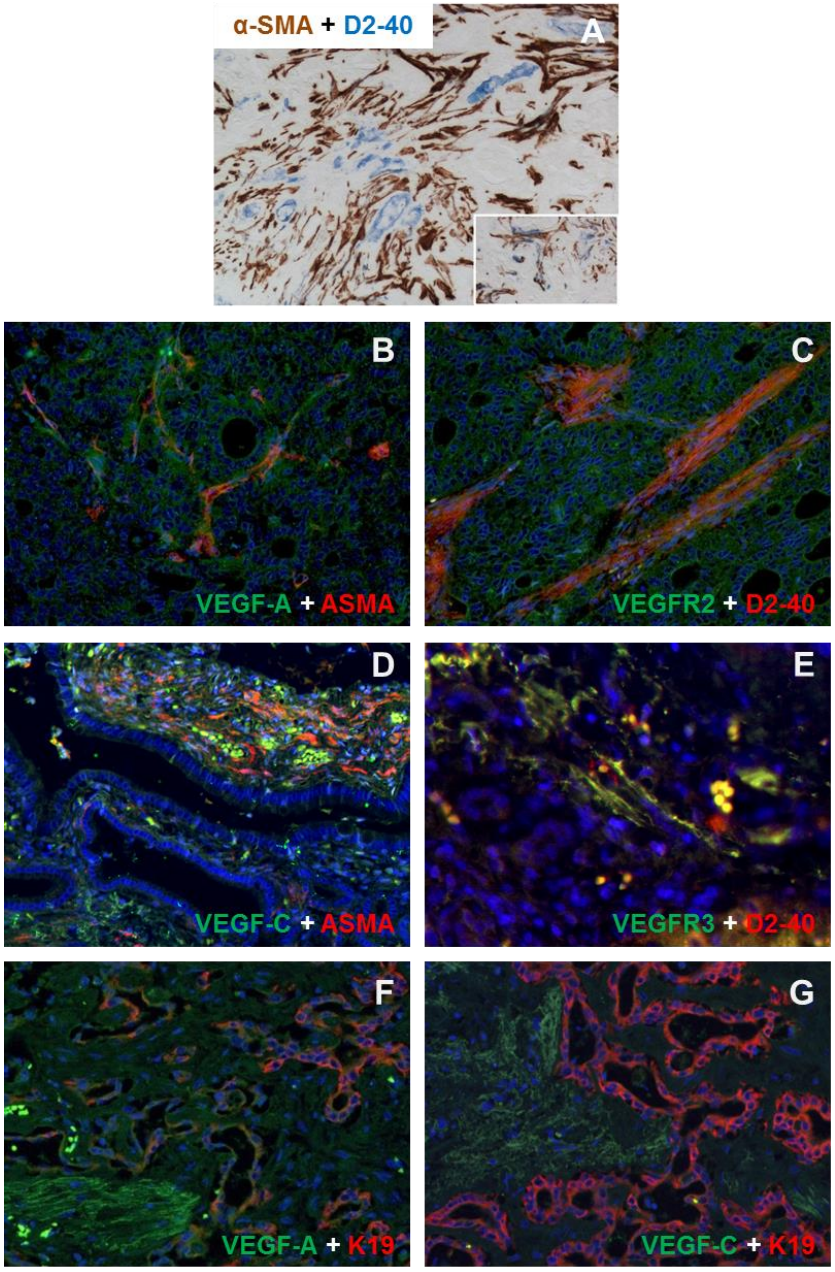

Figure 2. In human CCA specimens, cancer-associated fibroblasts (CAF) and lymphatic endothelial cells (LEC) are in close contiguity, and reciprocally

express VEGF ligands and receptors. Within the TRS of CCA, LEC were localized in close proximity to CAF, as shown by dual IHC for D2-40 (blue) and α-SMA (brown) (A, see inset for details). Moreover, α-SMA$^+$ CAF (red) expressed VEGF-A and VEGF-C (green) (B,D), while D2-40$^+$ LEC (red) expressed VEGFR2 and VEGFR3 (green) (C,E). K19$^+$ neoplastic cholangiocytes (red) showed a patchy expression of VEGF-A (green), whilst VEGF-C (green) was not expressed (F,G). Original magnification: A-D, F-G, 200x; E, 400x. Inset in A: 400x.

PDGF-D stimulates the secretion of VEGF-A and VEGF-C, but not of VEGF-D, Ang-1 and Ang-2 by human fibroblasts. To assess whether PDGF-D could provide fibroblasts with pro-lymphangiogenic functions, we challenged primary human fibroblasts with PDGF-D, and then we evaluated the secretion of paramount lymphangiogenic growth factors, i.e., VEGF-A, VEGF-C, VEGF-D, Ang-1 and Ang-2, by ELISA. PDGF-D-treated fibroblasts showed a significant and marked increased secretion of both VEGF-A and VEGF-C. Ang-1 was insensitive to PDGF-D stimulation, and remained at much lower levels (Table 1). Of note, VEGF-D and Ang-2 secretion was not detectable, no matter the exposure to PDGF-D.

	Ctrl	**PDGF-D**
Ang-1	190.57 ± 84.68	162.27 ± 84.10
Ang-2	ND	ND

VEGF-A	188.51 ± 87.56	1152.48 ± 297.11**
VEGF-C	696.47 ± 119.20	1715.30 ± 579.83**
VEGF-D	ND	ND

Table 1. Assessment of lymphangiogenic growth factors secreted in the supernatant by cultured human fibroblasts exposed to PDGF-D. **p<0.01 vs Ctrl; ND: not detectable.

ERK and JNK signaling mediates the PDGF-D-induced secretion of VEGF-A and VEGF-C by fibroblasts. We next investigated the signaling pathways regulating VEGF-A and VEGF-C secretion by fibroblasts upon stimulation with PDGF-D. To this end, VEGF-A and VEGF-C were assessed in supernatants harvested from fibroblasts challenged with PDGF-D, with or without inhibitors of PDGFRβ (imatinib mesylate), and of its downstream effectors ERK (U0126) and JNK (SP600125). PDGFRβ antagonism, as well as ERK or JNK inhibition, significantly counteracted the increase in VEGF-A and VEGF-C secretion induced by PDGF-D, with comparable decreasing effects (Fig. 3A,B). Overall, these data indicate that two distinct and likely redundant signaling pathways are activated in fibroblasts upon PDGF-D/PDGFRβ binding, and cooperate to promote VEGF-A and VEGF-C secretion. These findings are in line with previous observations performed in osteoblasts [20] and pericytes [21], with PDGFRβ activation dependent upon PDGF-B stimulation.

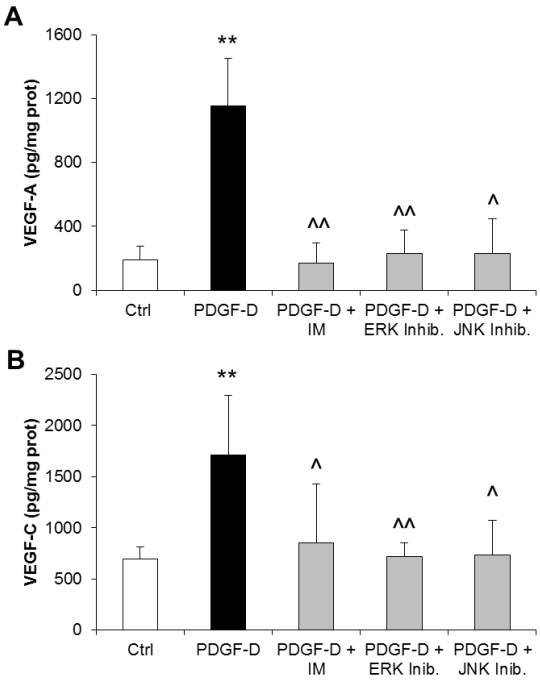

Figure 3. PDGF-D-stimulated secretion of VEGF-A and VEGF-C by human fibroblasts is dependent on ERK and JNK activation. While evaluating the intracellular signaling mediating VEGF-A and VEGF-C secretion by fibroblasts, we found that ERK and JNK inhibition abrogated the stimulatory effects of PDGF-D on both VEGF-A (A) and VEGF-C (B) secretory levels, similarly to what observed with imatinib mesylate (IM) (PDGFRβ inhibitor). n=6 *p<0.05 vs Ctrl; **p<0.01 vs Ctrl; ^p<0.05 vs PDGF-D; ^^p<0.01 vs PDGF-D.

The migration of LEC was potently stimulated by conditioned medium (CM) collected from fibroblasts challenged with PDGF-D. LEC migration is a prerequisite for tumor lymphangiogenesis [10]. To understand whether PDGF-D endowed fibroblasts with the ability to stimulate the chemotaxis of LEC, we studied LEC migration in Boyden chambers. We found that CM harvested from fibroblasts treated with

PDGF-D significantly increased the migration of LEC compared to controls, an effect completely abolished by challenging fibroblasts with imatinib mesylate. The recruiting effect of the CM from PDGF-D-stimulated fibroblasts on LEC was comparable to that exerted by VEGF-A or VEGF-C (Fig. 4A,B). Of note, WB analysis confirmed that LEC expressed VEGFR2 and VEGFR3, but not PDGFRβ, thus ruling out the possibility that they were influenced by residual exogenous PDGF-D potentially present in the CM (Supplementary Fig.1).

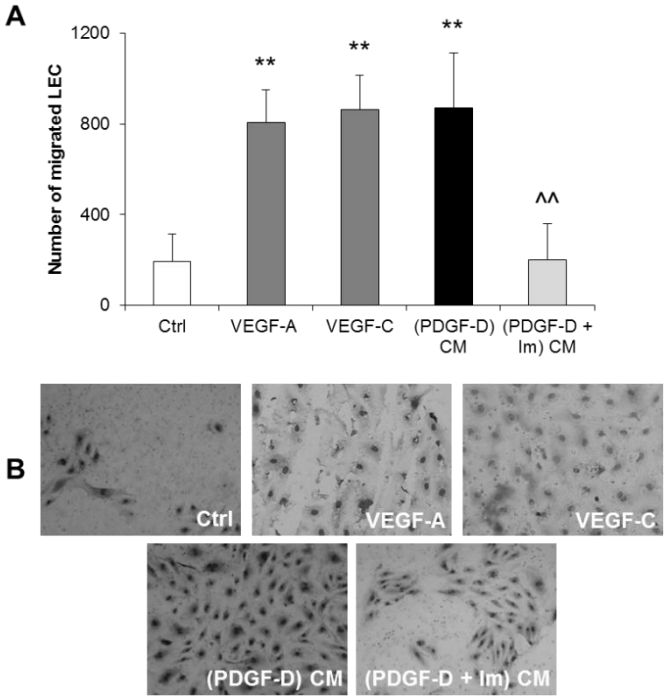

Figure 4. Upon PDGF-D stimulation, cultured human fibroblasts promote LEC recruitment, in vitro. Conditioned medium (CM) from fibroblasts exposed to PDGF-D, referred to as (PDGF-D) CM, potently stimulated LEC migration, an effect prevented by PDGFRβ antagonism with imatinib mesylate (Im), referred to as

(PDGF-D+Im) CM (A). Representative pictures of Boyden Chamber inserts (magnification = 200x) (B). n=6 **p<0.01 vs Ctrl; ^^p<0.01 vs (PDGF-D) CM.

Conditioned medium from PDGF-D-treated fibroblasts stimulated tubulogenesis in three-dimensional cultures of LEC. After showing the recruiting effect on LEC, we sought to evaluate whether, upon PDGF-D stimulation, fibroblasts could also prompt LEC to generate branched tubular structures. To this end, we generated 3D cultures of LEC, we exposed them to CM from PDGF-D-treated fibroblasts, and then we performed an AngioTool software-based tubulization assay in order to evaluate the percentage of area covered by vessels, the length of branches, and the number of junctions between branches [22]. Compared to controls, CM from PDGF-D-stimulated fibroblasts significantly increased all three morphometric parameters, similarly to VEGF-A and VEGF-C. Importantly, these effects were hampered by antagonizing either PDGFRβ on fibroblasts, or VEGFR2 (by SU5416) and VEGFR3 (by SAR131675) on LEC (Fig. 5A-D). Of note, SU5416 and SAR131675 were not cytotoxic on LEC at the chosen experimental doses, as shown by a dose-response MTS assay (Supplementary Fig. 2A,B). It must be borne in mind that VEGF-C can act by binding to either VEGFR2 or VEGFR3, whereas VEGF-A only binds to VEGFR2 [23]. Altogether, these data suggest that, following PDGF-D stimulation, fibroblasts can potently promote lymphangiogenesis.

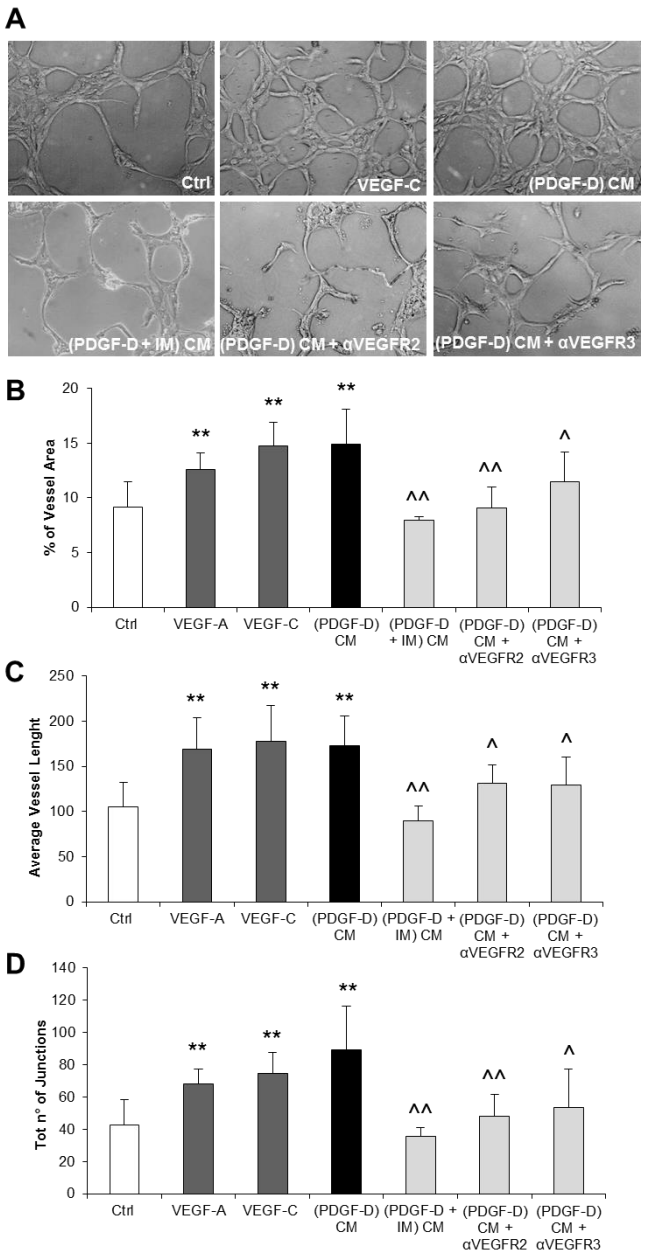

Figure 5. Upon PDGF-D stimulation, cultured human fibroblasts exert multiple lymphangiogenetic functions, inducing lumen formation, tubular branching

and tubular lengthening of cultured LEC, *in vitro*. Representative micrographs of LEC tubulization and branching in a fibronectin/matrigel sandwich for each treatment condition (A). CM from PDGF-D-treated fibroblasts, referred to as (PDGF-D) CM, induced 3D-cultured LEC to increase significantly the vessel area (B), the vessel length (C) and the number of junctions (D), with respect to controls. These effects were significantly attenuated by PDGFRβ antagonism in PDGF-D-treated fibroblasts, referred to as (PDGF-D + IM) CM, as well as by pre-treatment of LEC with inhibitors of either VEGFR2, referred to as (PDGF-D) CM + αVEGFR2, or VEGFR3, referred to as (PDGF-D) CM + αVEGFR3. n=minimum 4 experiments; **p<0.01 vs Ctrl; ^p<0.05 vs (PDGF-D) CM; ^^p<0.01 vs (PDGF-D) CM. Original magnification: 200x.

The permeability of LEC monolayers was markedly enhanced by conditioned medium from fibroblasts stimulated by PDGF-D. The high permeability of the lymphatic vasculature caused by defective tight junctions is conducive to tumor cell invasion [10,24]. Thus, to evaluate the effect of PDGF-D-stimulated fibroblasts on the permeability of lymphatic vessels, we allowed LEC to become confluent, and then we measured the TEER across the endothelial monolayer. We found that the TEER was significantly impaired by CM from PDGF-D-stimulated fibroblasts (Fig. 6A), and this effect could be prevented by treating fibroblasts with imatinib mesylate. Interestingly, exogenous VEGF-C increased the permeability of LEC monolayer, whereas VEGF-A did not. Consistently, VEGFR3 but not VEGFR2 antagonism on LEC challenged with CM from PDGF-D-stimulated fibroblasts restored the TEER to basal levels (Fig. 6A). Overall, these results suggest that fibroblasts treated with PDGF-D can dampen the integrity of the lymphatic endothelial barrier by secreting

VEGF-C, which is indeed capable of triggering the formation of intercellular gaps between adjacent LEC [10].

Conditioned medium from PDGF-D-treated fibroblasts supported the trans-endothelial migration of CCA cells across LEC monolayers. After showing that the permeability of LEC monolayers increased upon exposure to CM from PDGF-D-treated fibroblasts, we sought to determine whether the migration of CCA cells through the endothelial barrier was actually promoted as well. We seeded EGFP-expressing EGI-1 cells on the top of a LEC monolayer concurrently exposed to CM from PDGF-D-stimulated fibroblasts, and found that the number of trans-LEC migrated CCA cells was considerably increased, compared with controls. This effect was almost completely inhibited by antagonizing either PDGFRβ on fibroblasts, or VEGFR3 (but not VEGFR2) on LEC (Fig. 6B, and Supplementary Fig. 3).

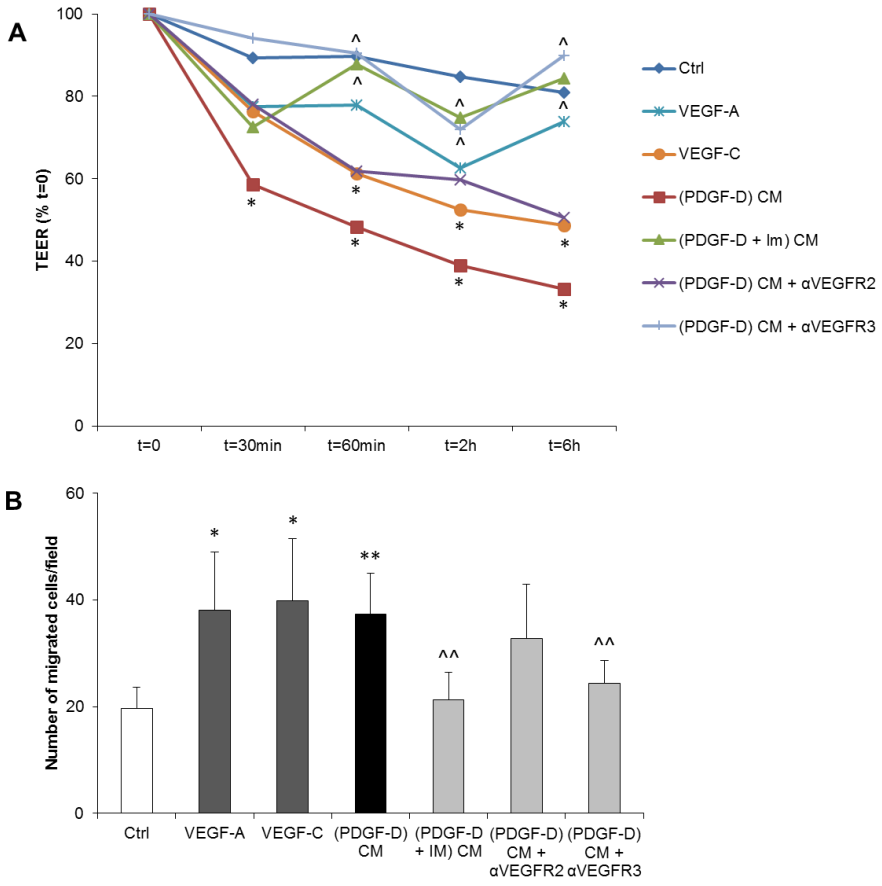

Figure 6. Upon PDGF-D stimulation, cultured human fibroblasts reduce trans-endothelial resistance of LEC monolayers (TEER) and stimulate trans-endothelial migration (TrEM) of CCA cells (EGI-1-EGFP). CM from PDGF-D-treated fibroblasts, referred to as (PDGF-D) CM, dramatically impaired the integrity of the lymphatic endothelial barrier, more effectively than VEGF-C and VEGF-A. This effect was only partially counteracted by the concomitant treatment with αVEGFR2, referred to as (PDGF-D) CM + αVEGFR2, but completely abrogated by the supplementation with αVEGFR3, referred to as (PDGF-D) CM + αVEGFR3, as well as by PDGFRβ antagonism in PDGF-D-treated fibroblasts, referred to as (PDGF-D + IM) CM (A). In TrEM experiments, CM from PDGF-D-treated fibroblasts enabled the CCA cell line EGI-1-EGFP to more easily cross the LEC monolayer (similar to VEGF-A and

VEGF-C), an effect blunted by the treatment of PDGF-D-stimulated fibroblasts with PDGFRβ antagonist, or by the treatment of LEC with αVEGFR3, but not with αVEGFR2 (B). n=minimum 7 experiments in duplicate *p<0.05 vs Ctrl, **p<0.01 vs Ctrl, ^p<0.05 vs (PDGF-D) CM, ^^p<0.01 vs (PDGF-D) CM.

Reduction of CAF by navitoclax markedly decreases the lymphatic vascularization in a syngeneic rat model of CCA. To confirm *in vivo* the strategic role played by CAF in directing tumor lymphangiogenesis, we used a well-established syngeneic rat model of CCA [19,25,26], featuring an intense expression of PDGF-D by CCA cells. Selective apoptotic depletion of CAF induced by navitoclax was accompanied by a significant decrease in the LMVD compared to control rats, without affecting the expression of PDGF-D by tumoral cholangiocytes (Fig. 7 and Supplementary Fig. 4). These data pinpoints the concept that CAF may represent a valuable target to hamper lymphatic dissemination in CCA.

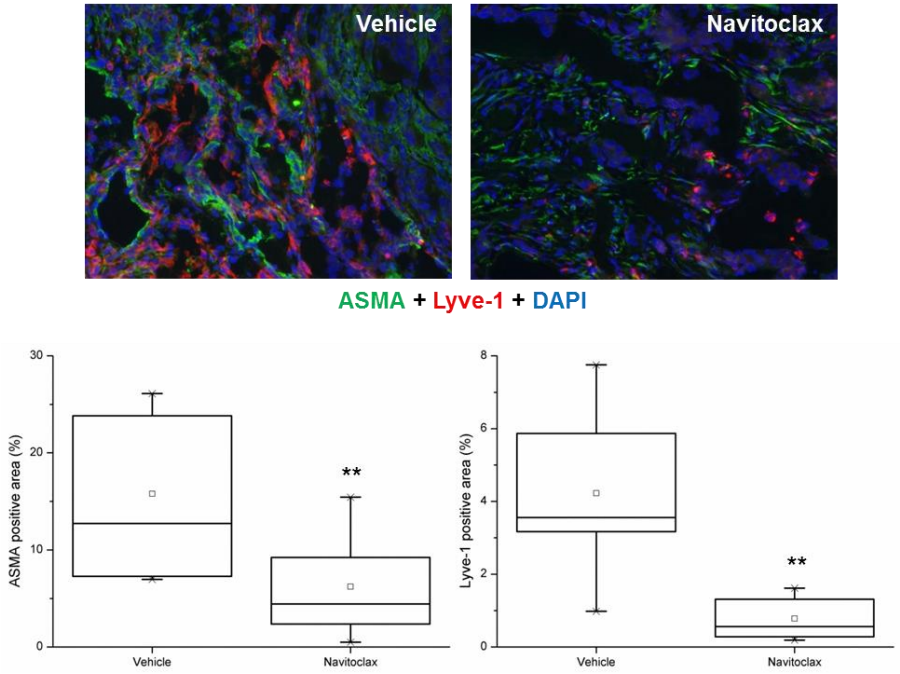

Figure 7. In a syngeneic rat model of CCA, targeting CAF by navitoclax correlates with a decreased lymphatic vascularization. In Fischer 344 male rats transplanted with BDE-neu rat CCA cells, selective depletion of α-SMA$^+$ CAF (graph left-sided) by navitoclax treatment was accompanied by a significant decrease in D2-40$^+$ LEC (graph right-sided) compared to untreated rats. In the top, representative images of CCA sections, with dual immunofluorescence for α-SMA (red) and D2-40 (green), show the stark difference between navitoclax and vehicle groups (n=6 each group). Original magnification: 100x. **p<0.01 vs Vehicle.

CONCLUSIONS

The generation of an exuberant lymphatic plexus within the tumor reactive stroma is a key event in CCA progression. Indeed, early metastatic dissemination through the lymphatic vessels occurs in 60-70% of CCA patients, often precluding curative surgery [27,28]. However, the molecular mechanisms modulating lymphangiogenesis

in CCA are still poorly elucidated, and more generally, tumor-associated lymphangiogenesis is still a major gap in knowledge in cancer research.

Among the multiple factors mediating the mutual epithelial-mesenchymal interactions typically fueling CCA aggressiveness, PDGF-D is attracting considerable interest, owing to its key role in the generation of the tumor reactive stroma, and its potential druggability [14,18]. As shown in different settings, PDGF-D exerts a repertoire of functions related to tumor-promotion, by fostering cancer cell proliferation and invasiveness, fibroblast recruitment and activation, and aberrant extracellular matrix deposition [18,29-31]. In this study, we provide evidence that in CCA, cancer cell-derived PDGF-D (which we previously showed to be up-regulated in malignant cholangiocytes under hypoxic conditions) triggers a multi-step paracrine sequence centered on CAF. This extensive paracrine signaling eventually leads to a massive recruitment of LEC, as well as to their assembly in highly branched and leaky tubular structures that can be easily invaded by cancer cells for their metastatic dissemination. Therefore, this model provides novel molecular insights into tumoral lymphangiogenesis in CCA.

First, we observed that CCA samples displayed a striking expansion of the lymphatic vascular bed compared to HCC, in sharp contrast to blood vessels, which were instead, much less represented. These findings lend strong support to the notion that the lymphatic

rather than the blood vasculature represents a preferential route for CCA cells to escape from the primary site of growth. Moreover, we found that the lymphatic structures thriving within CCA stroma were closely surrounded by CAF. This strict physical proximity was most likely related to the reciprocal expression of VEGF-A and VEGF-C (which were negligibly expressed in malignant cholangiocytes) by CAF, and of their cognate receptors VEGFR2 and VEGFR3 by LEC, suggesting the existence of an intimate cross talk between the two cell types. It is interesting to note that a similar pattern of expression was found in other desmoplastic epithelial cancers, such as colorectal [32] and ovarian [33] carcinomas.

In an effort to reproduce the biological interactions occurring within the tumor microenvironment, we next challenged human fibroblasts with recombinant PDGF-D. The modulatory effects of PDGF family members (especially, PDGF-B) on the secretion of VEGF ligands have been documented in various cell types, including hepatic stellate cells [34] and pulmonary fibroblasts [35]. However, no study has ever focused on the pro-lymphangiogenic properties of PDGF-D. Nonetheless, it was previously shown that PDGFRβ inhibition reduced VEGF, Ang-1, and Ang-2 mRNA expression in a mouse model of corneal neovascularization [36]. In our study, we demonstrated that PDGF-D potently elicits the secretion of VEGF-A and VEGF-C by fibroblasts, without affecting the release of other lymphangiogenic growth factors, such as VEGF-D, Ang-1, and Ang-2. In particular, the PDGF-D-

dependent production of both VEGF isoforms by fibroblasts was mediated by two partially redundant pathways, namely ERK and JNK. The latter are renowned downstream effectors of PDGFRβ activation, well-known to regulate the secretion of several growth factors, including VEGF, though their involvement has been investigated so far more in epithelial than in mesenchymal cells. Overall, these data add another piece to the puzzle of the pleiotropic functions played by CAF in response to the PDGF-D signaling originating from CCA cells: CAF are not only simply attracted, but are also empowered to direct tumor lymphangiogenesis.

To further address this issue, we assessed the influence of CM harvested from PDGF-D-stimulated fibroblasts on LEC motility, vascular assembly and permeability. In order to rule out confounding effects possibly related to the presence of residual exogenous PDGF-D, we preliminarily evaluated the expression of PDGFRβ on LEC. We found that LEC did not express PDGFRβ, while strongly expressing VEGFR2 and VEGFR3. It is fair to note that these findings are in contrast with data published in other studies. For instance, Cao et al. reported PDGFRβ expression on LEC; however, they used LEC of murine and rat origin, and moreover, they evaluated PDGFRβ expression only at the mRNA and not at the protein level [37]. Other studies in mice similarly described PDGFRβ expression on LEC, but only on LEC from large vessels; conversely, PDGFRβ expression was consistently negative on LEC lining the small vessels [38].

To evaluate the lymphangiogenic properties of CM from PDGF-D-treated fibroblasts, we employed the classic Boyden chamber system and the AngioTool software, which allows for a quick and reproducible quantification of different vessel morphological and spatial parameters, including vessel length, the percentage of area covered by vessels, and the number of branch points [39]. We found that cultured LEC exposed to CM from PDGF-D-stimulated fibroblasts were chemotactically recruited to aptly assemble branched vascular networks. Of note, the larger surface area covered by lymphatic structures increases the likelihood of contact with tumor cells, thereby favoring their access to lymphatics. This feature is regarded as a readout of paramount importance for lymph node metastatization [10,40].

In our model, enhanced lymphangiogenesis was dependent on the sequential activation of PDGFRβ on fibroblasts, and of VEGFR2 or VEGFR3 on LEC. In this regard, it is worth noting that the blockade of PDGFRβ resulted in a stronger inhibition of tubulogenesis compared to the specific antagonism of VEGFR2 or VEGFR3, thus suggesting that additional soluble factors released from PDGF-D-stimulated fibroblasts might act in concert with VEGF-A and VEGF-C to promote tumor lymphangiogenesis in CCA.

Although the correlation between the expression of lymphangiogenic growth factors and the propensity of the tumor to develop lymph node metastasis has been described in different cancer

types [41-43], the molecular mechanisms driving the lymphatic invasion of tumor cells remain elusive. Thus, to evaluate whether the pro-lymphangiogenic functions of CAF could also favor the entry of invasive cancer cells into the lymphatic vessels, we assessed the TEER across LEC monolayers, and the trans-LEC monolayer migration of CCA cells. Indeed, LEC monolayers challenged with CM from PDGF-D-stimulated fibroblasts showed an increased permeability compared to controls, in accordance with the observation that in colorectal cancer, VEGF-C makes the lymphatic endothelial barrier looser by weakening tight and adherent junctions [44]. Furthermore, CCA cells were able to cross LEC monolayers more easily upon exposure to CM from PDGF-D-stimulated fibroblasts. Of note, both effects were reverted by antagonizing either PDGFRβ on fibroblasts, or VEGFR3, but not VEGFR2, on LEC. This suggests that albeit VEGF-C and VEGF-A possess partially overlapping functions in the initial establishment of the lymphatic vascular network, the increase in endothelial permeability is a specific effect of VEGF-C. Taken together, these data suggest that PDGF-D is indeed a key factor secreted by CCA cells to recruit CAF and then shape them into potent pro-lymphangiogenic players, an essential step for permitting the lymphatic invasion and dissemination of tumor cells.

To confirm that CAFs are central actors in tumor lymphangiogenesis in CCA, we turned to a syngeneic rat model of CCA [25,26]. This animal model is characterized by a highly desmoplastic

tumor mass expressing PDGF-D (Supplementary Fig. 4), as well as by early metastatization. Selective reduction of CAF was obtained by treating rats with the anti-apoptotic protein inhibitor navitoclax [19]. Importantly, CAF depletion was paralleled by a stark decrease in the lymphatic vascular bed, thus supporting the great translational relevance of our working model.

In conclusion, our results unveil the presence of a paracrine sequence within the tumor reactive stroma of CCA, unleashed by PDGF-D, involving CCA cells, CAF and LEC, and able to orchestrate tumor-associated lymphangiogenesis and tumor cell intravasation (Fig. 8). This process is likely a pre-requisite for the dissemination of cancer cells to the regional lymph nodes, which is an early, frequent and feared event in CCA, placing the patient out of potential curative approaches. This working model provides a series of putative molecular targets amenable to therapeutic intervention, with the ultimate aim of halting the metastatic dissemination of CCA. Several small molecules are currently available to interfere with the different arms of the described paracrine mechanism, encompassing VEGFR inhibitors, PDGFR inhibitors, and inhibitors of CAF-specific anti-apoptotic proteins. For instance, regorafenib (or BAY 73-4506), a multi-kinase inhibitor already approved for the treatment of sorafenib-resistant HCC, definitely deserves our attention. In fact, regorafenib may allow to “kill two birds with one stone”, thanks to its ability to concurrently inhibit VEGFR-2 and -3, and PDGFR [45]. Of

note, regorafenib is already under phase II clinical trials for the treatment of CCA patients who did not benefit from first-line chemotherapy [46].

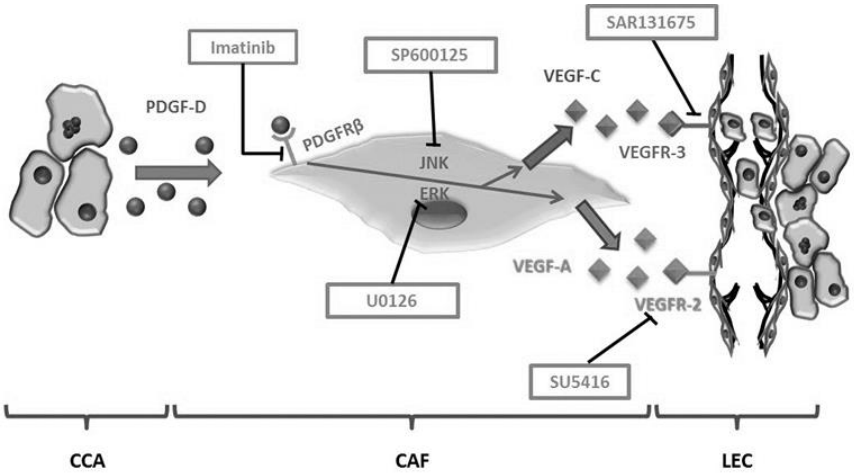

Figure 8. Molecular players mediating the pro-lymphangiogenic crosstalk among CCA cells, CAF and LEC. Upon being released by CCA cells, PDGF-D binds to PDGFRβ expressed on the surface of CAF, thereby triggering the activation of ERK and JNK pathways, which promote the secretion of VEGF-A and VEGF-C. Then, CAF-derived VEGF ligands trigger the activation of VEGFR2 (cognate receptor for VEGF-A and VEGF-C) and VEGFR3 (cognate receptor for VEGF-C) on the surface of LEC, which are thus induced to migrate and assemble highly branched and leaky vascular structures. The latter can be easily invaded by neoplastic cells, ultimately allowing for CCA metastatic spread.

REFERENCES

1. Banales JM, Cardinale V, Carpino V, Marzioni M, Andersen JB, Invernizzi P, et al. Expert consensus document: Cholangiocarcinoma: current knowledge and future perspectives consensus statement from the European Network

for the Study of Cholangiocarcinoma (ENS-CCA). Nat Rev Gastroenterol Hepatol 2016;13:261–280.

2. Razumilava N, Gores GJ. Cholangiocarcinoma. Lancet 2014;383:2168–2179.

3. Erice O, Merino-Azpitarte M, Arbelaiz A, Gutierrez-Larranaga M, Jimenez-Aguero R, Perugorria MJ, et al. Molecular Mechanisms of Cholangiocarcinogenesis: New Potential Targets for Therapy. Curr Drug Targets 2017;18:932-949.

4. DeOliveira ML, Cunningham SC, Cameron JL, Kamangar F, Winter JM, Lillemoe KD, et al. Cholangiocarcinoma: thirty-one-year experience with 564 patients at a single institution. Ann Surg 2007;245:755-762.

5. Brivio S, Cadamuro M, Fabris L, Strazzabosco M. Molecular mechanisms driving cholangiocarcinoma invasiveness: an overview. Gene Expr 2017; Epub ahead of print.

6. Thelen A, Scholz A, Benckert C, Weichert W, Dietz E, Wiedenmann B, et al. Tumor-associated lymphangiogenesis correlates with lymph node metastases and prognosis in hilar cholangiocarcinoma. Ann Surg Oncol 2008;15:791–799.

7. Thelen A, Scholz A, Weichert W, Wiedenmann B, Neuhaus P, Gessner R, et al. Tumor-associated angiogenesis and lymphangiogenesis correlate with progression of intrahepatic cholangiocarcinoma. Am J Gastroenterol 2010;105:1123-1132.

8. Luo X, Yuan L, Wang Y, Ge R, Sun Y, Wei G. Survival Outcomes and Prognostic Factors of surgical therapy for all potentially resectable intrahepatic cholangiocarcinoma: a large single-center cohort study. J Gastrointest Surg 2014;18:562-572.

9. Cao Y. Opinion: emerging mechanisms of tumor lymphangiogenesis and lymphatic metastasis. Nat Rev Cancer 2005;5:735-743.
10. Stacker SA, Williams SP, Karnezis T, Shayan R, Fox SB, Achen MG. Lymphangiogenesis and lymphatic vessel remodelling in cancer. Nat Rev Cancer 2014;14:159–172.
11. Kalluri R, Zeisberg M. Fibroblasts in cancer. Nat Rev Cancer 2006;6:392-401.
12. Qiao A, Gu F, Guo X, Zhang X, Fu L. Breast cancer-associated fibroblasts: their roles in tumor initiation, progression and clinical applications. Front Med 2016;10:33-40.
13. Pan B, Liao Q, Niu Z, Zhou L, Zhao Y. Cancer-associated fibroblasts in pancreatic adenocarcinoma. Future Oncol 2015;11:2603-2610.
14. Cadamuro M, Morton SD, Strazzabosco M, Fabris L. Unveiling the role of tumor reactive stroma in cholangiocarcinoma: an opportunity for new therapeutic strategies. Transl Gastrointest Cancer 2013;2:130-144.
15. Cadamuro M, Stecca T, Brivio S, Mariotti V, Fiorotto R, Spirli C, et al. The deleterious interplay between tumor epithelia and stroma in cholangiocarcinoma. Biochim Biophys Acta 2017; Epub ahead of print.
16. Mertens JC, Rizvi S, Gores GJ. Targeting cholangiocarcinoma. Biochim Biophys Acta 2017; Epub ahead of print.
17. Vaquero J, Guedj N, Clapéron A, Nguyen Ho-Bouldoires TH, Paradis V, Fouassier L. Epithelial-mesenchymal transition in cholangiocarcinoma: From clinical evidence to regulatory networks. J Hepatol. 2017;66:424-441.
18. Cadamuro M, Nardo G, Indraccolo S, Dall'olmo L, Sambado L, Moserle L, et al. Platelet-Derived Growth Factor and Rho GTPases regulate recruitment of Cancer-Associated Fibroblasts in Cholangiocarcinoma. Hepatology 2013;58:1042-1053.

19. Mertens JC, Fingas CD, Christensen JD, Smoot RL, Bronk SF, Werneburg NW, et al. Therapeutic effects of deleting cancer-associated fibroblasts in cholangiocarcinoma. Cancer Res 2013;73:897-907.
20. Tokuda H, Takai S, Hanai Y, Harada A, Matsushima-Nishiwaki R, Kato H, et al. Potentiation by platelet-derived growth factor-BB of FGF-2-stimulated VEGF release in osteoblasts. J Bone Miner Metab 2008;26:335-341.
21. Gaceb A, Özen I, Padel T, Barbariga M, Paul G. Pericytes secrete pro-regenerative molecules in response to platelet-derived growth factor-BB. J Cereb Blood Flow Metab 2017; Epub ahead of print.
22. Kazenwadel J, Secker GA, Betterman KL, Harvey NL. In Vitro Assays Using Primary Embryonic Mouse Lymphatic Endothelial Cells Uncover Key Roles for FGFR1 Signalling in Lymphangiogenesis. PLoS One 2012;7:e40497.
23. Ellis LM, Hicklin DJ. VEGF-targeted therapy: mechanisms of anti-tumour activity. Nat Rev Cancer 2008;8:579-591.
24. Duong T, Koopman P, Francois M. Tumor lymphangiogenesis as a potential therapeutic target. J Oncol 2012;2012:204946.
25. Lai GH, Zhang Z, Shen XN, Ward DJ, Dewitt JL, Holt SE, et al. ErbB-2/neu transformed rat cholangiocytes recapitulate key cellular and molecular features of human bile duct cancer. Gastroenterology 2005;129:2047-2057.
26. Sirica AE, Zhang Z, Lai GH, Asano T, Shen XN, Ward DJ, et al. A novel "patient-like" model of cholangiocarcinoma progression based on bile duct inoculation of tumorigenic rat cholangiocyte cell lines. Hepatology 2008;47:1178-1190.
27. Yamaguchi K, Chijiiwa K, Saiki S, Shimizu S, Takashima M, Tanaka M. Carcinoma of the extrahepatic bile duct: mode of spread and its prognostic implications. Hepatogastroenterology 1997;44:1256-1261.

28. Uenishi T, Hirohashi K, Kubo S, Yamamoto T, Yamazaki O, Kinoshita H. Clinicopathological factors predicting outcomes after resection of mass-forming intrahepatic cholangiocarcinoma. Br J Surg 2001;88:969–974.
29. Ustach CV, Taube ME, Hurst NJ Jr, Bhagat S, Bonfil RD, Cher ML, et al. A potential oncogenic activity of platelet-derived growth factor d in prostate cancer progression. Cancer Res 2004;64:1722-1729.
30. Xu L, Tong R, Cochran DM, Jain RK. Blocking platelet-derived growth factor-D/platelet-derived growth factor receptor beta signaling inhibits human renal cell carcinoma progression in an orthotopic mouse model. Cancer Res 2005;65:5711-5719.
31. Borkham-Kamphorst E, van Roeyen CR, Ostendorf T, Floege J, Gressner AM, Weiskirchen R. Pro-fibrogenic potential of PDGF-D in liver fibrosis. J Hep 2007;46:1064–1074.
32. Liang P, Hong JW, Ubukata H, Liu G, Katano M, Motohashi G, et al. Myofibroblasts Correlate with Lymphatic Microvessel Density and Lymph Node Metastasis in Early-stage Invasive Colorectal Carcinoma. Anticancer Res 2005;25:2705-2712.
33. Zhang Y, Tang H, Cai J, Zhang T, Guo J, Feng D, et al. Ovarian cancer-associated fibroblasts contribute to epithelial ovarian carcinoma metastasis by promoting angiogenesis, lymphangiogenesis and tumor cell invasion. Cancer Lett 2011;303:47-55.
34. Lu Y, Lin N, Chen Z, Xu R. Hypoxia-induced secretion of platelet-derived growth factor-BB by hepatocellular carcinoma cells increases activated hepatic stellate cell proliferation, migration and expression of vascular endothelial growth factor-A. Mol Med Rep 2015;11:691-697.
35. Nauck M, Roth M, Tamm M, Eickelberg O, Wieland H, Stulz P, et al. Induction of vascular endothelial growth factor by platelet-activating factor

and platelet-derived growth factor is downregulated by corticosteroids. Am J Respir Cell Mol Biol 1997;16:398-406.

36. Dell S, Peters S, Müther P, Kociok N, Joussen AM. The Role of PDGF Receptor Inhibitors and PI3-Kinase Signaling in the Pathogenesis of Corneal Neovascularization. Invest Ophthalmol Vis Sci 2006;47:1928-1937.

37. Cao R, Björndahl MA, Religa P, Clasper S, Garvin S, Galter D, et al. PDGF-BB induces intratumoral lymphangiogenesis and promotes lymphatic metastasis. Cancer Cell 2004;6:333–345.

38. Kodama M, Kitadai Y, Sumida T, Ohnishi M, Ohara E, Tanaka M, et al. Expression of platelet-derived growth factor (PDGF)-B and PDGF-receptor β is associated with lymphatic metastasis in human gastric carcinoma. Cancer Sci 2010;101:1984-1989.

39. Zudaire E, Gambardella L, Kurcz C, Vermeren S. A computational tool for quantitative analysis of vascular networks. PLoS One 2011;6:e27385.

40. Leu AJ, Berk DA, Lymboussaki A, Alitalo K, Jain RK. Absence of functional lymphatics within a murine sarcoma: a molecular and functional evaluation. Cancer Res 2000;60:4324–4327.

41. Mandriota SJ, Jussila L, Jeltsch M, Compagni A, Baetens D, Prevo R, et al. Vascular endothelial growth factor-C-mediated lymphangiogenesis promotes tumour metastasis. EMBO J 2001;20:672-682.

42. Skobe M, Hawighorst T, Jackson DG, Prevo R, Janes L, Velasco P, et al. Induction of tumor lymphangiogenesis by VEGF-C promotes breast cancer metastasis. Nat Med 2001;7:192-198.

43. Karnezis T, Shayan R, Caesar C, Roufail S, Harris NC, Ardipradja K, et al. VEGF-D promotes tumor metastasis by regulating prostaglandins produced by the collecting lymphatic endothelium. Cancer Cell 2012;21:181-195.

44. Tacconi C, Correale C, Gandelli A, Spinelli A, Dejana E, D'Alessio S, et al. Vascular endothelial growth factor C disrupts the endothelial lymphatic barrier to promote colorectal cancer invasion. Gastroenterology 2015;148:1438-1451.e8.
45. Bruix J, Qin S, Merle P, Granito A, Huang YH, Bodoky G, et al. Regorafenib for patients with hepatocellular carcinoma who progressed on sorafenib treatment (RESORCE): a randomised, double-blind, placebo-controlled, phase 3 trial. Lancet 2017;389:56-66.
46. Chong DQ, Zhu AX. The landscape of targeted therapies for cholangiocarcinoma: current status and emerging targets. Oncotarget 2016;7:46750-46767.

SUPPLEMENTARY MATERIALS AND METHODS

Cell lines. Human fibroblasts were seeded on plastic 25cm^2 flasks (Falcon®) and cultured in Dulbecco's Modified Eagle's medium (DMEM, Euroclone®) supplemented with 10% fetal bovine serum (FBS) and 1% penicillin/streptomycin (Euroclone®). Human lymphatic endothelial cells (LEC, purchased from ScienCell™) were seeded in 25cm^2 flasks (Falcon®) pre-coated with fibronectin 2µg/cm^2 (ScienCell™), and cultured in Endothelial Cell Basal Medium (ECM, ScienCell™) supplemented with 5% FBS (ScienCell™), 1% penicillin/streptomycin (ScienCell™) and 1% endothelial cell growth supplement (ECGS, ScienCell™). LEC were used until passage number 10. EGI-1 cells (PDGF-D expressing extrahepatic CCA cell line, purchased from Deutsche Sammlung von Mikroorganismen und

Zellkulturen) were seeded in 25cm^2 flasks (Falcon®) and cultured in RPMI-1640 Medium (Gibco™) supplemented with 10% FBS and 1% penicillin/streptomycin (Euroclone®). All cell lines were maintained in an incubator at 37°C and 5% CO_2 atmosphere (Galaxy S, RS Biotech).

Immunohistochemical staining. Briefly, after deparaffinization using xylene, sections were rehydrated in absolute ethanol and then washed in tap water; endogenous peroxidase activity was quenched incubating slides with methanol containing 10% H_2O_2 for 30 minutes. Antigen retrieval was performed by heating the slides in a steamer for 20 minutes in 10 mmol/L citrate buffer (pH 6) (Carlo Erba). Blocking of the aspecifics was achieved using UltraVision protein block (ThermoScientific) for 8 minutes. The sections were then incubated overnight at 4°C with primary antibodies against CD34 or D2-40 diluted in PBS + BSA 1% (Sigma-Aldrich®). After rinsing with phosphate-buffered saline (PBS) 1M supplemented with 0.05% Tween20 (PBS-T; both Sigma), slides were incubated for 30 minutes at room temperature with the specific horseradish peroxidase (HRP)-conjugated secondary antibody (EnVision, DAKO). Specimens were developed using 3,3-diaminobenzedine tetrahydrochloride 0.04 mg/mL (DAB, Sigma) with H_2O_2 0.01% diluted in PBS, counterstained with Gill's Hematoxylin N°2 (Sigma), and mounted using EuKitt (Bio-optica). Following immunostaining, lymphatic microvascular density (LMVD) and blood miscrovascular density (BMVD) were measured in

CCA and HCC samples using an Eclipse E800 microscope (Nikon). Briefly, 10 randomly taken micrographs were collected from each sample using a cooled digital camera (Nikon, DS-U1) and then analyzed using LuciaG 5.0 software, as previously described [1].

Double immunohistochemical staining. To match two antibodies developed in the same animal, we used a double immunohistochemical approach. Following deparaffinization and hydratation, as above described, CCA slides were incubated for 1h at room temperature with antibody against α-SMA and, following incubation with an appropriate HRP-conjugated secondary antibody, they were developed with DAB. Slides were then washed with distilled water for 15 min and then with PBS-T and incubated overnight at 4°C with antibody against D2-40. Following washing with PBS-T and incubation with the secondary antibody, staining was developed using TrueBlue (KPL), and then mounted as above described.

Double immunofluorescent staining. Briefly, following deparaffinization and hydratation, as above described, antigen retrieval was performed using 10 mmol/L citrate buffer (pH 6). Selected sections from CCA samples were incubated overnight at 4°C with primary antibodies against VEGF-A, VEGF-C, VEGFR2 or VEGFR3, together with antibodies against D2-40, α-SMA, or K19. Following washing in PBS-T, slides were then incubated for 30 minutes at room

temperature with the respective secondary Alexa Fluor 488- or 594-conjugated antibody (1:500, Life Technologies) and mounted with VECTASHIELD® Mounting Medium with DAPI (Vector Laboratories).

ELISA. Fibroblasts were seeded into a 24-well plate, and once confluent, were starved for 24h, before being exposed to recombinant human (rh) PDGF-D (100ng/ml, 24h, R&D Systems). To quantify the secretion of VEGF-A, VEGF-C, VEGF-D, Ang-1 or Ang-2, cultured fibroblast supernatants were harvested, stored at -80°C, and then analyzed by ELISA assay according to the supplier's instructions (RayBiotech). Absorbance levels were detected with FLUO Star Omega (BMG Labtech, Euroclone®). A calibration curve was generated for each experiment, and concentration levels were expressed in relation to the protein content of each experiment. In PDGF-D-stimulated fibroblasts, secretory levels were measured with or without treatment with imatinib mesylate (IM, PDGFRβ inhibitor, 1μM, 24h, Cayman Chemical Company), U0126 (ERK inhibitor, 10μM, 24h, Sigma-Aldrich®), and SP600125 (JNK inhibitor, 10μM, 24h, Sigma-Aldrich®), in order to dissect the intracellular pathways activated downstream of PDGFRβ, mediating the pro-lymphangiogenic functions of fibroblasts.

Western blotting. The expression of PDGFRβ, VEGFR2 and VEGFR3 was evaluated in untreated LEC and fibroblasts seeded into a 6-well plate. Total protein content (CelLytic M, Sigma) was obtained from

fibroblasts and LEC according to the supplier's instructions. Protein concentration was evaluated by Bradford assay (Sigma). Anti-PDGFRβ, anti-VEGFR2, anti-VEGFR3, and anti-GAPDH were used as primary antibodies. Equal concentrations of protein lysates were electrophoresed on a 4–12% NuPAGE® Novex Bis-Tris gel (Life Technologies) with MES (NuPage® Novex, Life Technologies in 500ml di H_2OmQ) for 40 minutes at 200 volt and 120 ampere and proteins were transferred to a nitrocellulose membrane (Life Technologies) for 60 minutes at 30 volt and 170 ampere. The membrane was then blocked with 5% non-fat dry milk (Euroclone) in Tris-buffered saline (TBS) supplemented with 0.1% Tween-20 (TBS-T) for 1 hour and then incubated overnight at 4°C with the primary antibody diluted in TBS-T + nonfat dry milk 5%. The membrane was washed 3 times with TBS-T before incubation with anti-rabbit (1:2000, Bio-Rad) or anti-mouse (1:2000, Sigma) HRP-conjugated secondary antibodies for 1 hour. Proteins were visualized using enhanced chemiluminescence (SuperSignal West Pico, Thermo Scientific). Bands were quantified with ImageJ and results were normalized versus reference proteins (GAPDH).

LEC migration assay. To assess the migratory abilities of LEC elicited by PDGF-D-stimulated fibroblasts, we used 6.5mm Transwell® with 8.0μm Pore Polycarbonate Membrane Insert (Corning), as previously described [2,3]. $5x10^4$ LEC in ECM medium + 0,5% FBS were added to

the upper chamber, whereas the lower chamber was filled with DMEM + 0,5% FBS harvested from fibroblasts challenged with PDGF-D (100ng/ml, 24h), with or without IM (1μM, 24h) (conditioned medium, CM). DMEM + 0,5% FBS from untreated fibroblasts and DMEM + 0.5% FBS supplemented with rh VEGF-A (100ng/ml, 24h, R&D Systems) or VEGF-C (100ng/ml, 24h, R&D Systems) served as negative and positive controls, respectively. After 24h, cells on the upper surface of the membrane were removed with a cotton swab, whereas cells adherent to the lower surface were fixed and stained using a Diff-Quick Staining Set (Medion Diagnostics). Finally, 10 random fields of each membrane were photographed at 10x magnification to count the number of clearly discernible nuclei.

Tube formation assay. To evaluate whether fibroblasts exposed to PDGF-D could also direct LEC to get-together in proper vascular structures, we performed a tube formation assay. LEC were re-suspended in ECM + 0,5% FBS, and seeded into a 24-well plate (Falcon®) at a density of $5x10^4$ cells/well. Each well was pre-coated with fibronectin 2μg/cm^2. After a 24h incubation, cultured LEC were covered with matrigel (Corning®) diluted at a 1:1 ratio in ECM + 0,5% FBS. Once matrigel solidified, cells were exposed to CM from fibroblasts challenged with PDGF-D (100ng/ml, 24h), with or without IM (1μM, 24h), and compared to cells exposed to medium from untreated fibroblasts, as negative control. Treatments with rhVEGF-A

(100ng/ml, 24h) or rhVEGF-C (100ng/ml, 24h) were used as positive controls. LEC exposed to CM from PDGF-D-treated fibroblasts were also simultaneously treated with antagonists of VEGFR2 (SU5416, 1μM, Sigma) or VEGFR3 (SAR131675, 15nM, Selleckchem). After a 24h exposure, analysis was performed in 5 random photos at 10x magnification (obtained through the same tools reported above for immunohistochemistry), by quantifying three parameters of tubulogenesis: a) length of vascular branches, b) number of junctions between branches, and c) luminal vascular area, using the AngioTool software, as described elsewhere [4].

Evaluation of trans-endothelial resistance (TEER). The following experiments were performed to understand whether, upon PDGF-D stimulation, fibroblasts could favor the lymphatic intravasation of CCA cells. To this end, $5x10^4$ LEC were seeded into a 24-well plate over a 0.4μm pore membrane (Corning) pre-coated with fibronectin 2μg/cm^2. Once LEC reached confluence, they were treated as reported for tube formation assay. Trans-endothelial electric resistance (TEER) was then evaluated by a Epithelial Volt/Ohm Meter (EVOM, World Precision Instruments) equipped with an STX2 electrode at different time points (0, 30, 60, 120, 360 min). To confirm the integrity of LEC monolayers, we ensured that TEER values at t=0 were higher than 1μΩ/μm^2.

Evaluation of trans-endothelial migration (TrEM). $5x10^4$ LEC were seeded over an 8.0μm pore polycarbonate membrane (Corning) pre-coated with fibronectin 2μg/cm^2. Once confluent, LEC were treated as reported for tube formation assay, and $5x10^4$ EGI-1 cells were seeded on the top of the endothelial monolayer. After 6h, cells on the upper surface of the membrane were removed, while cells on the lower side were fixed with ice-cold methanol and mounted with VECTASHIELD® Mounting Medium with DAPI (Vector Laboratories). To discriminate CCA cells from LEC, EGI-1 cells were originally transduced with a lentiviral vector encoding EGFP reporter gene, as previously performed [2,3]. The number of EGFP-positive cells was counted in 10 random pictures of each membrane taken at 10X magnification [5].

MTS assay. CellTiter 96® AQueous One Solution Cell Proliferation Assay (MTS) (Promega) was used to assess whether SU5416 (0,1μM, 1 μM, and 5 μM) and SAR131675 (1nM, 15nM, and 30nM) could affect LEC viability in response to a 24h treatment [6]. LEC were re-suspended in 0,5% FBS culture medium, and seeded into a 96-well plate at a density of $1x10^4$ cells/well. After a 24h incubation, cells were treated with SU5416 or SAR131675 diluted in 0,5% FBS culture medium. After treatment, 20μl of CellTiter 96® AQueous One Solution Reagent (Promega) were added to each well, and the plate was incubated at 37°C for 1 hour in a 5% CO_2 atmosphere. 490nm

absorbance was evaluated using FLUO Star Omega (BMG Labtech, Euroclone®). Each experiment was made in duplicate.

SUPPLEMENTARY FIGURES AND TABLES

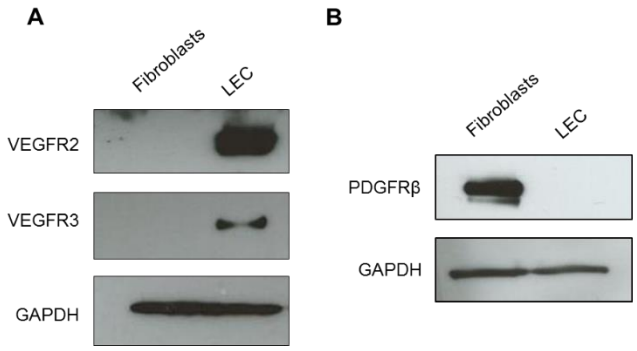

Figure S1. Opposite pattern of expression of VEGFR2, VEGFR3 and PDGFRβ on LEC compared with fibroblasts. In contrast to fibroblasts, LEC expressed VEGFR2 and VEGFR3 (A), whereas they did not express PDGFRβ (B), thereby indicating their unresponsiveness to PDGF-D.

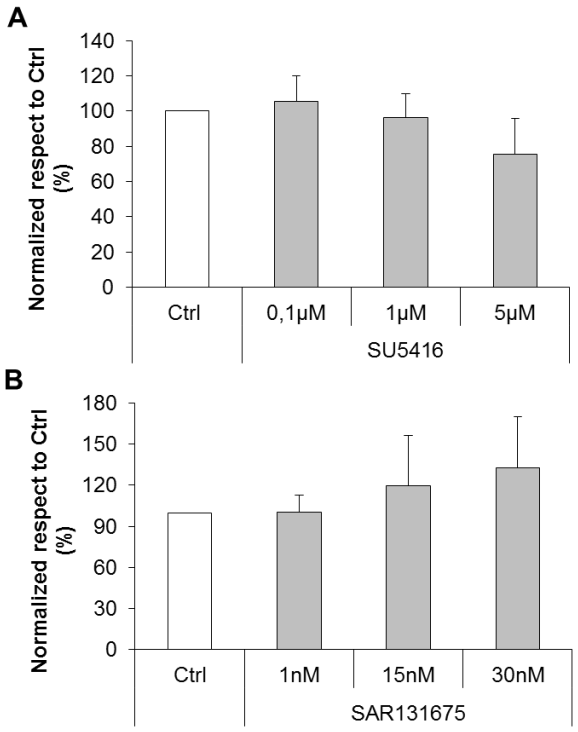

Figure S2. LEC viability is not affected by VEGFR2 or VEGFR3 antagonists. By MTS assay we evaluated the dose-response treatments of SU5416 (VEGFR2 inhibitor) (A) and of SAR131675 (VEGFR3 inhibitor) (B) on cultured LEC. No toxic effects could be observed with either compounds at the different concentrations tested in LEC cell experiments.

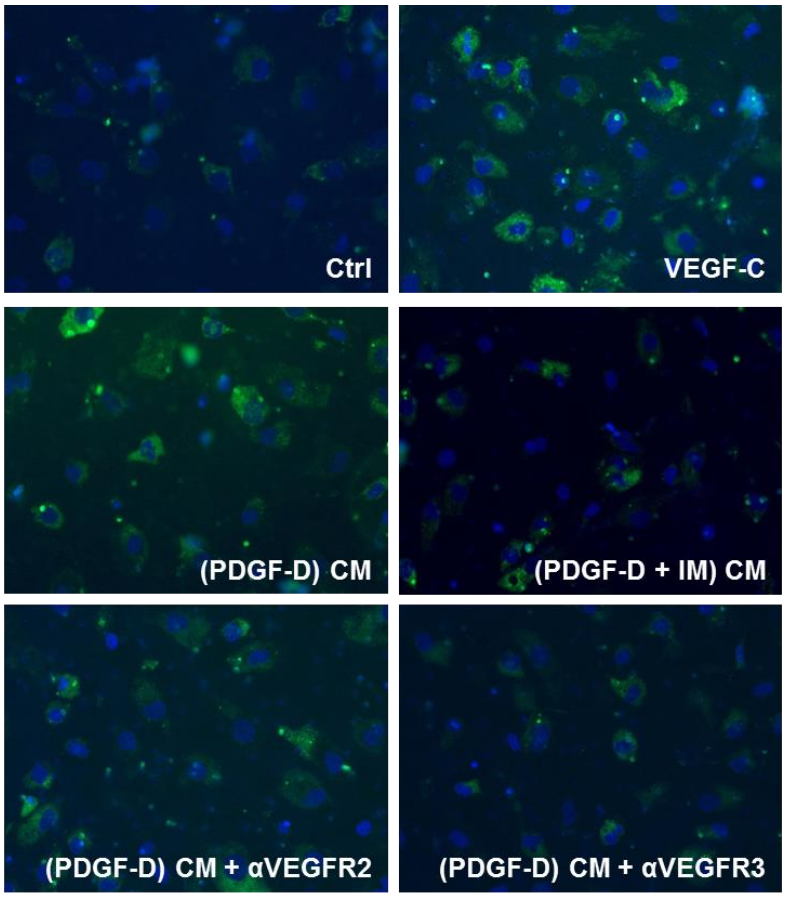

Figure S3. Trans-endothelial migration of EGI-1-EGFP cells is potently induced by CM from PDGF-D-stimulated fibroblasts. Representative micrographs of Boyden chamber experiments evaluating the amount of EGI-1-EGFP cells (green) crossing a LEC monolayer exposed to CM from fibroblasts challenged with PDGF-D, alone, (PDGF-D) CM, or in combination with IM, (PDGF-D + IM) CM, in the presence/absence of VEGFR2, (PDGF-D) CM + αVEGFR2, or VEGFR3, (PDGF-D) CM + αVEGFR3, antagonists. Nuclear marker, DAPI (blue). Original magnification: 200x.

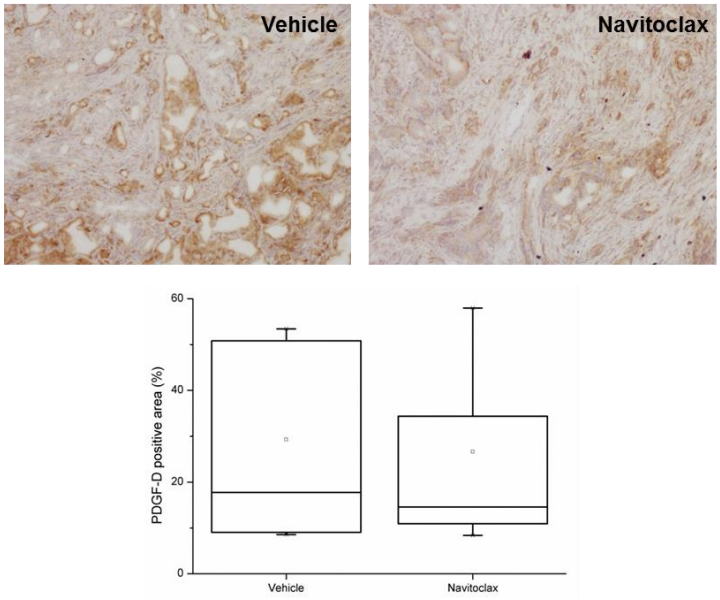

Figure S4. In a syngeneic rat model of CCA, targeting CAF by navitoclax did not affect PDGF-D expression by tumoral cells. In Fischer 344 male rats transplanted with BDE-neu rat CCA cells, treatment with navitoclax induced a selective depletion of CAF, without affecting PDGF-D expression by tumoral cells. In the top, representative images of CCA sections immunostained for PDGF-D, showing the comparable levels of expression by PDGF-D$^+$ tumoral areas between the two groups (n=6 each group). Original magnification: 100x.

Antibody	Isotype	(IHC/IF) dilution; antigen retrieval	(WB) dilution	Supplier
α-SMA (clone 1A4)	Mouse monoclonal	1:200; 10mmol/L citrate pH 6		DAKO
Actin	Rabbit polyclonal		1:5000	Sigma-Aldrich
CD34 (clone QBEnd/10)	Mouse monoclonal	1:50; 10mmol/L citrate pH 6		Leica Biosystems
D2-40	Mouse monoclonal	1:100; 10mmol/L citrate pH 6		DAKO

GAPDH (clone 0411)	Mouse monoclonal		1:5000	Santa Cruz Biotechnology
K19 (clone RCK108)	Mouse monoclonal	1:100 (frozen)		DAKO
Lyve-1	Rabbit polyclonal	1:100 (frozen)		Acris
PDGF-D	Rabbit polyclonal	1:100 (frozen)		Invitrogen
PDGFRβ	Rabbit polyclonal		1:1000	Cell Signaling
VEGF-A	Rabbit polyclonal	1:100; 10mmol/L citrate pH 6		Santa Cruz Biotechnology
VEGF-C	Rabbit polyclonal	1:100; 10mmol/L citrate pH 6		Santa Cruz Biotechnology
VEGFR2	Rabbit polyclonal	1:100; 10mmol/L citrate pH 6	1:1000	Cell Signaling
VEGFR3	Rabbit polyclonal	1:100; 10mmol/L citrate pH 6	1:500	Santa Cruz Biotechnology

Supplementary Table 1. List of primary antibodies.

SUPPLEMENTARY REFERENCES

1. Fabris L, Cadamuro M, Fiorotto R, Roskams T, Spirlì C, Melero S, et al. Effects of angiogenic factor overexpression by human and rodent cholangiocytes in polycystic liver diseases. Hepatology 2006;43:1001-1012.

2. Fabris L, Cadamuro M, Moserle L, Dziura J, Cong X, Sambado L, et al. Nuclear expression of S100A4 calcium-binding protein increases cholangiocarcinoma invasiveness and metastasization. Hepatology 2011;54:890-899.

3. Cadamuro M, Nardo G, Indraccolo S, Dall'olmo L, Sambado L, Moserle L, et al. Platelet-Derived Growth Factor and Rho GTPases regulate recruitment of

Cancer-Associated Fibroblasts in Cholangiocarcinoma. Hepatology 2013;58:1042-1053.

4. Kazenwadel J, Secker GA, Betterman KL, Harvey NL. In Vitro Assays Using Primary Embryonic Mouse Lymphatic Endothelial Cells Uncover Key Roles for FGFR1 Signalling in Lymphangiogenesis. PLoS One 2012;7:e40497.

5. Tacconi C, Correale C, Gandelli A, Spinelli A, Dejana E, D'Alessio S, et al. Vascular endothelial growth factor C disrupts the endothelial lymphatic barrier to promote colorectal cancer invasion. Gastroenterology 2015;148:1438-1451.e8.

6. Espagnolle N, Barron P, Mandron M, Blanc I, Bonnin J, Agnel M, et al. Specific Inhibition of the VEGFR-3 Tyrosine Kinase by SAR131675 Reduces Peripheral and Tumor Associated Immunosuppressive Myeloid Cells. Cancers (Basel) 2014;6:472-490.

CHAPTER 5

Summary, conclusions and future perspectives

During my PhD studies, I sought to gain insights into the molecular mechanisms underpinning the progression of cholangiocarcinoma (CCA), particularly focusing on the deleterious contribution of the tumor microenvironment, which is currently recognized as a driving force behind the emergence of the hallmarks of cancer [1-3]. Specifically, the studies presented here dissected the tumor-stroma interplay from various points of view. On the one hand (Chapters 2 and 3), we shed light on pro-oncogenic signaling systems that are deleteriously fueled by the crosstalk between the tumor and its stromal neighborhood, and provide CCA cells with enhanced aggressiveness. On the other hand (Chapter 4), we highlighted the capability of CCA cells to trigger a multi-step paracrine cascade that involve different stromal components, and ultimately give rise to a microenvironment conducive to tumor progression. Hopefully, a comprehensive understanding of the dense, multifaceted paracrine communications between cancer and reactive stromal cells in CCA will considerably help to identify prognostically relevant molecular signatures, as well as innovative therapeutic targets, with the ultimate goal to improve the management of this devastating malignancy.

In the first study, we demonstrated that the pleiotropic cytokine leukemia inhibitory factor (LIF) may strengthen the chemoresistant phenotype of CCA cells, through autocrine and paracrine mechanisms. Indeed, LIF is both overexpressed by CCA cells, and abundantly produced by cancer-associated fibroblasts (CAFs) and

inflammatory cells populating the tumor microenvironment. In addition, the cognate receptor for LIF is selectively up-regulated in neoplastic bile ducts. At the functional level, LIF enables CCA cells to escape from apoptosis induced by the combination of cisplatin and gemcitabine (i.e., the first-line chemotherapy regimen for patients with advanced CCA), an effect mediated by the up-regulation of the anti-apoptotic protein myeloid cell leukemia (Mcl)-1. As already discussed, the unbalance between anti-apoptotic and pro-apoptotic members of the Bcl-2 family is a primary mechanism of chemoresistance in several tumors, including CCA [4,5], and LIF seems to play a relevant role in this context. In our model, Mcl-1 up-regulation occurs downstream of the activation of the PI3K/Akt pathway, which in turn has been widely recognized as a paramount pro-oncogenic signaling network in human cancer [6]. It is important to underline that both pro-inflammatory cytokines [7,8], and intratumoral hypoxia [9] could be responsible for the overproduction of LIF in CCA, in line with the notion that the tumor reactive stroma (TRS) is an hectic microenvironment whose different (cellular and non-cellular) components support each other in fueling tumor progression.

In the second study, we showed that the nuclear import of the calcium-binding protein S100A4 confers strong metastatic properties upon CCA cells, an effect mediated by the activation of the small Rho GTPases RhoA and Cdc42, the overproduction of matrix

metalloproteinase (MMP)-9, and the enhanced expression of membrane-type (MT)1-MMP. Of note, RhoA and Cdc42 are key effectors of cell motility [10,11], whereas the proteolytic activity of MMP-9 and MT1-MMP is essential for massively degrading the extracellular matrix, and thus enabling a pervasive migration [12]. Importantly, we unveiled that the translocation of S100A4 into the nucleus of CCA cells is strictly dependent on its SUMOylation, a post-translational modification that may alter the activity, subcellular localization, or stability of several substrate proteins, mainly involved in gene transcription and DNA repair [13]. In experimental models of CCA, we finally proved that the pharmacological inhibition of S100A4 nuclearization by paclitaxel at nanomolar doses did not tackle tumor growth, but effectively halted the hematogenous metastasization to the lungs, which represent the preferential site of distant metastases in CCA patients [14]. Although we did not provide direct evidence that the nuclear expression of S100A4 in CCA cells is fostered by microenvironmental signals, it is worth considering that the up-regulation of epithelial-to-mesenchymal transition biomarkers, including S100A4, is a classic readout of tumor-stroma interactions [15] and moreover, in human chondrocytes, the SUMOylation-dependent nuclear entry of S100A4 can be potently stimulated by the pro-inflammatory cytokine interleukin 1β [16].

In the third study, we revealed that platelet-derived growth factor (PDGF)-DD, which is overexpressed by CCA cells under severe

hypoxia and exert motogenic effects on CAFs [17], is also able to endow fibroblasts with the ability to overproduce vascular endothelial growth factor (VEGF)-A and VEGF-C, which may then stimulate the chemotaxis of lymphatic endothelial cells (LECs), alongside their assembly in highly branched tubular structures. Specifically, PDGF-DD binds to its cognate receptor PDGFRβ on the surface of CAFs, thereby activating ERK and JNK signaling cascades, whereas VEGF ligands bind to VEGFR-2 (VEGF-A, VEGF-C) and VEGFR-3 (VEGF-C) on the surface of LECs. Therefore, tumor-derived PDGF-DD not only plays a prominent role in supporting fibroblast enrichment within the tumor microenvironment [17], but also molds the behavior of CAFs so that they can orchestrate lymphangiogenesis. As previously discussed, the establishment of an abnormally rich lymphatic vasculature is a histological hallmark of CCA, underlying its early metastatic spread [1,18,19]. In line with the notion that VEGF-C may also impair the integrity of lymphatic vessels by introducing intercellular gaps [20,21], we additionally found that PDGF-DD-treated fibroblasts could increase the permeability of LEC monolayers, ultimately favoring the trans-endothelial migration of CCA cells. It is finally worth noting that inflammatory cells represent an additional source of PDGF-DD [17] and, alongside CCA cells, may even contribute to the biosynthesis of VEGFs [22]. Overall, this further highlights that in CCA, the generation of a pro-metastatic microenvironment is finely orchestrated by the

redundant and synergistic activities of the cancer cells and their surrounding stromal cell populations.

Curative therapies for the management of CCA basically consist of surgical resection by partial hepatectomy and orthotopic liver transplantation. However, only a minority of patients can benefit from these treatment options, since CCA is frequently diagnosed at advanced stages [4]. Unfortunately, conventional chemotherapy is traditionally ineffective and so far, clinical trials with molecular targeted therapies failed to provide substantial survival benefits [23,24]. This paucity of potentially curative treatments ultimately results in a grim prognosis, which makes CCA a global health problem, especially considering its increasing incidence in Western Countries [4]. The development of effective pharmacological approaches to the management of CCA has been limited not only by the pronounced inter-tumor heterogeneity [24], but also by the fact that anti-cancer therapies have been classically designed to target intrinsic traits of neoplastic cells, without taking due account of the surrounding microenvironment [2]. However, we and others have provided evidence that reactive stromal cells may take a leading role in CCA progression, by both directly fostering cancer cell survival and invasiveness, and setting up a microenvironment conducive to metastatic dissemination. Therefore, interfering with the epithelial-mesenchymal crosstalk within CCA microenvironment might substantially hinder tumor progression, by deadening a driving force

behind the emergence of aggressive tumor phenotypes. Basically, the therapeutic targeting of the tumor stroma should seek to reduce the amount of reactive stromal cells or alternatively, to quench the pro-oncogenic pathways that they contribute to activate [2]. In this regard, in the studies presented here, we shed light on a wide range of putative novel targets potentially amenable to therapeutic modulation. For instance, targeting the LIF/PI3K/Mcl-1 axis could represents a feasible strategy to overcome CCA chemoresistance, whereas a selective reduction in S100A4 nuclear import by low-dose paclitaxel seems to be a promising approach to undermine CCA invasiveness. On the other hand, the therapeutic interference with either PDGF-DD/PDGFRβ or VEGF/VEGFR signaling systems should disrupt the crosstalk among CCA cells, CAFs and LECs, eventually preventing cancer cells to disseminate at distance through the lymphatic network. Interestingly, small molecules targeting some of the above mentioned molecular players are already approved for use or under clinical trials in other types of cancer. These include, for example, MK2206 (Akt inhibitor), MIK665 (Mcl-1 inhibitor), imatinib mesylate (PDGFRβ inhibitor), and fruquintinib (VEGFRs inhibitor). However, further studies are required to understand whether such TRS-oriented therapies could actually be successful in treating CCA, either alone or in combination with conventional anti-cancer treatments. It is also worth noting that several molecules may serve as both therapeutic targets and prognostic/predictive markers, and S100A4 is paradigmatic of this

concept. Indeed, our group previously found that nuclear expression of S100A4 by neoplastic bile ducts was associated with poor outcome, in terms of both metastasization and tumor-related death, thereby representing a promising tool in clinical decision-making [25]. In summary, the understanding of the dynamic and intricate interplay between CCA cells and the wide web of neighboring stromal components is undoubtedly an issue of great translational significance, with a view to open novel therapeutic avenues in CCA, as well as in other epithelial neoplasms characterized by an abundant stroma, such as breast and pancreatic cancers.

References

1. Cadamuro M, Morton SD, Strazzabosco M, Fabris L. Unveiling the role of tumor reactive stroma in cholangiocarcinoma: An opportunity for new therapeutic strategies. Transl Gastrointest Cancer. 2013;2:130-44.
2. Brivio S, Cadamuro M, Strazzabosco M, Fabris L. Tumor reactive stroma in cholangiocarcinoma: The fuel behind cancer aggressiveness. World J Hepatol. 2017;9:455-68.
3. Cadamuro M, Stecca T, Brivio S, Mariotti V, Fiorotto R, Spirli C, Strazzabosco M, Fabris L. The deleterious interplay between tumor epithelia and stroma in cholangiocarcinoma. Biochim Biophys Acta. 2017.
4. Banales JM, Cardinale V, Carpino G, Marzioni M, Andersen JB, Invernizzi P, Lind GE, Folseraas T, Forbes SJ, Fouassier L, Geier A, Calvisi DF, Mertens JC, Trauner M, Benedetti A, Maroni L, Vaquero J, Macias RI, Raggi C, Perugorria MJ, Gaudio E, Boberg KM, Marin JJ, Alvaro D. Expert consensus document: Cholangiocarcinoma: current knowledge and future perspectives consensus statement from the European Network for the Study of Cholangiocarcinoma (ENS-CCA). Nat Rev Gastroenterol Hepatol. 2016;13:261-80.
5. Cadamuro M, Brivio S, Spirli C, Joplin RE, Strazzabosco M, Fabris L. Autocrine and Paracrine Mechanisms Promoting Chemoresistance in Cholangiocarcinoma. Int J Mol Sci. 2017;18.
6. Fruman DA, Rommel C. PI3K and cancer: lessons, challenges and opportunities. Nat Rev Drug Discov. 2014;13:140-56.

7. Kamohara H, Ogawa M, Ishiko T, Sakamoto K, Baba H. Leukemia inhibitory factor functions as a growth factor in pancreas carcinoma cells: Involvement of regulation of LIF and its receptor expression. Int J Oncol. 2007;30:977-83.
8. Albrengues J, Bourget I, Pons C, Butet V, Hofman P, Tartare-Deckert S, Feral CC, Meneguzzi G, Gaggioli C. LIF mediates proinvasive activation of stromal fibroblasts in cancer. Cell Rep. 2014;7:1664-78.
9. Kuphal S, Wallner S, Bosserhoff AK. Impact of LIF expression in malignant melanoma. Exp Mol Pathol. 2013;95:156-65.
10. Ridley AJ. Rho GTPases and cell migration. J Cell Sci. 2001;114:2713-22.
11. Ridley AJ. Rho GTPase signalling in cell migration. Curr Opin Cell Biol. 2015;36:103-12.
12. Brown GT, Murray GI. Current mechanistic insights into the roles of matrix metalloproteinases in tumour invasion and metastasis. J Pathol. 2015;237:273-81.
13. Monribot-Villanueva J, Zurita M, Vázquez M. Developmental transcriptional regulation by SUMOylation, an evolving field. Genesis. 2017;55.
14. Fabris L, Alvaro D. The prognosis of perihilar cholangiocarcinoma after radical treatments. Hepatology. 2012;56:800-2.
15. Brivio S, Cadamuro M, Fabris L, Strazzabosco M. Epithelial-to-Mesenchymal Transition and Cancer Invasiveness: What Can We Learn from Cholangiocarcinoma? J Clin Med. 2015;4:2028-41.
16. Miranda KJ, Loeser RF, Yammani RR. SUMOylation and nuclear translocation of S100A4 regulate IL-1beta-mediated production of matrix metalloproteinase-13. J Biol Chem. 2010;285:31517–31524.

17. Cadamuro M, Nardo G, Indraccolo S, Dall'olmo L, Sambado L, Moserle L, Franceschet I, Colledan M, Massani M, Stecca T, Bassi N, Morton S, Spirli C, Fiorotto R, Fabris L, Strazzabosco M. Platelet-derived growth factor-D and Rho GTPases regulate recruitment of cancer-associated fibroblasts in cholangiocarcinoma. Hepatology. 2013;58:1042-53.
18. Thelen A, Scholz A, Benckert C, Weichert W, Dietz E, Wiedenmann B, Neuhaus P, Jonas S. Tumor-associated lymphangiogenesis correlates with lymph node metastases and prognosis in hilar cholangiocarcinoma. Ann Surg Oncol. 2008;15:791-9.
19. Thelen A, Scholz A, Weichert W, Wiedenmann B, Neuhaus P, Gessner R, Benckert C, Jonas S. Tumor-associated angiogenesis and lymphangiogenesis correlate with progression of intrahepatic cholangiocarcinoma. Am J Gastroenterol. 2010;105:1123-32.
20. Duong T, Koopman P, Francois M. Tumor lymphangiogenesis as a potential therapeutic target. J Oncol. 2012;2012:204946.
21. Stacker SA, Williams SP, Karnezis T, Shayan R, Fox SB, Achen MG. Lymphangiogenesis and lymphatic vessel remodelling in cancer. Nat Rev Cancer. 2014;14:159-72.
22. Leyva-Illades D, McMillin M, Quinn M, Demorrow S. Cholangiocarcinoma pathogenesis: Role of the tumor microenvironment. Transl Gastrointest Cancer. 2012;1:71-80.
23. Moeini A, Sia D, Bardeesy N, Mazzaferro V, Llovet JM. Molecular Pathogenesis and Targeted Therapies for Intrahepatic Cholangiocarcinoma. Clin Cancer Res. 2016;22:291-300.
24. Rizvi S, Gores GJ. Emerging molecular therapeutic targets for cholangiocarcinoma. J Hepatol. 2017;67:632-44.

25. Fabris L, Cadamuro M, Moserle L, Dziura J, Cong X, Sambado L, Nardo G, Sonzogni A, Colledan M, Furlanetto A, Bassi N, Massani M, Cillo U, Mescoli C, Indraccolo S, Rugge M, Okolicsanyi L, Strazzabosco M. Nuclear expression of S100A4 calcium-binding protein increases cholangiocarcinoma invasiveness and metastasization. Hepatology. 2011;54:890-9.

Contribution to international publications

Research articles

- Cadamuro M, Spagnuolo G, Sambado L, Indraccolo S, Nardo G, Rosato A, Brivio S, Caslini C, Stecca T, Massani M, Bassi N, Novelli E, Spirlì C, Fabris L, Strazzabosco M. *Low Dose Paclitaxel Reduces S100A4 Nuclear Import to Inhibit Invasion and Hematogenous Metastasis of Cholangiocarcinoma*. Cancer Res 2016; 76:4775-4784; doi: 10.1158/0008-5472.
- Morton SD, Cadamuro M, Brivio S, Vismara M, Stecca T, Massani M, Bassi N, Furlanetto A, Joplin RE, Floreani A, M, Fabris L, Strazzabosco M. *Leukemia Inhibitory Factor Protects Cholangiocarcinoma Cells from Drug-Induced Apoptosis via a PI3K/AKT-dependent Mcl-1 Activation*. Oncotarget 2015; 6:26052-26064; doi: 10.18632/oncotarget.4482.

Review articles

- Brivio S, Cadamuro M, Fabris L, Strazzabosco M. *Molecular mechanisms driving cholangiocarcinoma invasiveness: an overview*. Gene Expr 2017; Epub ahead of print; doi: 10.3727/105221617X15088670121925.
- Cadamuro M, Stecca T, Brivio S, Mariotti V, Fiorotto R, Spirli C, Strazzabosco M, Fabris L. *The deleterious interplay between tumor epithelia and stroma in cholangiocarcinoma*. Biochim

Biophys Acta 2017; Epub ahead of print; doi: 10.1016/j.bbadis.2017.07.028.

- Brivio S, Cadamuro M, Strazzabosco M, Fabris L. *Tumor reactive stroma in cholangiocarcinoma: The fuel behind cancer aggressiveness*. World J Hepatol 2017; 9:455-468; doi: 10.4254/wjh.v9.i9.455.
- Cadamuro M, Brivio S, Spirli C, Joplin RE, Strazzabosco M, Fabris L. *Autocrine and Paracrine Mechanisms Promoting Chemoresistance in Cholangiocarcinoma*. Int J Mol Sci 2017; 18; doi: 10.3390/ijms18010149.
- Fabris L, Brivio S, Cadamuro M, Strazzabosco M. *Revisiting Epithelial-to-Mesenchymal Transition in Liver Fibrosis: Clues for a Better Understanding of the 'Reactive' Biliary Epithelial Phenotype*. Stem Cells Int 2016; 2016:2953727; doi: 10.1155/2016/2953727.
- Brivio S, Cadamuro M, Fabris L, Strazzabosco M. *Epithelial-to-Mesenchymal Transition and Cancer Invasiveness: What Can We Learn from Cholangiocarcinoma*? J Clin Med 2015; 4:2028-2041; doi: 10.3390/jcm4121958.